Identification of Differentially Expressed Ferroptosis-Related Hub Genes and Their Association with Cigarette Smoke-Induced Chronic Obstructive Pulmonary Disease by Bioinformatic Analysis

by

Fatma Şimal Laçin

A Dissertation Submitted to the
Graduate School of Health Sciences
in Partial Fulfillment of the Requirements for
the Degree of

Master of Science

in

Immunology

October 4, 2024

Identification of Differentially Expressed Ferroptosis-Related Hub Genes and Their Association with Cigarette Smoke-Induced Chronic Obstructive Pulmonary Disease by Bioinformatic Analysis

Koç University

Graduate School of Health Sciences

This is to certify that I have examined this copy of a master's thesis by

Fatma Şimal Laçin

and have found that it is complete and satisfactory in all respects,
and that any revisions required by the final
examining committee have been made.

Committee Members:

Prof. Dr. Hasan Bayram (Advisor)

Prof. Dr. Öner Dikensoy

Assoc. Prof. Dr. Vahap Eldem

Date: 04.10.2024

To my dear father…

ABSTRACT

Identification of Differentially Expressed Ferroptosis-Related Genes and Their Association with Cigarette Smoke-Induced Chronic Obstructive Pulmonary Disease by Bioinformatic Analyses

Fatma Şimal Laçin

Master of Science in (Immunology)

04/10/2024

Chronic Obstructive Pulmonary Disease (COPD) is a complex and progressive respiratory disorder, primarily resulting from exposure to cigarette smoke. The disease is characterized by chronic inflammation, oxidative stress, and irreversible destruction of lung tissue. Recent studies have revealed that ferroptosis, a regulated form of cell death driven by iron-dependent lipid peroxidation, plays a significant role in COPD pathogenesis. The aim of this study was to identify ferroptosis-related genes (FRGs) involved in cigarette smoke-induced COPD, and to investigate the expression of these genes *in vitro*. Initially, an integrative bioinformatic analysis was performed that was followed by in vitro cigarette smoke extract (CSE) exposure and expression analysis of target genes. The datasets used in this study were obtained from the Gene Expression Omnibus (GEO) database. Differentially expressed genes (DEGs) were identified through dataset analysis, and ferroptosis-related genes were extracted using the FerrDb database gene list. The MCODE method, which was integrated into the Metascape online tool, was employed to identify hub genes. Subsequently, protein-protein interaction (PPI) analysis, functional enrichment analysis, and miRNA-gene interaction studies were conducted for the hub genes. Quantitative real-time polymerase chain reaction (qRT-PCR) was performed to analyse the expression of these hub genes after *in vitro* CSE exposure. Based on the analysis of multiple datasets and the FerrDb database, 20 FRGs involved in cigarette smoke-induced COPD were identified after removing redundant genes. MCODE analysis identified MDM2, EGFR, SRC, BRD4, GDF15, TP63, and CD44, as hub genes. Functional enrichment analysis revealed a strong association between these genes and ferroptosis-related biological pathways, including fatty acid and sulphur compound regulation that were mediated through the TP53 signaling pathway. miRNA-gene interaction analysis suggested that hsa-mir-203a-3p, hsa-mir-155-5p, and hsa-mir-34a-3p may regulate these genes. *In vitro* validation studies demonstrated that 24 hours incubation with CSE led to a significant reduction in the expression of six of the seven hub genes, except MDM2 gene in primary human bronchial epithelial cells (HBEC). However, CSE exposure did not cause any significant changes in the expression of genes studied in BEAS-2B cell line. In conclusion, we demonstrated the involvement of six ferroptosis-related hub genes in the pathogenesis of CSE-induced COPD by both bioinformatic tools and the validation by qRT-PCR. Our findings suggest that these genes may serve as potential targets for the diagnosis and treatment modalities of cigarette smoke-associated COPD; however, further studies are required.

Key words: COPD, Smoke, Ferroptosis, Differentially expressed genes (DEGs)

ÖZETÇE

Diferansiyel Olarak Eksprese Edilen Ferroptoz İlişkili Merkezi Genlerin ve Sigara Dumanına Bağlı Kronik Obstrüktif Akciğer Hastalığı ile İlişkilerinin Biyoinformatik Analizler Yoluyla Belirlenmesi

Fatma Şimal Laçin

İmmunoloji, Yüksek Lisans

04/10/2024

Kronik Obstrüktif Akciğer Hastalığı (KOAH), esas olarak sigara dumanına maruziyet sonucu ortaya çıkan, karmaşık ve ilerleyici bir solunum hastalığıdır. Bu hastalık, kronik inflamasyon, oksidatif stres ve geri dönüşü olmayan akciğer dokusu yıkımı ile karakterize edilmektedir. Son dönemde yapılan araştırmalar, demir bağımlı lipid peroksidasyonu tarafından yönlendirilen düzenlenmiş bir hücre ölüm türü olan ferroptozun, KOAH patogenezinde önemli bir rol oynadığını ortaya koymuştur. Bu çalışmanın amacı, sigara dumanı ile indüklenen KOAH'ın gelişiminde rol oynayan ve ferroptoz ile ilişkili genleri (FRG'ler) belirlemek ve bu genlerin ekspresyon seviyelerini in vitro olarak araştırmaktı. Çalışmamızda öncelikle integrative biyoinformatik analiz gerçekleştirildi ve sonrasında in vitro sigara dumanı ekstraktı (CSE) maruziyeti ve hedef genlerin ekspresyon analizleri gerçekleştirildi. Çalışmada kullanılan veri setleri gen ekpresyon omnibus (GEO) veri bankasından elde edildi. Veri setlerinin analizi sonucu diferansiyel eksprese genler (DEGs) belirlendi ve bu genler içinden ferroptoz ile ilişkili olanlar FerrDb veri bankasındaki gen listesi kullanılarak ayrıştırıldı. Bu genler içinde hub genlerin belirlenmesi için Metascape online aracına entegre MCODE yöntemi kullanıldı. Daha sonra bu genler protein-protein etkileşim analizi, fonksiyonel zenginleştirme analizi ve merkezi ilişkiye sahip genler ve miRNA etkileşimleri analiz edildi. Daha sonra belirlenen merkezi genler in vitro CSE maruziyet deneyi sonunda kantitatif gerçek zamanlı polimeraz zincir reaksiyonu (qRT-PCR) ile analiz edildi. Analiz sonuçlarına göre farklı data setlerinden belirlenen DEG'ler ve FerrDb veri bankası kullanılarak ferroptoz ilşkili genler belirlendi ve tekrarlı genler ayıklandıktan sonra sigara ile ilişkli KOAH'da rol oynayan ve feroptoz ilişkili 20 gen belirlendi. MCODE analizi sonucunda MDM2, EGFR, SRC, BRD4, GDF15, TP63 ve CD44 merkezi ilişkili genler olarak belirlendi. Bu genlerin fonksiyonel enrichment analiz sonucunda TP53 sinyallenme yolu ile ferroptozla ilişkili yağ asidi ve sülfür bileşenlerinin regülasyonunu içeren biyolojik sinyal yollarıyla güçlü ilişki saptadık. Bu genlerin miRNA ilişki analizinde hsa-mir-203a-3p, hsa-mir-155-5p ve hsa-mir-34a-3p miRNA'larının bu genlerin ortak regülasyonundan sorumlu olabileceğini belirledik. In vitro validasyon analizimizde, 24 saat CSE maruziyeti primer insan bronş epitel hücrelerinde 7 ortak gen içinden MDM2'yu kontrole göre anlamlı düzeyde etkilemezken diğer genlerin ekspresyonunu anlamlı düzeyde azalttığını belirledik. Ancak, 24 saat CSE maruziyeti BEAS-2B hücrelerinde bu genlerin ekspresyonuna kontrole göre anlamlı düzeyde etki etmedi. Sonuç olarak, CSE kaynaklı KOAH patogenezinde ferroptoz ile MDM2 dışındaki altı ortak geninin qRT-PCR ile

doğrulanan biyoinformatik analizlerle araştırılan ilişkisini ortaya koyduk. Elde ettiğimiz sonuçlara göre bu genler sigara ilişkili COPD'nin tanı ve tedavisinde hedef genler olabilir. Ancak, daha detaylı analizlerle verilerin doğrulanmasına ihtiyaç vardır.

Anahtar kelimeler: KOAH, Sigara, Ferroptoz, Differansiyel eksprese genler (DEGs)

ACKNOWLEDGMENTS

I am extremely grateful to my supervisor Prof. Dr. Hasan Bayram, for giving me a chance to start my early academic career in his laboratory. I am very thankful for his guidance and support throughout this process.

I would also like to extend my deepest gratitude to Dr. Özgecan Kayalar for sharing his extensive knowledge and always being there for me when needed, from day one until my graduation.

I am very thankful to Mr. Furkan Zahit Tunç for his huge support in the R-based bioinformatic analysis and for his time with me to discuss the results.

I also wish to thank all KUTTAM members. Sharing a laboratory with all of them was a real pleasure and fun that I will never forget.

I cannot begin to express my thanks to my family. They have been very supportive and kind to me through all the ups and downs that I faced during this process. I am deeply thankful for them, especially my mother and sister, who always encouraged me in every aspect of my life and were always there for me. I would not have accomplished any of the things I have so far if it were not for them.

Last but not the least, I need to thank one more person without whose support it would not have been possible for me to complete my thesis.

I gratefully acknowledge the support from Koç University School of Medicine and Graduate School of Health Sciences for the opportunities, which they provided me to conduct the experiments in this project.

TABLE OF CONTENTS

LIST OF TABLES

LIST OF FIGURES

ABBREVIATIONS

BEAS-2B	Bronchial Epithelial Cell Line (BEAS-2B)
cDNA	Complementary DNA
COPD	Chronic Obstructive Pulmonary Disease
CSE	Cigarette Smoke Extract
DEG	Differentially Expressed Gene
FRGs	Ferroptosis-Related Genes
FBS	Fetal Bovine Serum
GEO	Gene Expression Omnibus
GO	Gene Ontology
GSEA	Gene Set Enrichment Analysis
HAEC	Human Airway Epithelial Cells
KEGG	Kyoto Encyclopedia of Genes and Genomes
miRNA	MicroRNA
NCBI	National Center for Biotechnology Information
PBS	Phosphate-Buffered Saline
PCR	Polymerase Chain Reaction
qRT-PCR	Quantitative Real-Time Polymerase Chain Reaction
RNA	Ribonucleic Acid
ROS	Reactive Oxygen Species
RT	Reverse Transcription
SV40	Simian Virus 40
Tm	Melting Temperature

Chapter 1:
INTRODUCTION

1.1 Chronic Obstructive Pulmonary Disease (COPD)

1.1.1 Definition, Epidemiology, and Risk Factors

Chronic Obstructive Pulmonary Disease (COPD) is a chronic and progressive lung disease characterized by persistent airflow limitation in the airways and an increased inflammatory response in the lungs. The disease typically manifests as a combination of emphysema, which results from the destruction of the alveoli, and chronic bronchitis caused by the chronic inflammation of the bronchial tubes. COPD has a high morbidity and mortality rate worldwide, and it poses an economic burden on health systems and society. COPD was the third leading cause of death worldwide in 2019, resulting in approximately 3.23 million deaths annually, which represents 6% of all deaths globally. Based on epidemiological studies, in 2010, there were 384 million COPD cases with an 11.7% global prevalence (Adeloye et al., 2015). According to estimates, 251 million people worldwide were predicted to have COPD in 2019, with a prevalence of 10.1% among those 40 years of age and above. It is estimated that, by 2060, there may be over 5.4 million deaths annually from COPD and similar airway diseases (Agusti et al.,2024). In low- and middle-income nations, where indoor air pollution from biomass fuels and occupational dust exposure are frequent, the prevalence of COPD is highest. Male sex, smoking, body mass index (BMI) < 180.5 kg/m², biomass exposure, and dust or smoke exposure at work were significant risk factors for COPD (Adeloye et al., 2022). The prevalence rate of COPD varies significantly from region to region; higher rates are observed in Southeast Asia and the Western Pacific due to greater exposure to risk factors such as biomass smoke and occupational pollutants (Adeloye et al., 2022)

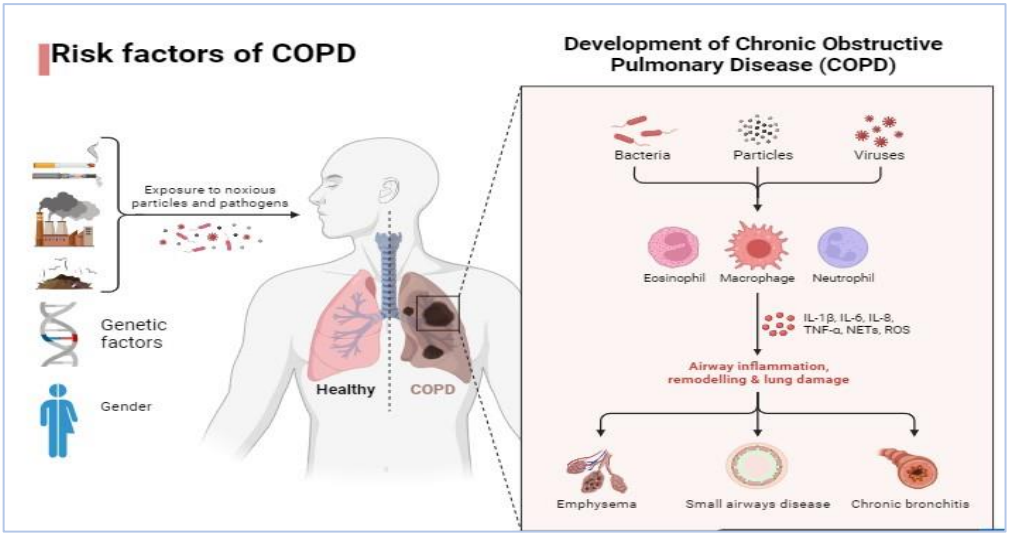

Figure 1.1: Development of COPD and risk factors (Produced and modified from Page, L. 2022, using BioRender. https://app.biorender.com/biorender-templates/figures/all/t-636d1c97be5ee0a7b22ae225-development-of-chronic-obstructive-pulmonary-disease-copd-2)

Risk factors for COPD include genetic factors, gender, developmental and social factors, bronchial hyperreactivity, respiratory infections, air pollution, and smoking (Figure 1). Smoking, especially, is the most significant risk factor, accounting for 85-90% of COPD cases in high-income countries (Soriano et al., 2020). In addition to smoking, other environmental factors also contribute to the risk of COPD. Among these, particularly for women in low-income countries, prolonged exposure to biomass smoke from cooking and heating indoors and occupational exposure to dust, chemicals, and toxic gases brought about by industrialization pose significant risks. Additionally, air pollution in industrial cities with high particulate matter is a considerable risk factor (Manisalidis et al., 2020)

Genetic factors also play a role in COPD susceptibility, with alpha-1 antitrypsin (AAT) deficiency being the most well-known genetic risk factor. AAT deficiency leads to unregulated protease activity in the lungs, resulting in tissue damage and emphysema. (Ferrarotti et al., 2012). Other genetic loci identified through genome-wide association studies (GWAS), such as *CHRNA3/5*, *HHIP*, and *FAM13A*, have been implicated in COPD, highlighting the complex interplay between genetic and environmental factors in disease development (Hardin et al., 2014).

COPD diagnosis is characterized by a gradual decline in lung function measured by the amount of air expelled with difficulty in one second (FEV1). The FVC is a forced vital capacity. A post-bronchodilator FEV1/FVC ratio of less than 0.07 confirms that airflow limitation is permanent. Spirometry is necessary to diagnose COPD (Miller et al., 2005). COPD is often seen alongside comorbidities such as cardiovascular disease, osteoporosis, and lung cancer; this situation increases the overall burden of the disease and complicates its management. The rate of decline increases with continued exposure to risk factors, particularly smoking, and genetic predisposition. (Barnes et.al., 2009).

1.1.2 Cigarette Smoke as a Major Risk Factor for COPD

Cigarette smoking is known to be a significant risk factor in the development of COPD (Wohnhaas et al., 2021). Cigarette smoke contains more than 7,000 chemicals, including tar, nicotine, carbon monoxide, and a variety of oxidants and free radicals that contribute to the pathogenesis of COPD through several mechanisms (US Department of Health and Human Services, [HHS], 2024; Hou et al.,2019). Exposure to cigarette smoke and other pollutants/toxicants leads to the generation of reactive oxygen species by inflammatory and epithelial cells in the lung. As a result, oxidative stress increases in the airways (Barnes, 2020). Cigarette smoke specifically affects small airway epithelial cell populations and triggers the expansion of inflammatory and squamous differentiation-associated basal cells. (Shaykhiev et al., 2014; Crystal, 2010). Cigarette smoke causes chronic inflammation in the airways and lung parenchyma (Figure 2), playing a role in the development of the COPD mechanism (Antunes et al., 2021). It is also known that there is a positive correlation between inflammation and disease severity in COPD patients (Parris et al., 2019). The inhalation of cigarette smoke triggers the recruitment of inflammatory cells, including neutrophils, macrophages, and CD8+ T lymphocytes, to the lungs. These cells release various pro-inflammatory cytokines, chemokines, and proteases, which lead to tissue damage, mucus hypersecretion, and airway remodeling. (Barnes, 2016) Chronic inflammation in COPD is perpetuated by ongoing exposure to cigarette smoke, which maintains the recruitment and activation of inflammatory cells, creating a self-sustaining cycle of inflammation and tissue destruction (Rahman, 2005).

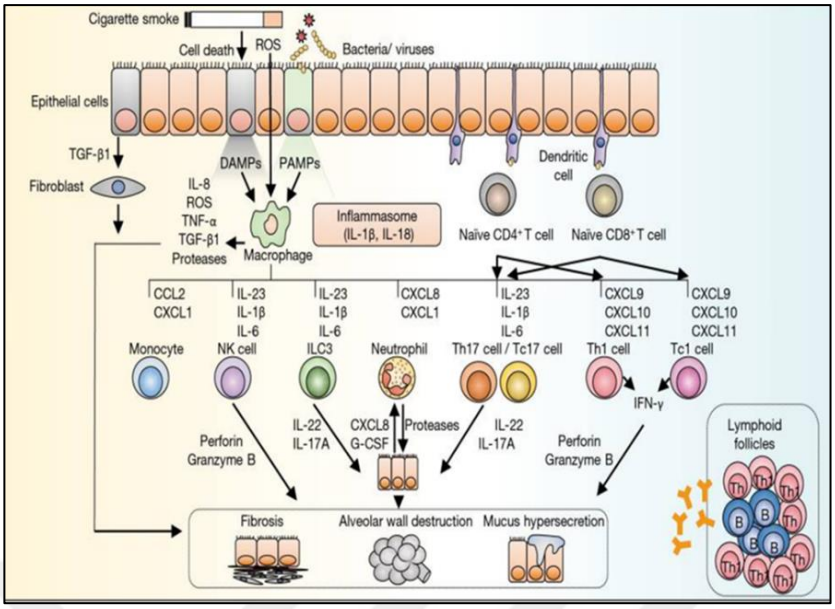

Figure 1.2: Airway inflammation in COPD; Cigarette smoke, irritants such as bacteria and viruses, penetrate the epithelial barrier and activate certain immune cells and inflammatory cytokines. Some inflammatory stimulating molecules, DAMPs, and PAMPs, are phagocytosed by macrophage cells, releasing cytokine stimulators such as IL-8, ROS, TNF-alpha, and TGF-B1 in the environment. Dendritic cells which are responsible for adaptive immunity stimulate naïve CD4 and CD8 T helper cells because of the release of certain chemokines, leading to the destruction of epithelial cells by the perforin granzyme B enzyme in the presence of IFN-y (Mucus hypersecretion). Again, due to the defence mechanisms of NK cells, neutrophils, and monocyte cells, fibrosis occurs because of the death of fibroblasts in the epithelial cells of the airways, leading to damage to the alveolar walls and the development of emphysema (Brightling et.al., 2019).

Cigarette smoke-induced oxidative stress is another critical mechanism in COPD pathogenesis. The oxidants in cigarette smoke directly damage the proteins, lipids, and DNA in the lung cells, leading to cellular dysfunction and death (Antunes et al., 2021). Oxidative stress also exacerbates inflammation by activating key signaling pathways, such as the nuclear factor-kappa B (NF-κB) pathway, which increases the expression of pro-inflammatory genes (Rahman, 2005). In addition, cigarette smoke disrupts the balance between proteases, such as neutrophil elastase and matrix metalloproteinases (MMPs), and their inhibitors, leading to the degradation of the extracellular matrix and the destruction of alveolar walls, which are characteristic of emphysema (Mercer et al., 2006).

The risk of developing COPD increases with both the intensity and duration of smoking, with a dose-response relationship between the number of pack years and the severity of airflow obstruction (Mannino et al. 2006). However, it is important to note that not all smokers develop COPD, indicating that genetic factors and other environmental exposures may also play a role in determining individual susceptibility (Hogg et al. 2017; Halpin et.al., 2021). Moreover, smoking cessation has been shown to slow the decline in lung function in individuals with COPD, highlighting the importance of smoking cessation as the most effective intervention for preventing and managing the disease (Scanlon et al., 2000).

1.1.3 Pathogenesis of COPD

COPD has a complex pathogenesis interplay of genetic predispositions, environmental exposures, airway epithelium's response to them and dysregulated immune responses (Barnes, 2016). The disease is characterized by chronic inflammation, oxidative stress, an imbalance between protease and antiprotease activity in the lungs, and cell death mechanisms, leading to the progressive destruction of lung tissue and persistent airflow limitation (Barnes, 2015; Barnes, 2016). Although various characteristics are involved in its pathology, the pathogenesis of COPD is mainly regulated through several signaling pathways, including oxidative stress and inflammation (Kaur et.al., 2022). The lungs of individuals with COPD are exposed to increased levels of reactive oxygen species (ROS), both from exogenous sources such as cigarette smoke and from endogenous sources such as activated inflammatory cells (Antunes et al., 2021). ROS can directly damage lung cells by oxidizing proteins, lipids, and DNA, leading to cellular dysfunction and death (Antunes et al., 2021). In addition, oxidative stress activates several pro-inflammatory signaling pathways, including the NF-κB pathway, which increases the expression of cytokines, chemokines, and adhesion molecules that perpetuate inflammation and proteolytic enzymes such as matrix metalloproteases, elastases, and other proteases (Stockley, 1999). Many studies have examined the role of matrix metalloproteases (MMPs) in emphysema. The data point to the direct involvement of some MMPs, including MMP-12, in the elastin breakdown, an essential constituent of the alveolar structure (Gharib et al., 2018; Vlahos et al., 2014). Furthermore, research suggests that an imbalance between these enzymes and AAT may

contribute to the pathophysiology of emphysema by causing considerable tissue degradation (Boschetto et al., 2006; Hao et al., 2019). For example, greater neutrophilic inflammation in COPD patients has been linked to raised levels of MMP-9 and neutrophil elastase, indicating the significance of these mediators in the course of the disease (Simpson et al., 2013; Beeh et al., 2003).

On the other hand, airway mucus hypersecretion is another important feature of COPD (Yang et al., 2021). Increased goblet cells and enlarged submucosal glands cause mucus hypersecretion, triggered by exposure to cigarette smoke and other noxious agents (Shen et al., 2018).

Epigenetic changes are also associated with susceptibility to COPD. In a genome-wide association study, DNA methylation profiling was performed in lung tissue from COPD patients, identifying differences in methylation loci related to lung function, asthma diagnosis, nicotine addiction, T-cell development, and other factors (Agustí et.al., 2019).

Immunopathogenically, COPD is associated with the activation of a variety of immune cells, including neutrophils, macrophages, and $CD8^+$ T lymphocytes, which release pro-inflammatory cytokines such as interleukin (IL)-1β, -6, -8, and -13 , tumor necrosis factor-alpha (TNF-α), and interferon-gamma (IFN-γ). These cytokines promote the recruitment and activation of additional immune cells, perpetuating the inflammatory response and leading to tissue damage (Gadgil et.al., 2008; Zheng et al., 2000; Hata et al., 2004, Yamamoto et al., 1997; Chung, 2001; Keatings et al., 1996).

Furthermore, genome wide association studies (GWAS) studies performed in COPD patients have reported genes associated with COPD susceptibility. These genes include SERPINA1 (Rotondo et al., 2021), MUC5AC (Van Buren et al., 2023), Glutamate Cysteine Ligase Catalytic Subunit (GCLC) (Siedlinski et al. 2008), Cytochrome p450 Family 1 Subfamily B Member 1 (CYP1B1) (Pierrou et al., 2007), CHRNA3/5 (Pillai et al, 2009), HHIP (Pillai et al, 2009; Zhou et al., 2012; Wang et al., 2013a), fibroblast growth factor-7 (FGF7) (Brehm et al. 2011), FAM13A (Hancock et al., 2010; Wang et al., 2013b), XRCC5 (Wang et al., 2014), PDE4D (Yoon et al., 2014), FBXO38 (Saferali et al. 2019), PPP1R12B (Diaz-Pena et al., 2020), testis-specific protein Y-encoded-like 4

(TSPYL-4), 5'-nucleotidase domain containing 1 (NT5DC1) (Guo et al., 2012), BICD1 (Kong et al., 2011), RAB4B, EGLN2, MIA and CYP2A6 (Cho et al., 2012). These genes were obtained from studies with large patient and control populations. Changes in these genes are closely related to factors such as decreased lung function in COPD, emphysema, and response to cigarette smoke.

1.1.4. COPD and Airway Epithelium

The airway epithelium is the first line of defence against inhaled pathogens, pollutants, and allergens, playing a crucial role in maintaining respiratory health and it is repeatedly exposed to harmful agents such as cigarette smoke, leading to chronic injury, dysfunction, and remodelling (van der Does et al., 2022).

One of the key functions of the airway epithelium is to provide a physical barrier against inhaled particles and pathogens. This barrier function is maintained by tight junctions such as occludens claudins, and zonula occludens (ZO-1) between epithelial cells (Heijink et al., 2012). In COPD, chronic exposure to cigarette smoke disrupts these tight junctions, leading to increased epithelial permeability and allowing harmful substances to penetrate deeper into the lung tissue (Heijink et al., 2012; Aghapour et al., 2018). This increased permeability is associated with enhanced inflammation, as it facilitates the influx of inflammatory cells and the release of pro-inflammatory cytokines into the airway lumen.

The airway epithelium also plays an active role in the immune response by producing a variety of cytokines and chemokines that recruit and activate immune cells. In COPD, the epithelial cells are a major source of pro-inflammatory mediators, including IL-8, TNF-α, and MCP-1, which contribute to the chronic inflammation observed in the disease (Kayalar et al., 2024). Additionally, the epithelium in COPD patients exhibits features of epithelial-mesenchymal transition (EMT), a process in which epithelial cells acquire mesenchymal characteristics, including increased migratory capacity and resistance to apoptosis. EMT is thought to contribute to airway remodelling and fibrosis in COPD, further exacerbating airway obstruction (Hikichi et al., 2019).

1.2 Cell Death Mechanisms in COPD

COPD involves several cell death mechanisms that contribute to its pathogenesis and progression. Among these, apoptosis, autophagy, pyroptosis, and ferroptosis are particularly significant. Apoptosis is a form of programmed cell death that leads to the systematic dismantling and removal of damaged cells, often exacerbated by oxidative stress and inflammation (Song et al., 2021). Autophagy involves the degradation and recycling of cellular components, which, when dysregulated, can contribute to cell death and tissue damage (Goldklang et.al., 2016). Pyroptosis is an inflammatory form of cell death triggered by the activation of inflammasomes, leading to the release of pro-inflammatory cytokines (Khawas et.al., 2024). Ferroptosis is characterized by iron-dependent lipid peroxidation, resulting in cell membrane damage and cell death (Khawas et.al., 2024). These mechanisms collectively contribute to the structural and functional deterioration observed in COPD, highlighting the complexity of the disease and the potential for targeted therapeutic interventions (Chung et.al., 2008).

It is worth noting that each abovementioned mechanism occurs under specific conditions and involves distinct molecules: Apoptosis in COPD is primarily triggered by oxidative stress, chronic inflammation, and exposure to harmful substances such as cigarette smoke. Key molecules involved in apoptosis include caspases (e.g., caspase-3 and caspase-9), which are responsible for the execution phase of apoptosis, and Bcl-2 family proteins (e.g., Bax and Bcl-2), which regulate mitochondrial membrane permeability and cytochrome c release. Additionally, p53, a tumor suppressor protein, plays a significant role in inducing apoptosis in response to DNA damage and cellular stress (Chung et.al., 2008; Demedts et al., 2006). The imbalance between pro-apoptotic and anti-apoptotic signals in COPD exacerbates lung tissue damage and impairs repair mechanisms, highlighting the importance of targeting apoptotic pathways for potential therapeutic interventions (Demedts et al., 2006; Guo et al., 2022). On the other hand, autophagy in COPD is often dysregulated and contributes to disease progression. This mechanism is typically activated in response to cellular stress, nutrient deprivation, and hypoxia. In COPD, harmful stimuli such as cigarette smoke and oxidative stress can induce autophagy. In this process, autophagy-related genes (ATGs), Beclin-1, LC3 (microtubule-associated protein 1A/1B-light chain 3), and mTOR (mechanistic target of rapamycin) play vital roles. Beclin-1 and LC3 are essential for the formation of

autophagosomes, while mTOR acts as a negative regulator of autophagy. Dysregulation of autophagy in COPD can lead to either excessive degradation of cellular components or insufficient removal of damaged organelles, both of which contribute to cellular dysfunction and lung tissue damage (Li et al., 2021; Zhang et al.,2022). Understanding the role of autophagy in COPD provides insights into potential therapeutic targets for mitigating disease progression (Levra et al.,2023; Lv et., al 2020). Pyroptosis with a significant role in the pathogenesis of COPD is typically triggered by microbial infections and chronic inflammation, leading to the activation of inflammasomes, such as the NLRP3 inflammasome. Upon activation, inflammasomes facilitate the maturation and release of pro-inflammatory cytokines like IL-1β and IL-18. In pyroptosis caspase 1, cleaves gasdermin D (GSDMD) to form membrane pores, resulting in cell swelling, lysis, and the release of inflammatory mediators (Feng et al., 2022). The excessive inflammatory response and cell death associated with pyroptosis contribute to lung tissue damage and the progression of COPD (Liu et al., 2023; Liang et al., 2024). Understanding the molecular mechanisms of pyroptosis in COPD provides insights into potential therapeutic targets to mitigate inflammation and tissue damage. Eventually, ferroptosis is another form of regulated cell death characterized by iron-dependent lipid peroxidation, distinct from apoptosis and necrosis. In the context of COPD, ferroptosis plays a significant role in disease pathogenesis. The mechanism involves the accumulation of iron and ROS, leading to oxidative damage and cell death. In this process, glutathione peroxidase 4 (GPx4), which inhibits lipid peroxidation, and system Xc-, which regulates cystine uptake and glutathione synthesis are the main role players. Dysregulation of these molecules contributes to increased oxidative stress and inflammation in COPD (Meng et al.,2023).

1.2.1 Ferroptosis: Definition and its Mechanism

Ferroptosis is a new form of programmed cell death due to iron-dependent excess accumulation of lipid peroxides and differs from other programmed cell deaths in morphological and biochemical characteristics (Yu et al., 2021). Ferroptosis is distinct from apoptosis, necroptosis, and autophagy, and it is characterized primarily by iron-dependent lipid peroxidation and the catastrophic failure of cell membrane integrity. Regarding morphology, the nuclear fragmentation and chromatin agglutination that occur

during cell apoptosis, do not exist. Additionally, the formation of autophagic vacuoles with double-layered membrane structures is observed during autophagy, and the swelling of organelles and rupture of the plasma membrane during necrosis is not observed during ferroptosis (Dixon et al., 2012). Its primary morphological features include shrinking mitochondria and thickening the mitochondrial membrane, along with a decrease in or absence of mitochondrial cristae and destruction of the outer membrane (Dixon et al., 2012).

Ferroptosis was first described in 2012 as an iron-dependent form of non-apoptotic cell death characterized by the accumulation of lipid peroxides to lethal levels, leading to cell death (Dixon et al., 2012). This process is distinct in that it is driven by the oxidation of PUFAs in cellular membranes, catalysed by iron through the Fenton reaction, which generates highly reactive hydroxyl radicals (Gryzik et al., 2021) Central to the regulation of ferroptosis is the glutathione peroxidase 4 (GPX4) enzyme, which reduces lipid hydroperoxides to non-toxic lipid alcohols, thus protecting cells from oxidative damage (Yang et al., 2016b). The inhibition of GPX4, either through genetic manipulation or chemical inhibitors like RSL3, leads to an overwhelming build-up of lipid peroxides, precipitating ferroptosis (Imai et al., 2017). Another critical regulator is the cystine/glutamate antiporter system Xc-, which imports cystine into cells for the synthesis of glutathione (GSH), the cofactor required for GPX4 activity (Kwon et al., 2020). Disruption of this system, as seen with the ferroptosis inducer elastin, depletes intracellular GSH levels, further sensitizing cells to ferroptosis (Yang et al., 2016b).

Recent advances have expanded our understanding of ferroptosis, revealing additional layers of complexity. For example, the enzyme ACSL4 (acyl-CoA synthetase long-chain family member 4) has been identified as a key modulator of ferroptosis by facilitating the incorporation of PUFAs into phospholipids, making them substrates for peroxidation (Moerke et al., 2019). Moreover, emerging evidence suggests that the mitochondria may play a dual role in ferroptosis, both contributing to and protecting against lipid peroxidation, depending on the cellular context (Tang et al., 2019). This expanding knowledge underscores the intricate regulatory network governing ferroptosis and highlights its potential as a therapeutic target in diseases characterized by oxidative stress and lipid peroxidation, such as COPD (Liao, 2022).

Ferroptosis Inducers and Suppressors

The regulation of ferroptosis is governed by a delicate balance between inducers and suppressors, which determine cell fate under conditions of oxidative stress. Among the most well-characterized inducers of ferroptosis are small molecules such as erastin, which inhibits the system Xc- antiporter, and RSL3, which directly inhibits GPX4 (Yang et al., 2016a). These compounds have been instrumental in dissecting the molecular pathways leading to ferroptosis and have provided valuable tools for investigating the role of ferroptosis in various diseases, including COPD (Li et al., 2020). Beyond these chemical inducers, endogenous factors such as iron overload and increased ROS production can also trigger ferroptosis. Iron plays a dual role as both a catalyst for lipid peroxidation and as a regulator of ferroptosis through its impact on the cellular redox state. Conditions that lead to increased intracellular iron, such as dysregulated ferritinophagy or iron supplementation, can enhance susceptibility to ferroptosis (Yoshida et al., 2019; Bartos et al., 2023).

On the other side of the regulatory spectrum are ferroptosis suppressors, which include molecules that either scavenge ROS or inhibit lipid peroxidation. Ferrostatin-1 and liproxstatin-1 are synthetic inhibitors that have been shown to prevent ferroptosis by blocking the peroxidation of lipids, thereby preserving membrane integrity 8Zeng et al., 2023). Additionally, the role of selenium as a cofactor for GPX4 underscores the importance of micronutrients in modulating ferroptosis susceptibility (Liao, 2022). The transcription factor Nrf2 (nuclear factor erythroid 2–related factor 2) also plays a protective role by upregulating the expression of genes involved in antioxidant defense, including GPX4 and ferritin, thereby reducing the risk of ferroptosis under conditions of oxidative stress (Liu et al., 2022). The intricate interplay between these inducers and suppressors reflects the complex regulatory mechanisms that control ferroptosis and highlights potential therapeutic targets for modulating this form of cell death in COPD and other diseases (Dos Santos et al., 2023).

<u>Ferroptosis is driven by two main pathways:</u>

1-Cystine/Glutamate Reverse Transport System and Glutathione Peroxidase 4 (Transporter-dependent) Pathway

The cell membrane contains the cystine/glutamate reverse transporter (system Xc-), which is made up of the disulfide-bonded SLC3A2 and SLC7A11 (Dixon et al., 2014). Glutamic acid (Glu) is transported outside by System Xc in a 1:1 ratio to cystine inside. Once within the cell, cysteine is reduced from cysteine and is one of the building blocks needed to make GSH and contributes to Glutathione metabolism. Glutathione peroxidase 4 (GPX4) needs GSH as a substrate to break down Lipid Peroxides (LPOs) which are oxidation products of phospholipids and polyunsaturated fatty acids (PUFAs) (Meng, et.al.,2023). The only anti-membrane peroxidase that is known to decrease lipoxygenases (LOXs) and stop overactivation is GPX4. Additionally, it can effectively prevent LPO-induced damage to cell membranes and eliminate LPO that is created by iron accumulation (Stoyanovsky et al., 2019) (Figure 3).

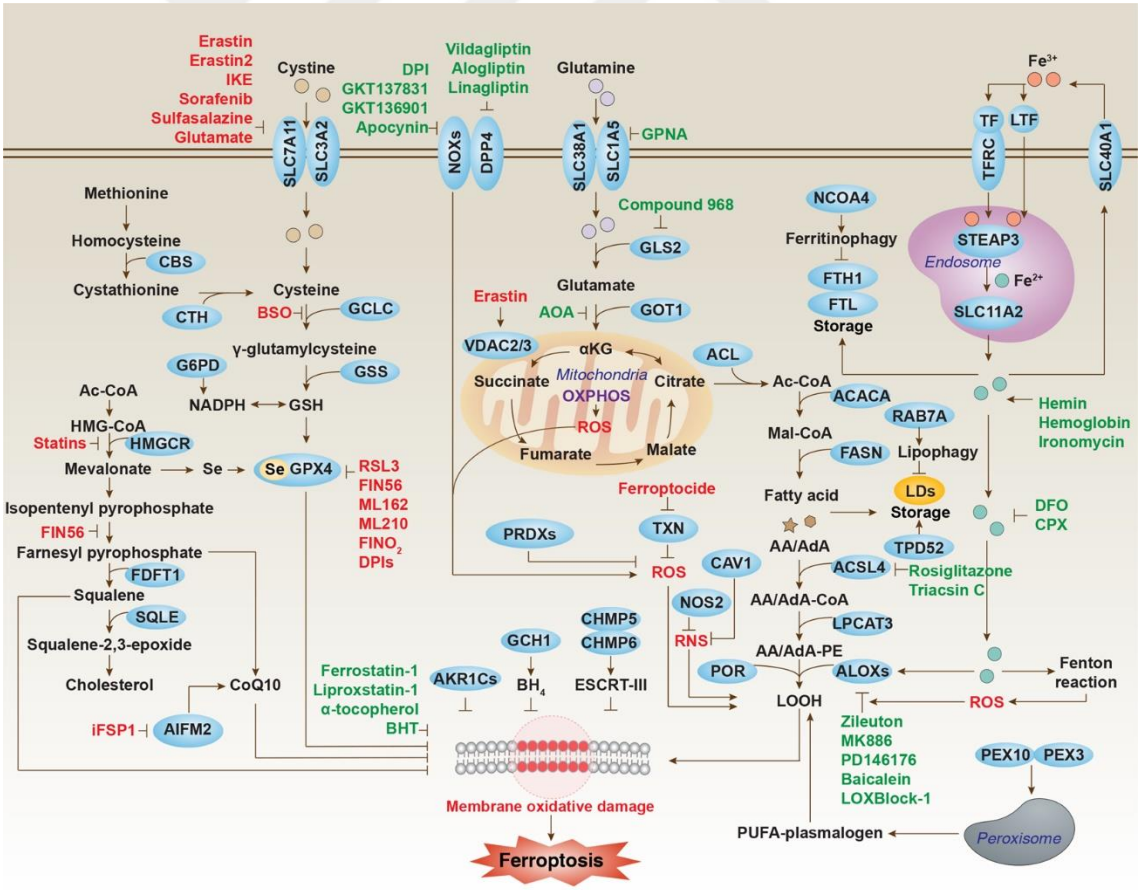

Figure 1.3: Two main mechanisms can lead to ferroptosis: the intrinsic or enzyme-regulated pathway (e.g., suppression of GPX4) and the extrinsic or transporter-dependent

pathway (e.g., decreased cysteine or glutamine uptake and increased iron uptake) (Tang et al., 2021).

2- Lipid Metabolism (Enzyme-regulated) Pathway

Lipid peroxides are the leading trigger factor of ferroptosis. Excessive accumulation of LPO will cause plasma membrane damage and eventually lead to cell ferroptosis. Polyunsaturated fatty acids (PUFAs) are prone to oxidation because they are double-bonded fatty acids and, in the presence of reactive oxygen species, they turn into lipid peroxides, causing the cell membrane to break down, resulting in ferroptosis (D'Herde et al., 2017). With the help of two enzymes, long-chain acyl-CoA synthetase family member 4 (ACSL4) and lysophosphatidylcholine acyltransferase 3 (LPCAT3) (Dixon et al., 2015), multiple unsaturated fatty acids (PUFAs) in cell membranes esterify to form PUFA-Pes. PUFA-Pes can promote enzymatic reactions mediated by lipid oxides to form lipid alcohols, and lipid oxides can promote the peroxidation of PUFAs (Yang et al., 2016b) and the inhibition of GPX4, which triggers ferroptosis.

The significant role of iron in this process makes ferroptosis uniquely sensitive to disruptions in iron metabolism and redox homeostasis, both of which are prevalent in the pathophysiology of COPD. The identification of ferroptosis as a key mechanism in COPD offers new insights into how chronic oxidative stress and iron dysregulation contribute to the progressive lung damage seen in this disease (Conrad & Costa da Silva, 2019; Imai et al., 2017).

1.2.2. Cigarette Smoke and Ferroptosis

Cigarette smoke is the primary etiological factor in the development of COPD and is a potent inducer of oxidative stress in the lungs. The components of cigarette smoke, including reactive aldehydes, free radicals, and heavy metals, contribute to the overwhelming oxidative burden placed on lung tissue (Hikichi et al., 2019). This oxidative stress depletes cellular antioxidants such as GSH, disrupts iron homeostasis, and leads to the accumulation of lipid peroxides, all of which are key triggers of ferroptosis (Wu et al., 2023). The connection between cigarette smoke and ferroptosis has been substantiated by studies showing that exposure to cigarette smoke extract induces

ferroptosis in lung epithelial cells, as evidenced by increased lipid peroxidation, iron accumulation, and decreased GPX4 activity (Liu et al., 2022).

Moreover, cigarette smoke has been shown to interfere with cellular mechanisms that normally protect against ferroptosis. For instance, it impairs the function of the cystine/glutamate antiporter system Xc-, leading to reduced cystine uptake and GSH synthesis, thereby sensitizing cells to ferroptotic death (Yoshida et al., 2019). The relationship between cigarette smoke-induced oxidative stress and ferroptosis is further complicated by the fact that cigarette smoke also induces inflammation, which can enhance iron uptake and ROS production through the activation of inflammatory signaling pathways (Wang et al., 2023). This creates a vicious cycle where inflammation and oxidative stress mutually reinforce each other, driving the progression of COPD through mechanisms that include ferroptosis.

Given the significant role of cigarette smoke in inducing ferroptosis, therapeutic strategies that target this pathway hold promise for mitigating lung damage in smokers and individuals with COPD. Such strategies might include the use of ferroptosis inhibitors, antioxidants, or agents that restore iron homeostasis, all aimed at breaking the cycle of oxidative stress and cell death that characterizes COPD (Liu et al., 2022). Future research should continue to explore the molecular details of how cigarette smoke induces ferroptosis and identify potential intervention points for therapeutic development.

1.2.3. COPD and Ferroptosis

The relevance of ferroptosis to COPD has become increasingly apparent as more studies reveal the connection between oxidative stress, iron metabolism, and lung tissue destruction (Yoshida et al. 2019; Günes Günsel et al., 2022). COPD is characterized by chronic oxidative stress, which not only drives inflammation but also sets the stage for ferroptotic cell death (Mizumura et al., 2021). The lung tissue in COPD patients shows signs of disrupted iron homeostasis, with increased levels of free iron and decreased expression of iron-binding proteins such as ferritin (Sato et al., 2020). This iron dysregulation is coupled with reduced antioxidant defenses, particularly in the form of

diminished GPX4 activity, which further predisposes cells to ferroptosis (Jeridi et al., 2023).

The levels of iron, serum ferritin, and non-heme iron in lung cells rose when human bronchial epithelial cells were exposed to CS (Ghio et al. 2008). The cytoplasm contained endoplasmic reticulum stress and mitochondrial malfunction, after which bronchial epithelial cells underwent ferroptosis (Park et al., 2019). Free iron builds up, as a result of nuclear receptor coactivator 4 (NCOA4)-mediated ferritin autophagy that is triggered by CS. The pathophysiology of COPD involves a number of factors, including decreased GPX4 activity, low GSH, and other factors that result in human bronchial epithelial cell peroxidation and ferroptosis (Dowdle et al.,2014; Yoshida et al., 2019). The primary reasons of iron homeostasis imbalance, which ultimately results in ferroptosis, are modifications in transferrin and ferritin expression (Wang et al., 2019). Ferrostatin-1 and deferoxamine, an iron chelator, can help endothelial cells reduce their levels of GSH and NADPH.

The role of ferroptosis in COPD is also supported by findings from animal models, where the inhibition of ferroptosis leads to reduced lung injury and inflammation in response to oxidative stress (Meng et al., 2023). These studies suggest that targeting ferroptosis could be a viable strategy for preventing or mitigating the tissue damage seen in COPD. Furthermore, the link between ferroptosis and COPD extends to the immune response, with evidence that ferroptotic cell death in the lung can exacerbate inflammation by releasing damage-associated molecular patterns (DAMPs), which activate surrounding immune cells and perpetuate the inflammatory cycle (Sun et al., 2020; Rajabi et al., 2022). This connection between ferroptosis and the immune response underscores the potential for ferroptosis inhibitors to not only protect lung cells from death but also to modulate the inflammatory environment in COPD (Yoshida et al., 2019).

1.3 Bioinformatic Approach in Biomedical Research

1.3.1 Introduction to Bioinformatic Tools and Databases

Bioinformatics is an interdisciplinary field that leverages computational tools and databases to analyze and interpret biological data (Pathak et al., 2022). In the era of high-

throughput sequencing technologies, bioinformatics has become indispensable for managing and making sense of the vast amounts of data generated in biomedical research. Bioinformatic tools facilitate tasks such as sequence alignment, structural prediction, gene expression analysis, and functional annotation, among others. Key bioinformatics databases include the Kyoto Encyclopedia of Genes and Genomes (KEGG) for pathway analysis, the Gene Expression Omnibus (GEO) for gene expression data, and STRING for protein-protein interaction networks (Kanehisa et al., 2023; Szklarczyk et al., 2023).

These tools and databases are essential for integrating and interpreting complex datasets to generate hypotheses about gene function and disease mechanisms. For instance, in the study of COPD, bioinformatics can be used to identify DEGs, predict their roles in biological pathways, and explore their interactions with other proteins and genes. Such analyses can lead to the identification of novel biomarkers or therapeutic targets that might be overlooked using traditional experimental approaches (Kanehisa et.al., 2000; Shannon et al., 2003). In COPD research, bioinformatics plays a crucial role in identifying the genetic and molecular factors that contribute to the disease. By analyzing large datasets from patient samples, researchers can pinpoint specific genes and pathways that are altered in COPD, offering potential targets for drug development. (Zhang et al., 2022; Zhong et al., 2022). For example, through the integration of multi-omics data, researchers can uncover the molecular signatures that distinguish diseased tissues from healthy ones, providing insights into the pathogenesis and progression of diseases (Subramanian et al., 2020).

1.3.2 Identification of DEGs with Transcriptomic Data

The identification of DEGs using transcriptomic data is a cornerstone of modern biomedical research. Transcriptomics, which involves the comprehensive analysis of RNA transcripts in a given sample, provides a snapshot of gene expression at a specific time and under specific conditions. RNA-seq is the most widely used technique for transcriptomic analysis, offering high sensitivity and the ability to detect both known and novel transcripts (Wang et al., 2009; Trapnell et al., 2012).

In the context of COPD, transcriptomic data can be used to compare gene expression profiles between healthy individuals and COPD patients, or between smokers and non-

smokers. This comparison allows for the identification of DEGs that are associated with the disease or its risk factors, such as cigarette smoke exposure. Once identified, DEGs can be further analyzed to understand their roles in disease-related pathways, such as those involved in inflammation, oxidative stress, and cell death. Moreover, bioinformatic tools like DESeq2 and R are commonly employed to statistically validate the significance of DEGs, ensuring that the results are robust and reliable (Love et al., 2014).

1.4 Hypothesis

We hypothesized that the ferroptosis genes contribute to the pathogenesis of cigarette smoke-induced COPD by triggering the ferroptosis pathway in human bronchial epithelial cells.

1.4.1 Aim and our objectives:

The primary aim of my studies was to elucidate the role of ferroptosis-related genes in the pathogenesis of cigarette smoke-induced COPD, and to validate this in both BEAS-2B cell lines and primary human airway epithelial cells (HAECs).

The main objectives of my studies were as follows:

1. To find upregulated and downregulated genes from 4 different datasets GSE87098, GSE151052, GSE76925, and GSE10006

2. To determine hub genes with common changes after the intersections of 4 different dataset

2. To perform functional enrichment analysis with the identified hub genes.

3. To validate the expressions of the hub genes in BEAS-2B cells and HAECs, following incubation with CSE.

Chapter 2: **METHODOLOGY**

2.1 Materials: Bioinformatic Tools

This study's methodological approach was based on the integration of bioinformatic tools and databases that enable rigorous analysis of gene expression data, especially when considering the relationship between COPD and cigarette smoke. The selection of each tool has been predicated on its ability to offer profound insights into the molecular foundations of disease mechanisms, including ferroptosis's function in the pathophysiology of COPD. The bioinformatics tools used in this research are explained below, emphasizing their applicability and usefulness.

2.1.1 National Center for Biotechnology Information (NCBI)

National Center for Biotechnology Information (NCBI), as one of the cornerstones of biomedical research, is a unique big data resource for genomic and transcriptomic analyses. The benefit of NCBI is not only to obtain data but also to provide data for advanced tools like BLAST for sequence alignment and access to annotated sequences through GenBank. In this study, the application of NCBI resources was vital for the identification and characterization of genes associated with COPD in both smokers and non-smokers. Additionally, the genes we filtered from this data provided a solid platform for literature review in comprehensive databases within NCBI, such as PubMed and the Protein Data Bank (PDB), and for contextualizing findings within broader scientific discussions (Sayers et al., 2021).

2.1.2 Gene Expression Omnibus (GEO)

The GEO database maintained by NCBI is a valuable resource for accessing high-throughput gene expression datasets. In this study, GEO was used as a source to obtain microarray and RNA-seq datasets (for example, GSE87098, GSE151052, GSE76925, and GSE10006) that were important for identifying differentially expressed genes (DEGs) associated with COPD and smoking. The datasets have been meticulously compiled and re-analyzed to ensure consistency and relevance with the objectives of the study. The use of GEO allows for the comparison of gene expression profiles across

multiple studies, thereby contributing to the reliability of the identified DEGs and their subsequent functional interpretation (Barrett et al., 2013).

2.1.3 R Studio (Version 4.2.1)

R Studio is used as the primary environment for statistical computing and bioinformatics analysis. This study extensively utilized R packages such as DESeq2 and limma to determine statistically significant gene expression changes between COPD patients and the control group, focusing on both smoking and non-smoking groups. Additionally, a cluster profile package is used for gene set enrichment analysis, which facilitates the identification of overrepresented biological processes and pathways. The ggplot2 package (Love et al., 2014, version 4.2.1, September/12/2022) is used for data visualization and enables the clear and effective presentation of complex bioinformatics results. The flexibility and power of R Studio in processing large-scale genomic data make it indispensable for this research (Yu et al., 2012).

2.1.4 Gene Set Enrichment Analysis (GSEA)

In this study, GSEA was a valuable tool to determine the enrichment of predefined gene sets in gene expression profiles associated with COPD. Unlike traditional single-gene approaches, GSEA provides insights into systemic changes in biological processes by considering the collective behavior of genes within pathways, particularly those related to cell death pathways such as oxidative stress and ferroptosis. In this case, applying GSEA allows for the identification of the main pathways that drive the pathogenesis of COPD and provides a more comprehensive understanding of the disease mechanism. (Subramanian et al., 2005)

2.1.5 FerrDb

FerrDb is the first database specifically designed for genes related to ferroptosis, classifying these genes as drivers, suppressors, and markers (http://www.zhounan.org/ferrdb/current/). This tool is necessary to validate the role of ferroptosis in COPD by comparing the identified DEGs with known regulators of

ferroptosis. The compiled content of the database, enriched with information from recent publications, ensures that the genes under study are relevant and up to date; this facilitates the identification of new therapeutic targets and biomarkers in the context of lung damage caused by cigarette smoke (Bao et.al., 2020).

2.1.6 METASCAPE

METASCAPE is utilized for comprehensive gene annotation and enrichment analysis, integrating data from authoritative sources such as KEGG, and GO. This tool allows for the functional analysis of DEGs identified in the study, providing insights into the biological processes and pathways most affected by COPD. The platform's ability to generate protein-protein interaction (PPI) networks and perform multi-gene analysis enhances the depth of the analysis, allowing for the identification of key regulatory networks involved in disease progression (Zhou et al., 2019).

2.1.7 STRING (Search Tool for the Retrieval of Interacting Genes/Proteins)

STRING is a critical tool for constructing protein-protein interaction networks that reveal the complex interactions between proteins encoded by DEGs. This study leveraged STRING to map the interactions of ferroptosis-related proteins, shedding light on their roles in COPD. The PPI networks generated provide a visual representation of the molecular interplay within cells, identifying potential hubs that could be targeted for therapeutic intervention. STRING's integration with other databases such as KEGG further enhances the pathway analysis, linking proteins to specific biological functions and disease pathways (Szklarczyk et al., 2021).

2.1.8 miRmap

miRmap is a comprehensive tool used to predict miRNA targets and assess their potential regulatory impact on gene expression. In this study, miRmap was employed to explore the post-transcriptional regulation of ferroptosis-related genes by miRNAs. This analysis is crucial for understanding the fine-tuning of gene expression in COPD, where miRNAs may function as critical modulators of cell death pathways. The predictions

generated by miRmap are validated through integration with experimental data, ensuring their relevance to the disease context (Vejnar et al., 2012).

2.1.9 Venn Diagram Tool

The Venn diagram tool from Ghent University's Bioinformatics & Evolutionary Genomics group is utilized to visualize the overlap of DEGs across different datasets. This visualization is crucial for identifying common hub genes that are consistently dysregulated in COPD across multiple studies. The identification of these common genes strengthens the robustness of the findings, ensuring that the conclusions drawn are based on reproducible and reliable data (Chen et.al., 2011).

2.1.10 KEGG Pathway: Kyoto Encyclopaedia of Genes and Genomes

KEGG is employed for the pathway analysis of identified DEGs, mapping them to specific biological processes and disease pathways. The use of KEGG allows for the contextualization of gene expression changes within well-defined metabolic and signaling pathways, particularly those related to ferroptosis and oxidative stress. This pathway-centric approach facilitates the identification of potential therapeutic targets and enhances the understanding of the molecular mechanisms underlying COPD (Kanehisa et al., 2021).

Each of these bioinformatic tools contributes a unique capability to the study, collectively enabling a comprehensive analysis of gene expression data. By integrating these tools, the study aimed to uncover the molecular mechanisms by which cigarette smoke induces COPD, with a particular focus on the role of ferroptosis in disease progression. This methodological approach not only ensures the thorough exploration of the data but also enhances the potential for discovering novel therapeutic targets.

2.2 Data Collection

Gene microarray datasets associated with COPD and smoking in airway (bronchial) epithelial cells and lung tissues were downloaded from the National Center for Biotechnology Gene Expression Omnibus, GEO, (https://www.ncbi.nlm.nih.gov/geo/) (Table 1). The datasets GSE76925 and GSE151052 contain gene expression profiles of lung tissue samples that have originated from healthy control donors and COPD patients (Morrow et al., 2017; Hobbs et al., 2023; Xu et al., 2022). The dataset GSE87098 contains a gene expression profile of airway epithelial cells on a chip that has been challenged with cigarette smoke for 24 h and originated from healthy control donors and COPD patients (Benam et al., 2016). The dataset GSE10006 contains gene expression profiles of airway epithelial cells that have originated from non-smokers and smokers (Carolan et al., 2008).

Table 2.1: Details of GEO COPD Data

Accession	Platform	Sample	COPD	Control	Smoker	Non-smoker
GSE76925	GPL10558	Airway epithelial	111	40		
GSE87098	GPL16686	Airway epithelial	8	7		
GSE151052	GPL17556	Airway epithelial	77	40		
GSE10006	GPL570	Airway epithelial			14	13

These datasets encompass a range of experimental conditions, including untreated controls and samples exposed to CSE, thus providing a broad spectrum of gene expression profiles pertinent to the studies of COPD. The selection of these datasets was determined by a comprehensive review of the literature, ensuring that they were representative of the current state of research in COPD and ferroptosis.

Raw data from these datasets were obtained in their CSV file formats. These files were converted to xls files and manipulated. We wrote special codes to pre-processing of these raw data, which involved several critical steps, including dropping non-gene ID correction, and duplicate IDs.

2.3 Identification of DEGs

Following the data collection, the data pre-processing was conducted using GEO2R which is an interactive web tool designed in the limma package of R program. It involved the comparison and analysis of two different groups of samples (i.e., control and COPD) under the same experimental conditions at the significance level of $P < 0.05$, and therefore could assist in the identification of DEGs in the dataset. Multiple probe-containing genes were eliminated from the dataset. A freely accessible web program called GEO2R compares and analyses of two different sample groups under identical experimental settings. The obtained results were downloaded and the genes with adjusted P-value < 0.05 and logFC value > 1 on the Benjamini-Hochberg (BH) were considered as upregulated, whereas genes with same Adj.P value and logFC < 1 on the BH were considered as downregulated genes. Using this free online tool, a volcano plot was created to visually identify up-regulated and down-regulated genes. The UMAP dimensionality reduction graph is used to visualize the relationship between samples and how the samples are discriminated well each other. And the other graphs, expression density and box plots demonstrated that the chosen samples' expression value distribution was cross-compatible, normalized, and appropriate for comparing differences.
(https://www.ncbi.nlm.nih.gov/geo/geo2r/, [accessed on.20.11.2022]).

The DEG results obtained from the COPD and control datasets analyzed in the GEO2R program were intersected with the GSE 1006 dataset, which consisted of smokers and non-smokers, to establish the relationship between COPD and smoking. Venn diagrams were used to visualize the number of overlapped and intersected genes.
(https://bioinformatics.psb.ugent.be/webtools/Venn/ [accessed on.23.11.2022]).

2.4 Identification of Differentially Expressed Ferroptosis Genes (FRGs)

The identification of differentially expressed ferroptosis-related genes (FRGs) is a critical component in understanding the molecular mechanisms by which ferroptosis contributes to the pathogenesis of COPD, particularly in the context of cigarette smoke-induced inflammation. This process involves a multi-step bioinformatics pipeline designed to isolate genes whose expression levels significantly differ between diseased and control conditions, with a specific focus on those implicated in ferroptosis.

Once the DEGs are identified, they are cross-referenced with the FerrDb database (http://www.zhounan.org/ferrdb/current/, [accessed on 29.11.2022]) a specialized resource for ferroptosis-related genes, to isolate those that are directly involved in ferroptosis. This step involves matching gene identifiers and annotations from the DEGs list with those cataloged in FerrDb, focusing on genes categorized as drivers, suppressors, or markers of ferroptosis. The integration of these two datasets—DEGs from COPD studies and the curated list of FRGs—yields a refined set of ferroptosis-related DEGs that are likely to play pivotal roles in the disease process. The Venn diagram tool used to visualize the FRGs for COPD smoker's vs COPD non- smokers and Ferroptosis Genes.

2.5 Gene Ontology (GO) Terms and Kyoto Encyclopedia of Genes and Genomes (KEGG) Pathways Analyses

Gene Ontology (GO) and Kyoto Encyclopedia of Genes and Genomes (KEGG) pathway analyses are indispensable tools in bioinformatics for elucidating the biological significance of differentially expressed genes (DEGs), particularly in complex diseases like COPD. These tools provide a structured framework for understanding how changes in gene expression translate into alterations in cellular functions, biological processes, and disease pathways.

GO analysis involves categorizing the identified FRGs into three main domains: biological processes (BP), molecular functions (MF), and cellular components (CC). This classification allows for a detailed examination of how these genes contribute to specific biological functions relevant to COPD. For instance, in the context of ferroptosis, GO terms related to iron ion binding, lipid peroxidation, and regulation of oxidative stress are expected to be significantly enriched. This enrichment indicates that the DEGs are likely playing crucial roles in these processes, which are central to both ferroptosis, and the oxidative damage observed in COPD.

The GO analysis is performed using specialized software tools such as DAVID (Database for Annotation, Visualization, and Integrated Discovery) or Metascape, which provide statistical assessments of the enrichment of specific GO terms among the identified FRGs. The results are typically presented in the form of enrichment scores or p-values, with lower p-values indicating stronger associations between the genes and the

GO terms. These results not only help in confirming the relevance of the identified genes but also in generating new hypotheses about their roles in disease pathogenesis.

KEGG pathway analysis complements GO analysis by mapping the identified FRGs onto specific metabolic and signaling pathways. This analysis helps to contextualize the role of these genes within broader biological systems, providing insights into how they interact with other molecules and pathways to drive disease processes. In the case of COPD, pathways related to ferroptosis, glutathione metabolism, and inflammation are of particular interest. For example, the KEGG pathway analysis might reveal that several FRGs are involved in the regulation of glutathione peroxidase 4 (GPX4) activity, a key enzyme that protects cells from ferroptosis by reducing lipid hydroperoxides.

The integration of GO and KEGG pathway analyses provides a comprehensive view of the functional landscape of the identified FRGs. This dual approach not only highlights the individual roles of these genes but also reveals how they might work together to contribute to the pathogenesis of COPD. The insights gained from these analyses are critical for identifying potential therapeutic targets, as they highlight key nodes within the disease network that could be modulated to alleviate disease symptoms or halt disease progression.

2.6 Screening Ferroptosis-Related Differentially Expressed Genes

The STRING database (Search Tool for the Retrieval of Interacting Genes/Proteins) and Cytoscape software are pivotal tools for exploring and visualizing the complex networks of protein-protein interactions (PPIs) that underpin biological processes in health and disease. In the context of COPD and ferroptosis, these tools enable researchers to construct and analyze interaction networks for the differentially expressed ferroptosis-related genes (FRGs), offering deeper insights into their functional interrelationships and their potential roles in disease pathogenesis.

The STRING database is a comprehensive resource that integrates known and predicted protein-protein interactions from a wide array of organisms. These interactions

are derived from various sources, including experimental data, computational prediction methods, and text mining of the scientific literature. For this study, the identified FRGs are input into STRING to generate a PPI network, which visually represents how these proteins interact with each other and with other key molecules involved in ferroptosis and COPD.

STRING assigns confidence scores to each interaction based on the strength of the supporting evidence, allowing researchers to prioritize interactions that are most likely to be biologically relevant. High-confidence interactions are typically used to build the core of the network, while lower-confidence interactions may be included for exploratory purposes. The resulting network can reveal key hub proteins—those with the most connections—which are often critical regulators of biological processes. In the context of ferroptosis and COPD, these hub proteins may represent potential therapeutic targets or biomarkers for disease progression.

Cytoscape is a powerful open-source software platform that complements STRING by providing advanced tools for the visualization and analysis of complex networks. Once the PPI network is generated in STRING, it can be imported into Cytoscape for further refinement and analysis. Cytoscape offers a wide range of functionalities, including the ability to customize network layouts, annotate nodes and edges with additional biological information, and perform network clustering to identify modules of highly interconnected proteins.

One of the key advantages of using Cytoscape is its ability to integrate multiple types of data, such as gene expression profiles, GO annotations, and KEGG pathway data, into a single network visualization. This integration allows for a multi-dimensional analysis of the FRGs, providing a more comprehensive understanding of how these genes contribute to COPD pathogenesis. For example, by overlaying gene expression data onto the PPI network, researchers can identify which interactions are likely to be most relevant under specific experimental conditions, such as exposure to cigarette smoke.

Moreover, Cytoscape’s plugin architecture allows for the use of various specialized tools that can enhance the analysis. For instance, the MCODE plugin can be used to

identify highly interconnected clusters within the network, which may represent functional modules or complexes that are particularly important in ferroptosis regulation. Other plugins, such as CytoHubba, can be used to identify essential nodes within the network that could serve as key targets for therapeutic intervention.

2.7 Validation of Seven Hub Genes with Experimental Methods

Validation of bioinformatic findings through experimental methodologies is essential for bridging the gap between in silico predictions and biological reality. In the context of this study, the experimental validation focused on confirming the expression and functional relevance of seven FRGs implicated in cigarette smoke-induced COPD. These genes were selected based on their differential expression and potential involvement in ferroptosis pathways as identified through rigorous bioinformatic analyses. The experimental strategies employed include precise molecular biology techniques such as primer design, gradient PCR, cell culture experiments using both immortalized and primary human airway epithelial cells, cigarette smoke exposure, RNA isolation, cDNA synthesis, and quantitative real-time polymerase chain reaction (qRT-PCR).

2.7.1 Primer Design of Seven Hub Genes

The design of primers for the seven FRGs was executed with meticulous attention to the specificity and efficiency of the subsequent PCR amplifications. Given the critical role that primer design plays in the accuracy of PCR, we employed Primer-BLAST, a sophisticated tool from the NCBI to design primers that would anneal specifically to the target regions of each gene. The selection criteria for the primers included a balance between GC content and melting temperature ®, typically aiming for a GC content of 50-60% and a temperature within the range of 58-62°C. This approach minimizes the risk of secondary structures such as hairpins or primer-dimers that could compromise the PCR's efficiency and specificity.

In addition, the designed primers were subjected to in silico validation using tools like OligoAnalyzer to ensure the absence of significant secondary structures and to predict their binding efficiency under experimental conditions. The specificity of each

primer pair was further confirmed by aligning the sequences against the human genome to avoid off-target amplification. These primers were synthesized by a reputable commercial provider, and their performance was initially assessed through a series of test PCRs before proceeding to experimental validation.

2.7.2 Culture of Human Bronchial Epithelial Cells (BEAS-2B)

Human bronchial epithelial cells (BEAS-2B) were chosen as the primary in vitro model to investigate the cellular and molecular mechanisms underlying COPD, particularly in response to cigarette smoke exposure (Reddel et al., 1988; Veljkovic et al., 2011; Li et al., 2024). Bronchial epithelial cells are becoming a relevant model for respiratory studies by preserving many functional properties, including barrier function and mucus secretion ability. To avoid having the effects of cell age on the outcomes, experiments were carried out between passage numbers of P27 and P34.

Cells were cultured in RPMI-1640 (Cat number: R8758, Sigma,USA) medium supplemented with 10% fetal bovine serum (FBS, Cat number: S160H-500, Biowest, France), 1% penicillin and streptomycin (100 U/mL, Cat number: L0022-100X, Biowest, France). Cultural conditions were carefully maintained at 37°C in a humidified incubator with 5% CO_2. When the cells reached 70-80% confluence (Figure 2.1), they were detached from the bottom of the plate by using trypsin (Cat number: 325-045-EL, Wisent, Canada) enzyme and then re-seeded into the 75 cm2 culture flasks (Cat number: 83.3911, Sarsted, Germany) in the necessary amounts. Culture medium was changed every two days. For our experimental design, the cells were treated with CSE at different concentrations, ranging from 2.5% to 7.5%. This concentration was chosen based on previous studies that made these levels physiologically significant for modelling the oxidative and inflammatory responses observed in the lungs of smokers (Li et al., 2024, Chen et al., 2024).

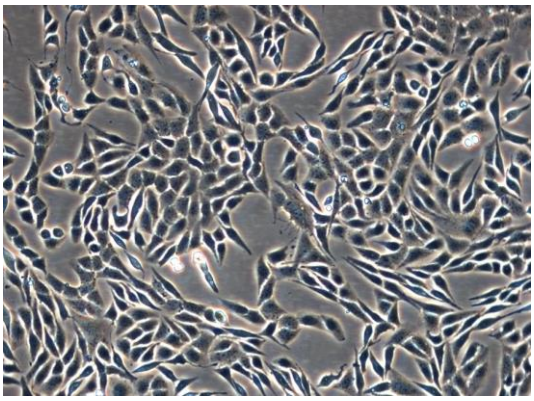

Figure 2.1: Light microscopy image of BEAS-2B cell cultures in 70% confluence.

BEAS-2B cells were seeded in 6-well plates (n=3 biological replicates for each concentration) at a density of $2x10^5$ cell/well and kept for 24 hours to reach %70-80 confluency. Cells were washed with 1X DPBS (Biowest, L0615-500), and then the medium was changed to serum free medium (SF) containing %99 RPMI-1640 (Sigma Life Science) medium and 1% penicillin/ streptomycin (Biowest, L0022-100). Cells were incubated for another 24 hours at 37°C under 5% CO2 condition. SF medium was removed, and cells were washed with 1X dPBS (Biowest, L0615-500) to remove dead cells from the plate. Cells were then treated with different CSE concentrations for 24 hours. Images of BEAS-2B cells treated with each particle concentration are shown in Figure 2.1. Each experimental set-up had a control group (0% CSE, only SF medium). Cells were collected for RNA isolation to perform qPCR analysis.

2.7.3 Culture of Primary Human Airway Epithelial Cells (HAEC)

To confirm the findings obtained by BEAS-2B cell cultures, primary human airway epithelial cells (HAEC, Cat number: EP51AB, Epitelix, Switzerland) were cultured and used in similar experiments, as a more physiologically relevant model. HAECs were isolated from a healthy non-smoker male's bronchial tissue. These cells can differentiate into mucociliary epithelium, a characteristic feature of the airway epithelial layer that plays a critical role in respiratory defense mechanisms.

HAEC medium (1 ml) was added to the cryovial in passage 2, which contained approximately 1 million HAEC cells, and mixed. In a falcon of 15 ml, 3 ml of medium was added to the cell suspension, and it was centrifuged at 2000 rpm for 10 minutes. The

supernatant was discarded, and 1 ml of HAEC medium was added to the cell pellet, then transferred to a T25 flask. Three days later, the medium changed, and the growth of the cells was monitored. After approximately 2 weeks of continuous growth in fresh medium, when the cells reached 70% confluence, they were seeded into 12-well plates. Three biological and three technical replicates were conducted (Figure 7).

The cells were exposed to the same CSE concentrations (2.5%, 5%, and 7.5%) as the BEAS-2B cells, with an exposure duration of 24 hours.

2.7.4 The preparation of Cigarette Smoke Extract (CSE) and its exposure on BEAS-2B and HAEC Cell Cultures.

CSE was prepared by adapting the methods used in the literature (Aoshiba et al. 2001; Sarı et al. 2020). According to this method, three reference cigarette (1R6F, Kentucky, USA) is used with the aspiration machine until it reaches the filter. The smoke emitted from cigarettes was mixed with 30 ml of sterile phosphate-buffered saline (PBS, 0.01) at 37˚C. The solution containing CSE was filtered through a 0.22µm-millipore filter. The resulting extract was considered as stock of 100% CSE. Extracts with an OD value between 2-2.4 at 290 nm in spectrophotometric measurement was used in the experiment (Figure 2.2). CSE was prepared fresh for each experiment.

Cells were seeded and after 80% confluence, while some of the cells formed the control group, the others made CSE group. CSE concentration was determined as 2.5%, 5%, and 7.5% doses. The next day, after treatment, RNA was collected from the cells at 24h.

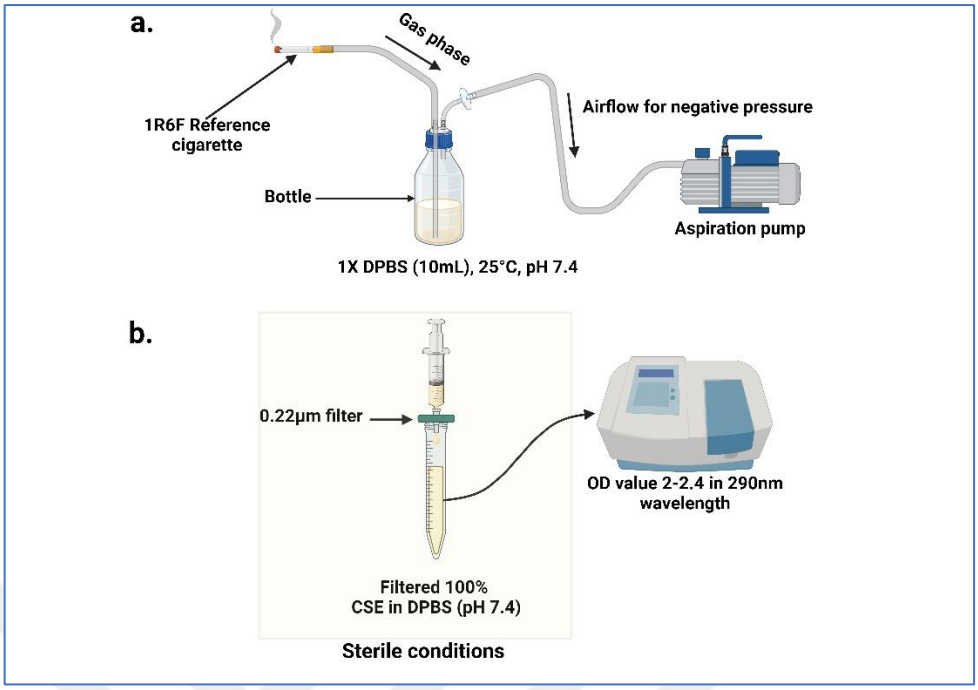

Figure 2.2: Preparation of 100% Cigarette Smoke Extract (CSE)

For each 3 sets of 6 well plates; the cigarette media for a total of 9 wells corresponding to the SF control and other doses were prepared in a volume of 20 ml.

For 2.5% CSE, 500 µl was taken, for 5% CSE, 1 ml, and for 7.5% CSE, 1.5 ml was taken from the 100X extract, and mixed with medium to a total of 20 ml (Figure 2.3).

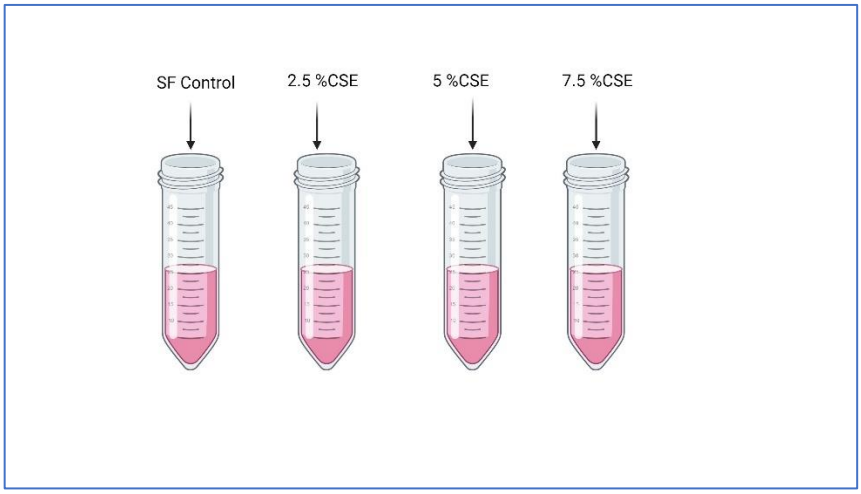

Figure 2.3: Cigarette smoke extract aliquots

After 24h incubation of CSE exposure, dead cells were seen under the light microscopy (Figure 2.4):

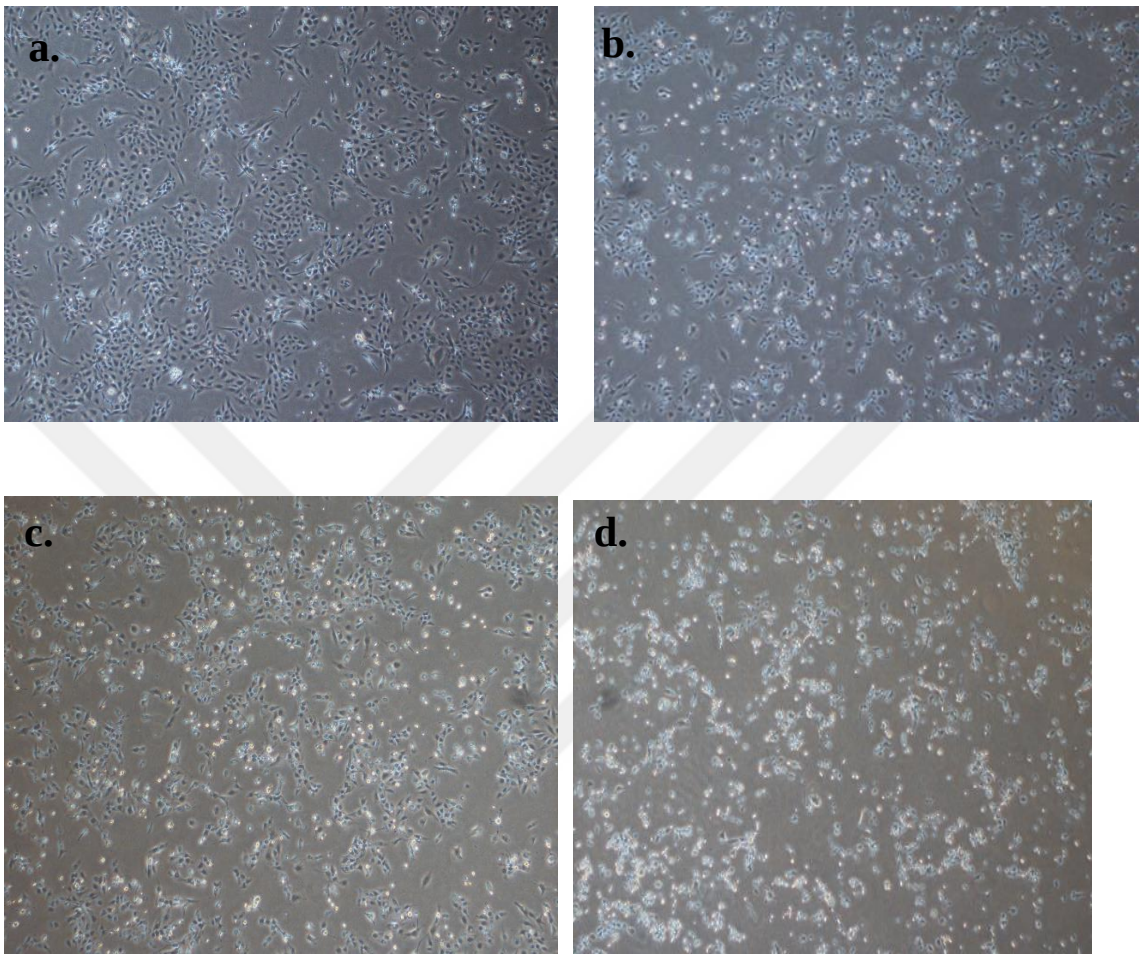

Figure 2.4: Images of cells under a light microscope after the application of cigarette smoke extract (CSE) at doses of; a. SF Control, **b.** %2.5, **c.** %5, **d.** and %7.5.

2.7.5 RNA Isolation

Following CSE exposure, total RNA was extracted from BEAS-2B and HAEC cells using the TRIzol reagent (15596018, Thermo Fischer-Invitrogen, USA), a phenol-based method that allows for the simultaneous extraction of RNA, DNA, and proteins (Figure 2.5). The protocol was performed according to the manufacturer's instructions.

The cells were detached by trypsin and centrifuged at 400 g for 4 min (for BEAS-2B cells) / 2000 rpm, 10 min (for HAEC cells). The supernatant was aspirated, and the pellet

was washed with 1ml DPBS (1X, Gibco, Thermo) and centrifuged at 400g for 4 min (BEAS-2B) / 2000 rpm, 10 min (for HAEC cells), respectively. The supernatant was aspirated and 1 ml Trizol was added to the pellet and incubated at room temperature for 5 minutes. Consequently, 200 µl chloroform (Cat number: 102445, Merck, Germany) was added and shaked slowly for 15 seconds to see the phases. After 10 minutes of incubation at room temperature, the tubes were centrifuged at 12000 g for 15 minutes at 4 ºC. The upper phase was taken slowly (do not touch the lower phase). An amount of 500 µl of Isopropyl alcohol (100272, Merck, Germany) was added and shaken slowly. The tubes were kept at -20 ºC for 30 minutes. After the tubes were centrifuged at 12000 rpm for 5 minutes, 1 ml of 75 % ethanol (Cat number: 920.026, Isolab, Germany) was added and vortexed until the pellet detached. For the third time, tubes were centrifuged at 12000 rpm for 5 minutes. The supernatant was taken, and the tubes were left to dry under the hood. Then, pellets were dissolved in 30 µl of nuclease-free water. Finally, total RNA samples were analysed for their concentrations and purities according to A260/280 with Nanodrop^{TM} 2000c (Thermo, USA). Total RNAs were stored at -80 until used in subsequent experiments.

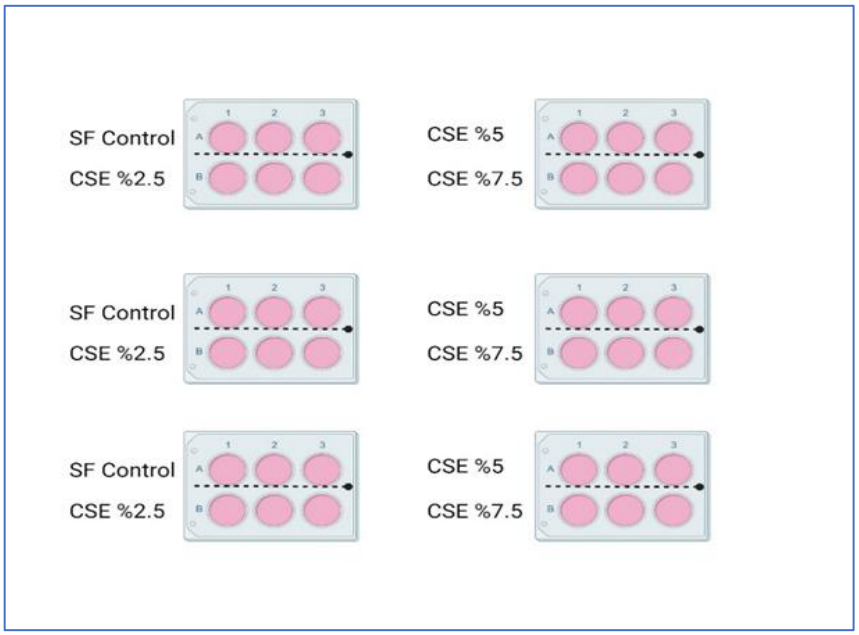

Figure 2.5: The 6 well plates configurations for RNA isolation

2.7.6 cDNA Synthesis

Complementary DNA (cDNA) was synthesized from the isolated RNA using a iScript TM cDNA Synthesis Kit (1708891, Biorad, USA) according to the manufacturer's instructions. In a 96-well T100 PCR thermal cycler (Bio-rad, USA) device, PCR reactions were carried out. Priming was performed at 25°C for 5 minutes, followed by reverse transcription at 46°C for 20 minutes and 95°C for 1 minute for the inactivation. This temperature range ensures efficient synthesis of cDNA from both the 5' and 3' ends of the mRNA, capturing the entire transcriptome for subsequent analysis. After incubation, each well has 1000 ng cDNA/ 20µl total volume. The synthesized cDNA was stored at -20°C until further use.

2.7.7 Gradient PCR of Seven Genes

The optimization of PCR conditions for each of the seven FRGs was critical for ensuring the success of subsequent quantitative analyses. Gradient PCR, a method allowing the simultaneous testing of a range of annealing temperatures, was utilized to determine the optimal annealing temperature for each primer pair. This step is vital to maximize the specificity and yield of the desired amplicons while minimizing nonspecific amplification.

We employed a thermal cycler capable of gradient temperature control, typically testing a range from 50°C to 70°C. For 5 different temperatures (56°C, 58°C, 60°C 62°C, 64°C), samples were prepared. Negative controls were also studied for each primer to check if there was any contamination. The total volume of 20 µl reaction mix was prepared. Each tube contained 10 µl of DreamTaq Green PCR Master Mix (2X) (Thermo Scientific), 0.8 µl from 10 µM primer mix and 8.2 µl nuclease-free water (NFW). 1 µl of cDNA was added at the end. cDNA concentration in each tube was 25 ng. Negative controls did not contain any cDNA. NFW (9.2 µl) was added to these tubes. All samples were run in the thermal cycler (Veriti 96 Well Thermal Cycler, Applied Biosystems), in different temperatures. Reaction conditions for thermal cycler were shown in the reactions including the designed primers, a high-fidelity DNA polymerase, and cDNA synthesized from RNA isolated from BEAS-2B cells exposed to cigarette smoke extract (CSE). The PCR products were resolved on a 1.5 % agarose gel, and the optimal annealing temperature was selected based on the intensity and clarity of the bands,

ensuring the amplification of a single, specific product corresponding to the target gene (Figures 2.6a-g).

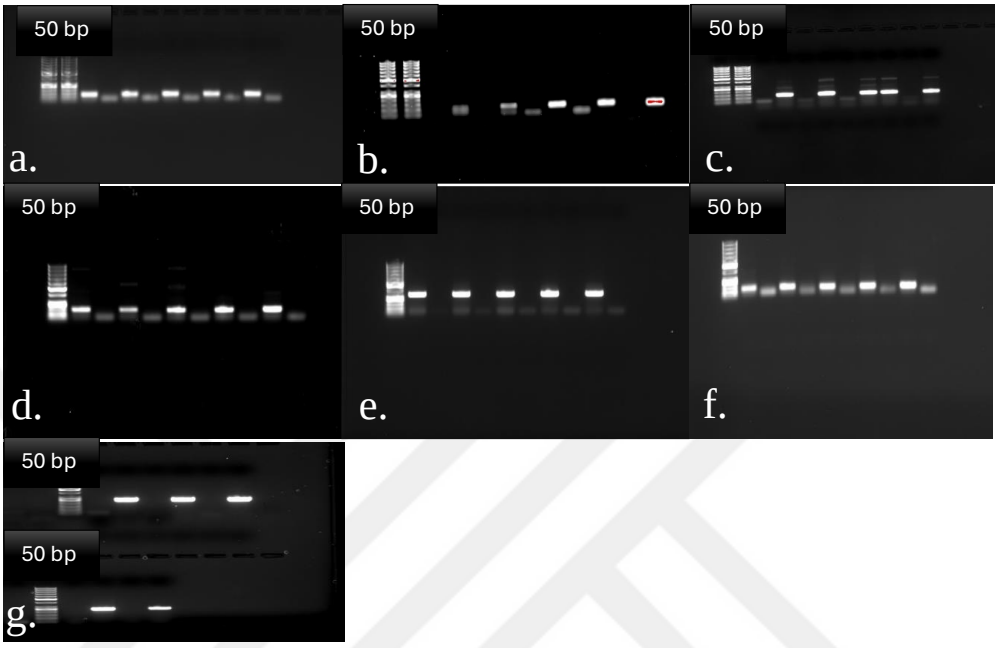

Figure 2.6. Gradient PCR images of seven genes. The bands given in each annealing temperatures 54°C, 56°C, 58°C, 60°C and 62°C belongs to **a.** *MDM2*, **b.** *EGFR*, **c.** *TAP63*, **d.** *SRC*, **e.** *BRD4*, **f.** *GDF15*, and **g.** *CD44*, respectively.

2.7.8 Quantitative Real-Time Polymerase Chain Reaction (qRT-PCR)

Quantitative real-time polymerase chain reaction (qRT-PCR) was employed to quantify the expression levels of the seven ferroptosis-related genes in response to CSE exposure. This technique, known for its high sensitivity and specificity, allows for the precise quantification of mRNA levels in real-time, providing insights into the molecular changes induced by cigarette smoke in airway epithelial cells. Using the QuantiNova SYBR Green PCR kit (Qiagen, Germany) and an Applied Biosystem PCR equipment (Thermo Scientific), cDNA was analyzed quantitatively in real-time (qRT-PCR) using specific primer sequences listed in Table 2.2.

Briefly, 20 µl of the mixture was added to each well, along with 5 µl of SYBR Green Master Mix, 12.5 ng of cDNA, forward (F) and reverse ® primers at a working

concentration of 10 µM, and nuclease-free water. The sample underwent 40 cycles of denaturation for 15 seconds, annealing for 30 seconds, and extension for 30 seconds at 72 °C after first being heated to 95 °C for five minutes. After that, a melting curve was produced by heating the material between 65 and 95 °C in increments of 0.5 °C. The qRT-PCR tests were conducted in duplicate. The relative expression levels of the target genes were normalized to housekeeping gene GAPDH which is stably expressed across different experimental conditions. The data were analyzed using the $2^{-\Delta\Delta Ct}$ method, allowing for the comparison of gene expression levels between CSE-treated and control samples (Livak et al., 2001)

Table 2.2: Primer sequences used in the quantitative real-time polymerase chain reaction (qRT-PCR).

Gene	Primer	Sequence (5'-3')	Amplicon Size(bp)
MDM2	Forward	AGGAGATTTGTTTGGCGTGC	20
	Reverse	TGAGTCCGATGATTCCTGCTG	21
EGFR	Forward	GGAGAAACTGCCAGAAACTGACC	22
	Reverse	GCCTGCAGCACACTGGTTG	19
TAP63	Forward	TGTATCCGCATGCAGGACT	19
	Reverse	CTGTGTTATAGGGACTGGTGGAC	23
SRC	Forward	GCGAGAAAGTGAGACCACGA	20
	Reverse	CCATCGGCGTGTTTGGAGTA	20
GDF15	Forward	GCAAGAACTCAGGACGGTGA	20
	Reverse	TGGAGTCTTCGGAGTGCAAC	20
BRD4	Forward	GTTACATCTACAACAAGCCTGGA	23
	Reverse	GACAGGGGTCTGGACGATGA	20
CD44	Forward	GTTATCCCTGGGGCCCTATTTCAT	24
	Reverse	ACTCCCCAGGCACTTAACTCATCC	24
GAPDH	Forward	ATGGAAATCCCATCACCATCTT	22
	Reverse	CGCCCCACTTGATTTTGG	18

2.7.9 Statistical Analysis

Continuous variables were compared utilizing One-way analysis of variance (ANOVA), and ANOVA multiple comparison tests, or the Kruskal-Wallis multiple comparison tests. One-way ANOVA was used to compare control and CSE groups. Results are expressed as the mean standard error of the mean (SEM) or median interquartile ranges (Q1 and Q3). P values below 0.05 were considered significant. PRISM version 8 was used to perform statistical analysis (GraphPad Software Inc, San Diego, CA, USA).

Chapter 3:
RESULTS

3.1 The Results of Gene Expression Omnibus (GEO) data

GEO2R is a program based on R, designed to analyse genes that are expressed differently between experimental and control groups based on Gene Expression Omnibus (GEO) datasets. The GEO2R analysis was conducted between the mRNA data of patients with COPD and the mRNA data of healthy individuals (control group), and the expression of these genes was analyzed differentially with various statistical visual data. The threshold for log fold change is greater than 1 (absolute value) and the p-value is less than or equal to 0.05. Numerous studies commonly use this criterion to determine whether genes are significantly upregulated or downregulated. According to the results, the joint genes were expressed as the P value <= 0.05, logFc >= 1 for upregulated genes, and P value <= 0.05, logFc <= -1 for downregulated genes to obtain hub genes (Gu et, al.,2016).

This research included four mRNA expression profiles in GSE87098, GSE151052, GSE76925, and GSE10006 from GEO to identify DEGs of airway epithelial cells in smoke-induced COPD. We obtained the comparison results by intersecting the differential genes in different datasets, which included the airway epithelial cells and lung tissue of control and COPD donors. Among them, GSE87098 includes chip data following 8 control samples and 7 COPD samples. GSE151052 includes 77 control samples and 40 COPD samples, GSE76925 includes 111 control samples and 40 COPD samples, and GSE10006 includes 14 smoker samples and 13 Non-smoker samples. These samples were from small airway epithelial cells. Volcano plots were used to visualize differential expression, with red indicating up-regulated genes and blue indicating down-regulated genes. According to the results obtained from the screening conditions and compared with the control group, GSE76925 had 1102 upregulated and 1792 downregulated genes (Figure 3.1a), GSE87098 had 113 upregulated genes and 16823 downregulated genes (Figure 3.2a), GSE151052 had 44 upregulated genes and 3629 downregulated genes (Figure 3.3a), and GSE10006 had 755 upregulated genes and 2831 downregulated genes (Figure 3.4a). The UMAP dimensionality reduction graph was used to visualize the relationship between samples (Figures 3.1b, 3.2b, 3.3b, and 3.4b). The

graph showed that the sample data from the three datasets collected were well discriminated, and there were significant differences overall, which is important for screening. Boxplots and expression density plots demonstrated that the distribution of expression values for selected samples were normalized and was suitable for comparing differences (Figures 3.1c and d-3.4 c and d).

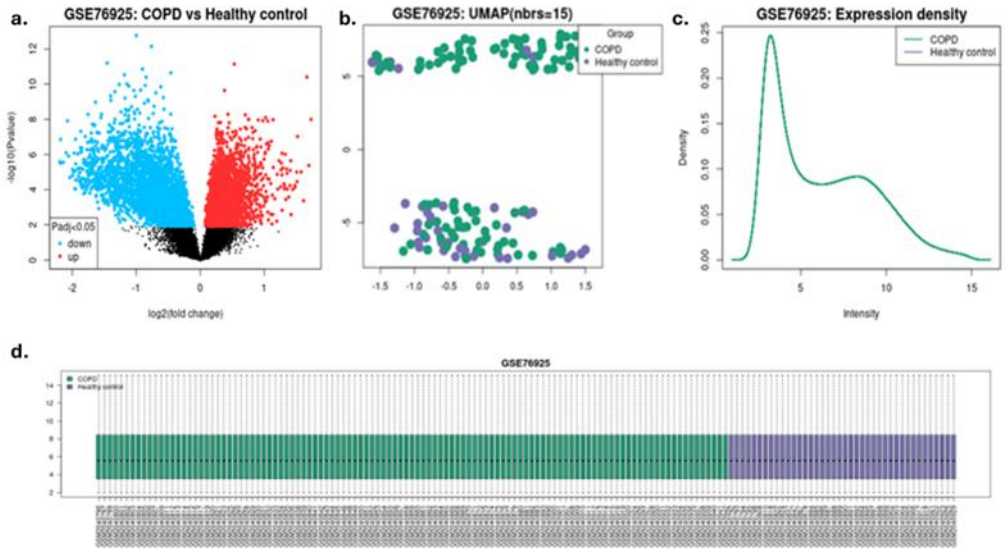

Figure 3.1: Discrimination visualization of COPD and control samples and up and down DEGs from the GSE76925 dataset. **A**. Volcano plot of the filtered dataset. **B**. UMAP graph of GSE76925. **C**. The density plots of the dataset. The density plot displays the points' uniform distribution along the numerical axis. The locations with the highest point concentrations are where the density plot's peaks are found. **D**. Box plot illustrates the normalization of the chosen samples in the dataset.

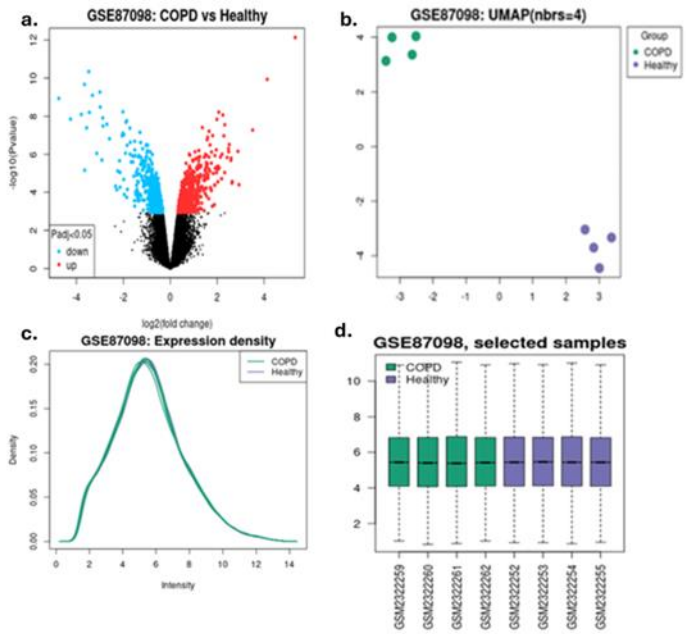

Figure 3.2: Discrimination visualization of COPD and control samples and up and down DEGs from the GSE87098 dataset. **A**. Volcano plot of the filtered dataset. **B**. UMAP graph of GSE87098. **C**. The density plots of the dataset. The density plot displays the points' uniform distribution along the numerical axis. The locations with the highest point concentrations are where the density plot's peaks are found. **D**. Box plot illustrates the normalization of the chosen samples in the dataset.

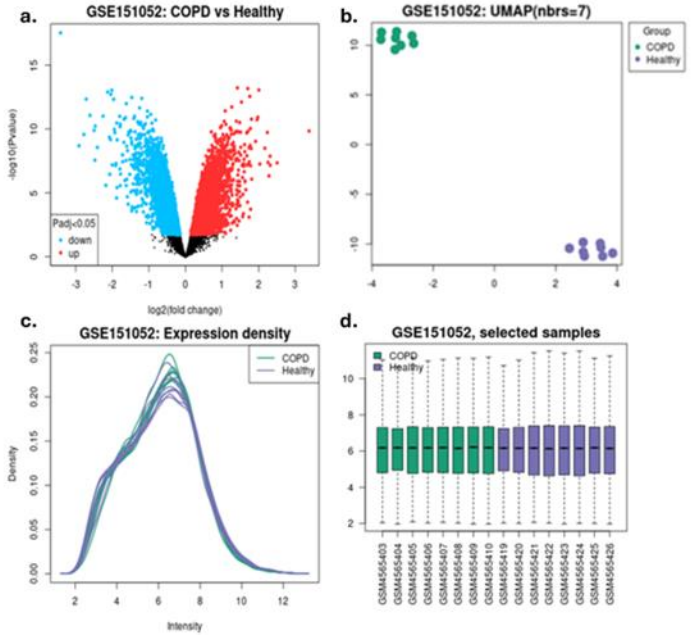

Figure 3.3: Discrimination visualization of COPD and control samples and up and down DEGs from the GSE151052 dataset. GEO2R analysis of GSE151052. **A**. Volcano plot of the filtered dataset. **B**. UMAP graph of GSE151052. **C**. The density plots of the dataset. The density plot displays the points' uniform distribution along the numerical axis. The

locations with the highest point concentrations are where the density plot's peaks are found. **D**. Box plot illustrates the normalization of the chosen samples in the dataset.

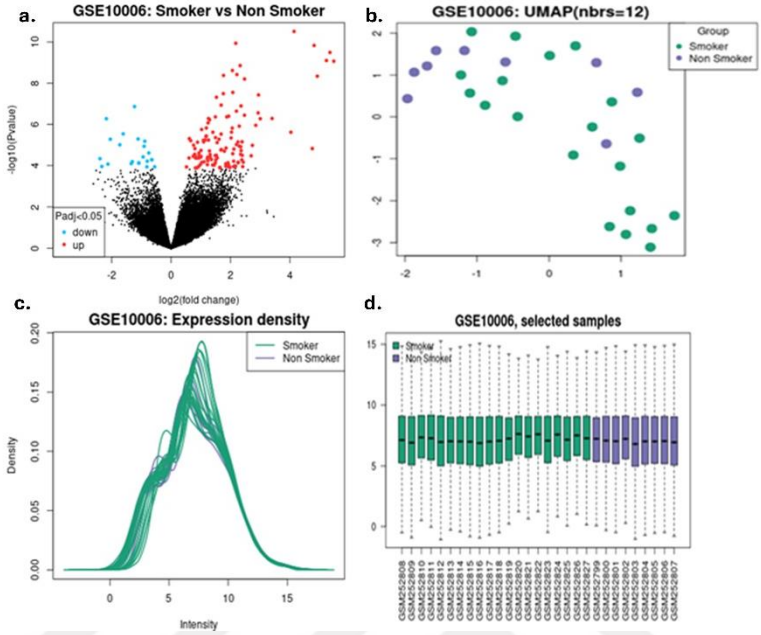

Figure 3.4: Discrimination visualization of COPD smoker and COPD non-smoker samples and up and down DEGs from the GSE10006 dataset. **A**. Volcano plot of the filtered dataset. **B**. UMAP graph of GSE10006. **C**. The density plots of the dataset. The density plot displays the points' uniform distribution along the numerical axis. The locations with the highest point concentrations are where the density plot's peaks are found. **D**. Box plot illustrates the normalization of the chosen samples in the dataset.

We compared the common differentially expressed genes of cigarette smoking related dataset (CSE10006) to COPD related datasets (GSE76925, GSE87098, and GSE151052). We found 507 common DEGs from the 3497 differentially expressed genes of COPD patients' airway epithelium in GSE76925 and 3018 differentially expressed genes of CSE exposed airway epithelial cells in GSE10006. Also, we determined 1757 common DEGs from the 15635 differentially expressed genes of COPD patients' airway epithelium in GSE87098 and 3018 differentially expressed genes of CSE exposed epithelial cells in GSE10006. Moreover, we found 513 common DEGs from the 3301 differentially expressed genes of COPD patients' airway epithelium in GSE151052 and 3018 differentially expressed genes of CSE exposed airway epithelial cells in GSE10006 (Figure 3.5).

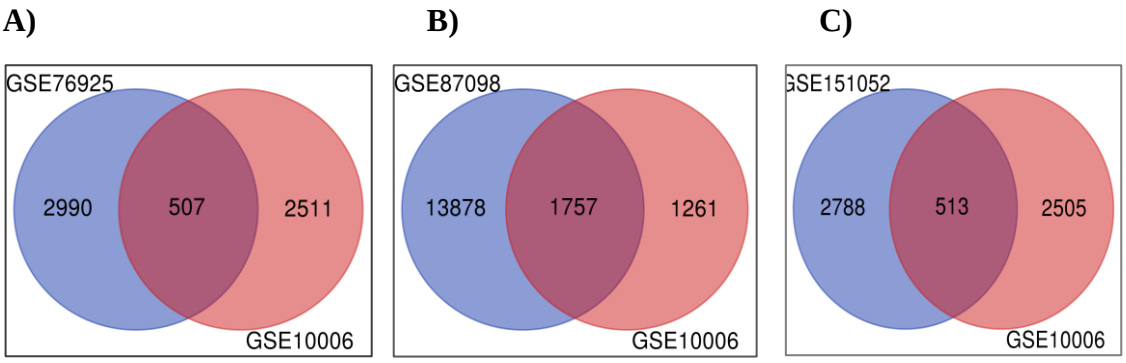

Figure 3.5: The intersection of COPD vs Healthy Control DEGs with Smokers and Non-smoker DEGs. It visualizes the comparison of common differentially expressed genes of cigarette smoking-related dataset (GSE10006) against COPD-related datasets (GSE76925, GSE87098, and GSE151052). **A)**. It was found 507 common DEGs between GSE76925 and GSE10006 **B)**. It was found 1757 common DEGs between GSE87098 and GSE10006. **C)**. It was found 513 common DEGs between GSE151052 and GSE10006.

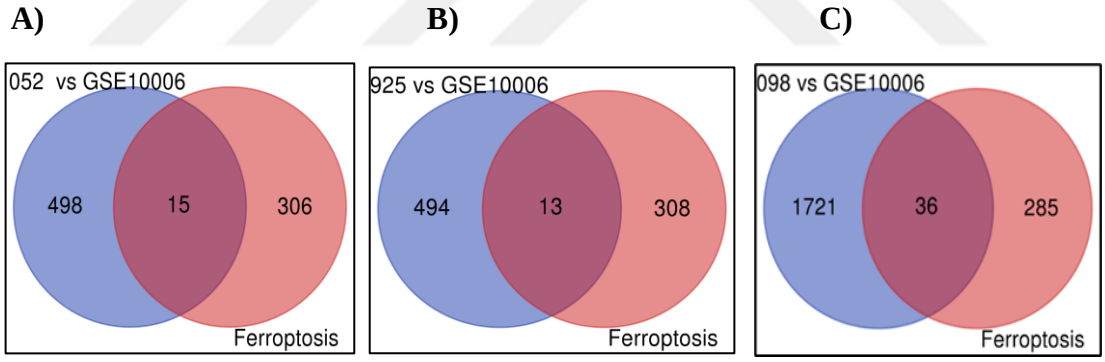

Figure 3.6: The intersection of COPD and smoker DEGs with the ferroptosis genes. It visualizes the comparison of common differentially expressed genes of ferroptosis genes dataset against COPD vs smoking datasets (GSE76925, GSE87098, GSE151052 and GSE10006). It was found 15 DEGs between GSE151052 and GSE10006 and Ferroptosis. B). It was found 13 DEGs between GSE76925 and GSE10006 and Ferroptosis c). It was found 36 DEGs between GSE87098 and GSE10006 and Ferroptosis. The intersected genes were totally 20 genes which are obtained from 3 different intersections some of them were repeated genes.

3.2 Identified Differentially expressed Ferroptosis Genes (FRGs)

Comparative analysis of COPD datasets associated with cigarette smoke exposure revealed 507 common genes between GSE76925 and GSE10006, 1757 common genes between GSE87098 and GSE10006, and 513 common genes between GSE151052 and GSE10006 (Figure 3.5). When these common genes were individually compared with the ferroptosis gene list obtained from FerrDb v1 (http://www.zhounan.org/ferrdb; Zhou et al., 2020) on [accessed at 23.02.2023], a total of 20 genes involved in COPD associated with cigarette smoke exposure were identified, comprising 11 upregulated and 9 downregulated genes (Tables 3.1 and 3.2).

Table 3.1: Upregulated ferroptosis genes (FRGs)

Adj P value	Log Fc	Upregulated Genes	Gene name
0.0000785	1.48012.713	GP6D	Glucose 6 phosphate dehydrogenase
0.012361	2.05729.477	TP63	Tumor protein 63
0.0122	1.34821477	GDF15	Growth differentiation factor 15
0.0195	1.090094	CD44	CD44 molecule (IN blood group)
0.0235	1.212228	ASMTL-AS1	ASMTL antisense RNA 1
0.000881	1.72576291	PANX2	Pannexin2
0.003251	1.6497898	BRD4	Bromodomain-containing protein 4
0.00054	1.50258364	AIFM2	Apoptosis Inducing Factor Mitochondria Associated 2
0.008386	1.41453131	PROM2	Prominin 2
0.018455	1.36779733	MDM2	Mouse double minute 2
1.44E-08	1.07388	CIRBP	Cold-inducible RNA-binding protein

Table 3.2: Downregulated ferroptosis genes (FRGs)

Adj P value	LogFc	Downregulated Genes	Gene name
0.00544	-1.40392	PAQR3	Progestin and adipoQ receptor family member 3
0.00969	-1.30538	ATF2	Activating transcription factor 2
0.0171	-1.42312	EGFR	Epidermal growth factor receptor
0.0306	-1.45566	CHAC1	ChaC glutathione specific gamma-glutamylcyclotransferase 1
0.014363	-1.4869	SRC	Proto-oncogene tyrosine-protein kinase Src

0.007745	-1.62329	ACSL3	Acyl-CoA synthetase long-chain family member 3
0.000652	-1.8838	ALOX5	Arachidonate 5-lipoxygenase
2.66E-10	-2.776731	PRKAA2	Protein kinase AMP-activated catalytic subunit alpha 2
7.53E-04	-1.45078	MEF2C	Myocyte enhancer factor 2C

3.3 Functional enrichment and pathway analyses of 20 FERGs

The functional enrichment analysis of 20 common genes associated with ferroptosis, cigarette smoke, and COPD, conducted using METASCAPE, revealed several key pathways. According to WikiPathways (WP), these genes are enriched in the VEGFA-VEGFR2 signaling pathway, the gastrin signaling pathway, and malignant pleural mesothelioma. In the GO biological process database, they are linked to positive regulation of phosphorylation, response to nutrient levels, regulation of growth, regulation of defense responses, sulfur compound metabolic processes, and regulation of vesicle-mediated transport. KEGG pathway analysis highlights enrichment in proteoglycans in cancer, while reactome indicates involvement in TP53 transcriptional regulation and the regulation of fatty acid metabolism. Additionally, protein interaction database (PID) analysis points to the regulation of p53 downstream pathways as significant signaling routes (Figure 3.7a).

GO molecular function analysis of these 20 genes further demonstrates enrichment in positive regulation of biological processes, response to stimulus, and metabolic processes (Figure 3.7b).

a.

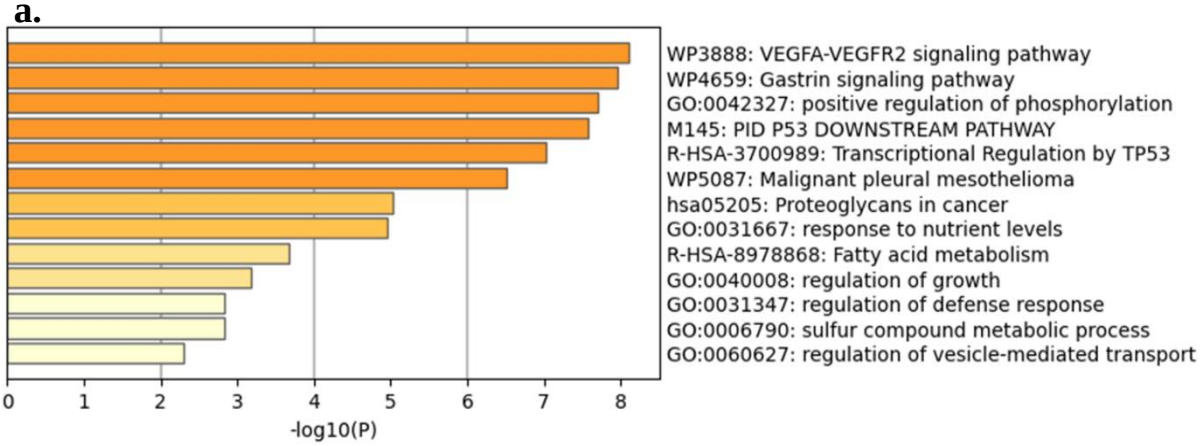

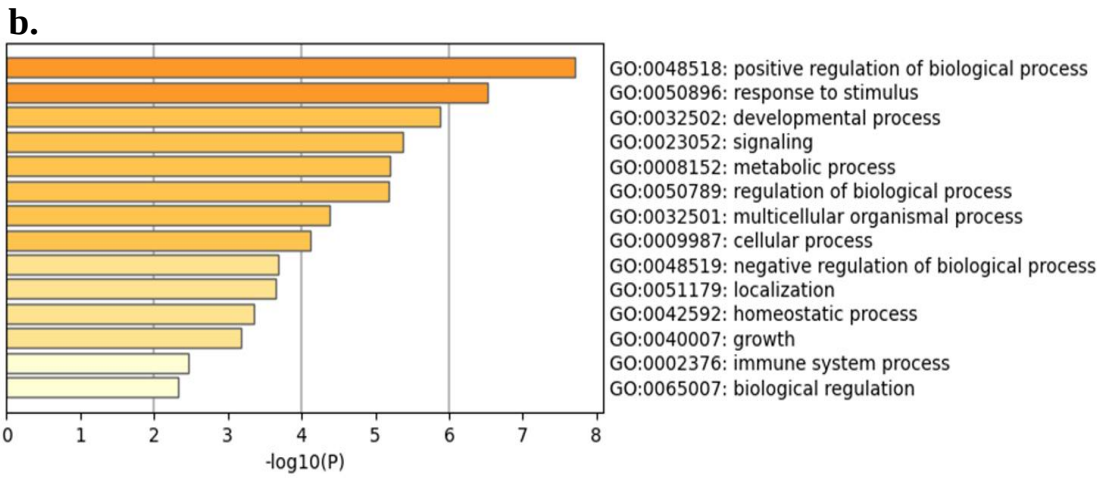

Figure 3.7: Functional enrichment analysis with Metascape. **A**). The pathway analysis results were identified by METASCAPE using KEGG, GO Biological Function, Wiki Pathways, Reactome, and Pathway Interaction Database. **B)**. According to the combined score of GO molecular function (MF), highest enriched GO MF terms were identified. The higher enrichment score states the higher number of genes are involved in a certain ontology. The results of the pathway terms were identified through the combined score (-log10(P)). GO molecular function analysis of these 20 genes further demonstrates enrichment in positive regulation of biological processes, response to stimulus, and metabolic processes.

3.4 The Interaction Between COPD-Related Ferroptosis Genes by Metascape Analyses

3.4.1 MCODE Analysis of 20 FERGs

According to MCODE analysis, a highly interconnected interaction network was identified among the 20 common ferroptosis-related COPD genes. This network includes the genes *CD44*, *SRC*, *MDM2*, *G6PD*, and *EGFR*, which were found to be highly associated (Figure 3.8). To strengthen their relationships with each other, an analysis was conducted in STRING. As a result, a network of 7 interconnected genes was created, with 2 of them located at the center. The confidence rate was settled medium level and Ferroptosis proteins were analyzed according to their interactions with each other, and the central genes were found to be *MDM2* and *EGFR* (Figure 3.9).

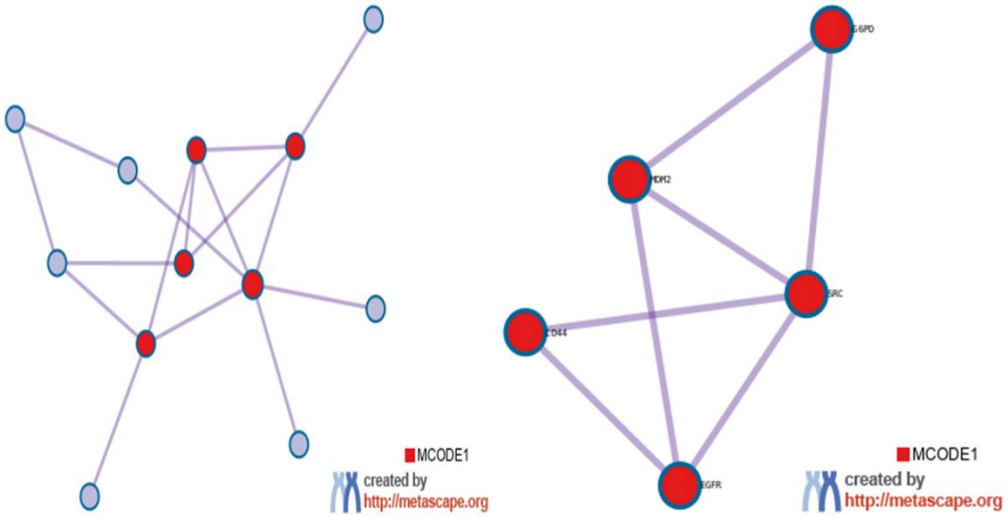

Figure 3.8: MCODE analysis. The bioinformatics analysis results showed that when we performed Metascape-based MCODE analysis on the 20 genes we identified, 5 of these genes were interconnected in a cross-relation network. This shows a strong connection between *MDM2*, *SRC*, *CD44*, *G6PD*, and *EGFR*.

3.4.1.2 Protein-Protein Interaction of 7 Hub Genes

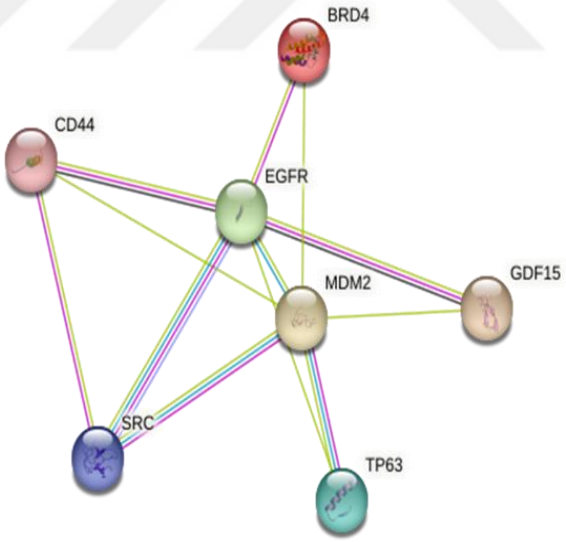

Figure 3.9: Protein-protein interaction of seven hub genes.

3.5 mRNA-miRNA interaction of Seven Hub Genes

Based on the integrated mRNA-miRNA analysis of these seven genes, hsa-mir-203a-3p was identified as a common miRNA regulating *SRC*, *MDM2*, and *TP63* genes. Hsa-mir-155-5p was found to be a common miRNA for *SRC*, *GDF15*, and *MDM2*, while hsa-mir-34a-3p regulates *SRC*, *GDF15*, *CD44*, and *MDM2* (Figure 3.10a). The *EGFR* gene was associated with miRNAs hsa-mir-21-5p, hsa-mir-335-5p, hsa-mir-218-5p, hsa-mir-16-5p, and hsa-mir-128-3p. *MDM2* was linked to hsa-mir-92a-3p, hsa-mir-26b-5p, hsa-mir-335-5p, and hsa-mir-218-5p. *CD44* was connected to hsa-mir-204-5p, hsa-mir-218-5p, and hsa-mir-16-5p. *TP63* was related to hsa-mir-92a-3p and hsa-mir-21-5p, while *BRD4* was associated with hsa-mir-26b-5p and hsa-mir-204-5p. *GDF15* was linked to hsa-mir-335-5p and hsa-mir-128-3p. Several of these miRNAs interacted with multiple genes. The most highly interacting miRNAs were hsa-mir-218-5p (associated with *MDM2*, *EGFR*, and *CD44*) and hsa-mir-335-5p (associated with *MDM2*, *EGFR*, and *GDF15*). MiRNAs that interacted with at least two genes include hsa-mir-204-5p (*BRD4* and *CD44*), hsa-mir-26b-5p (*BRD4* and *MDM2*), hsa-mir-92a-3p (*MDM2* and *TP63*), hsa-mir-21-5p (*TP63* and *EGFR*), hsa-mir-128-3p (*GDF15* and *EGFR*), and hsa-mir-16-5p (*EGFR* and *CD44*) (Figure 3.10b).

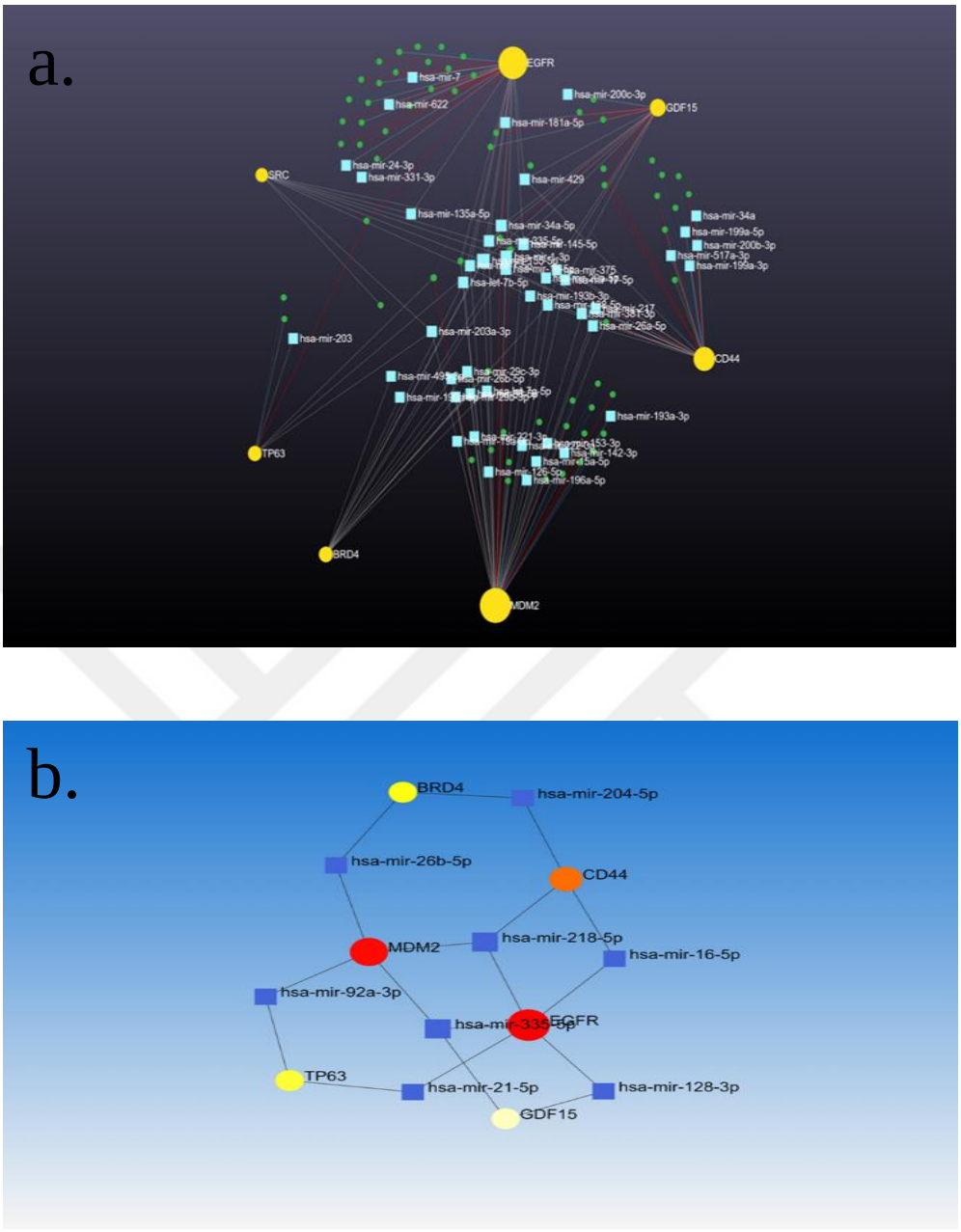

Figure 3.10: miRmap analysis **a.** miRmap Analysis for 7 Central Ferroptosis Genes. **b.** The miRmap analysis and network worked for central degree genes. MDM2 and EGFR are the most centrally genes, and completed miRNAs were found. A correlation has been identified between specific microRNAs (miRNAs), specifically HSA-mir-21-5p, HSA-mir-34a-3p, HSA-mir-155-5p, HSA-mir-203a-3p, and HSA-mir-218-5p, which suggests a potential mechanism by which these miRNAs may contribute to the downregulation of these genes at the transcriptional level.

3.6 The Validation of Bioinformatic Data by qPCR

3.6.1 The mRNA expression of Ferroptosis related COPD genes in CSE-exposed BEAS-2B cells

24-hour exposure to CSE applied at different doses did not cause significant changes in any of the *MDM2*, *EGFR*, *BRD4*, *SRC*, *GDF15*, *TAP63* and *CD44* genes in BEAS-2B cells compared to the control group (Figures 3.11a-g).

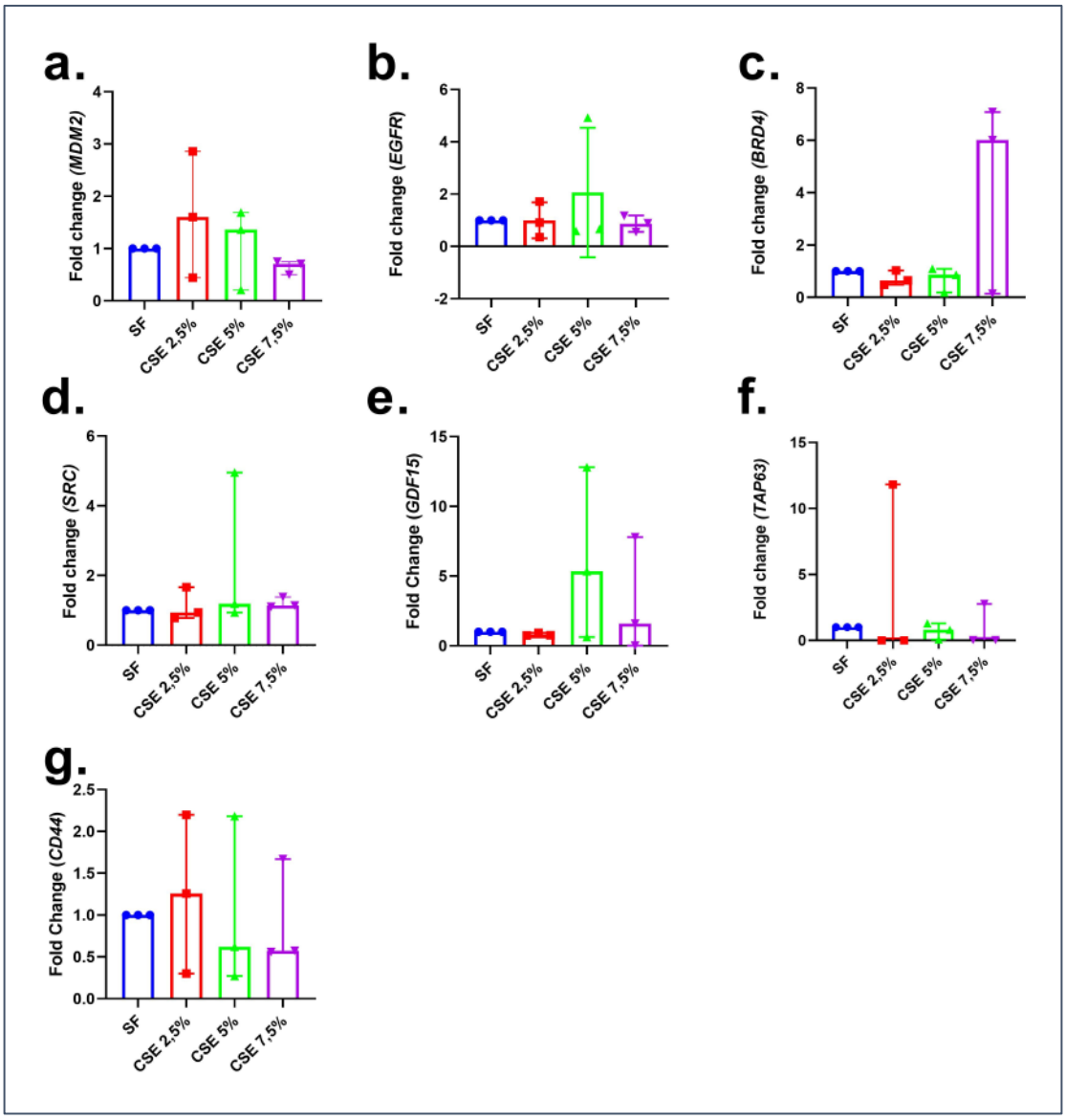

Figure 3.11: Effect on mRNA expression (fold change) of seven hub genes at different doses of CSE (*MDM2, EGFR, SRC, GDF15, TAP63, CD44, and BRD4*) in BEAS-2B cells. Data are given as median ± interquartile ranges (Q1 and Q3).

3.6.2 Effects of CSE on mRNA expression of Ferroptosis related COPD genes in HAECs

HAECs cells were exposed to CSE at concentrations of 2.5%, 5% and 7.5% for 24 hours. No concentration of CSE significantly changed the MDM2 gene level in HAEC cells compared to the control (Figure 3.11a). On the other hand, 2.5% CSE exposure significantly reduced EGFR ($p<0.0001$), BRD4 ($p<0.0001$), SRC ($p<0.0001$), GDF15 ($p<0.0001$), and CD44 ($p<0.001$) mRNA levels in these cells. CSE (5%) exposure significantly increased the mRNA levels of EGFR ($p<0.0001$), BRD4 ($p<0.0001$), SRC ($p<0.0001$), GDF15 ($p<0.0001$), TAP63 ($p<0.01$) and CD44 ($p<0.001$) in these cells. At 7.5% dose, CSE exposure also increased mRNA expression for EGFR ($p<0.0001$), BRD4 ($p<0.0001$), SRC ($p<0.0001$), GDF15 ($p<0.0001$), TAP63 ($p<0.01$) and CD44 ($p<0.0001$) in these cells (Figures 3.12b-g).

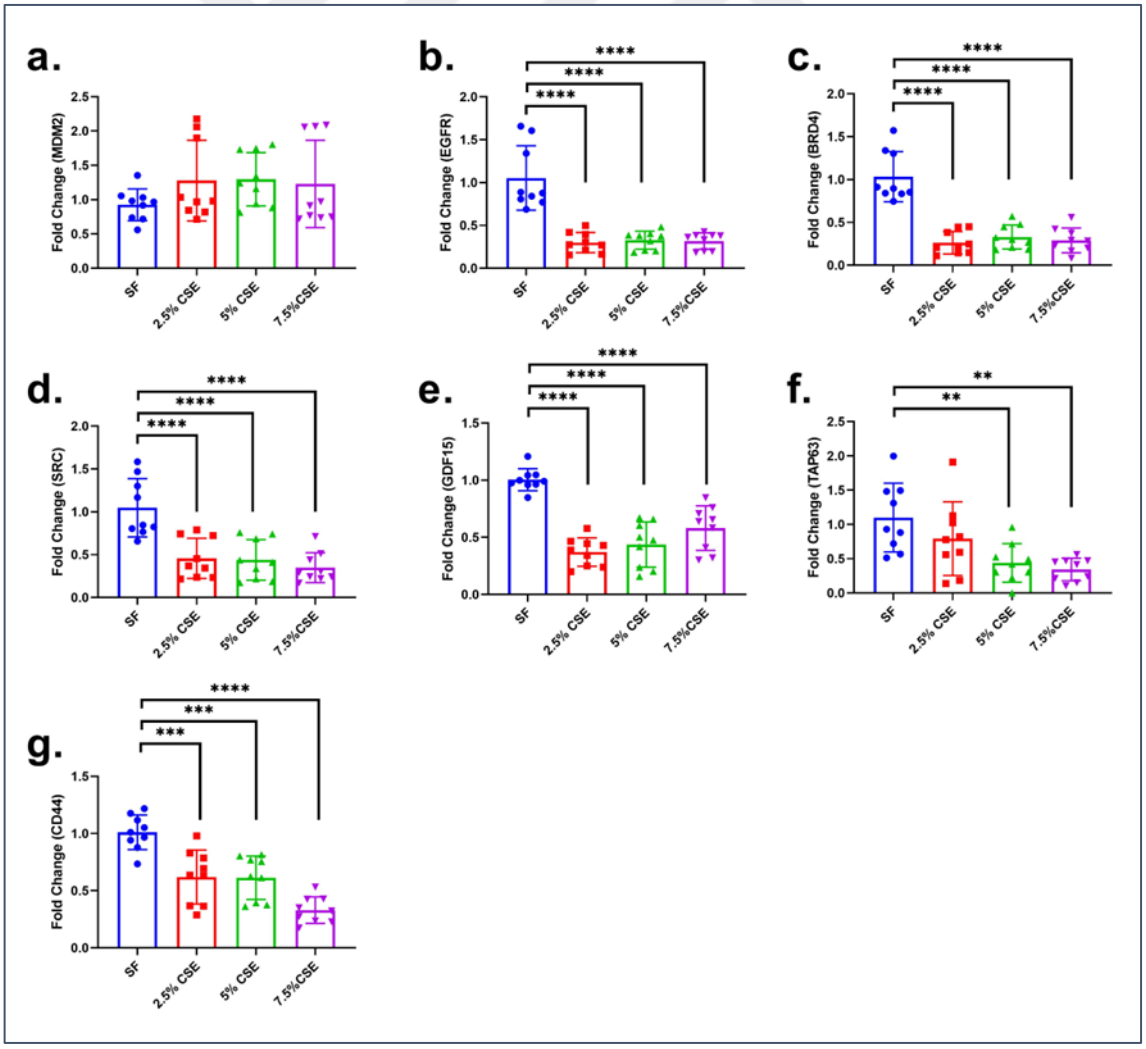

Figure 3.12: Effect on mRNA expression (fold change) of seven hub genes (*MDM2, EGFR, SRC, GDF15, TAP63, CD44, and BRD4*) at different doses of CSE in primary human airway epithelial cells (HAECs). Data are given as mean ± standard deviation (SD). **p<0.01, ***p<0.001, and ****p<0.0001 vs control (0% CSE).

The summary of methods and results found in our studies are demonstrated in a flowchart (Figure 3.13).

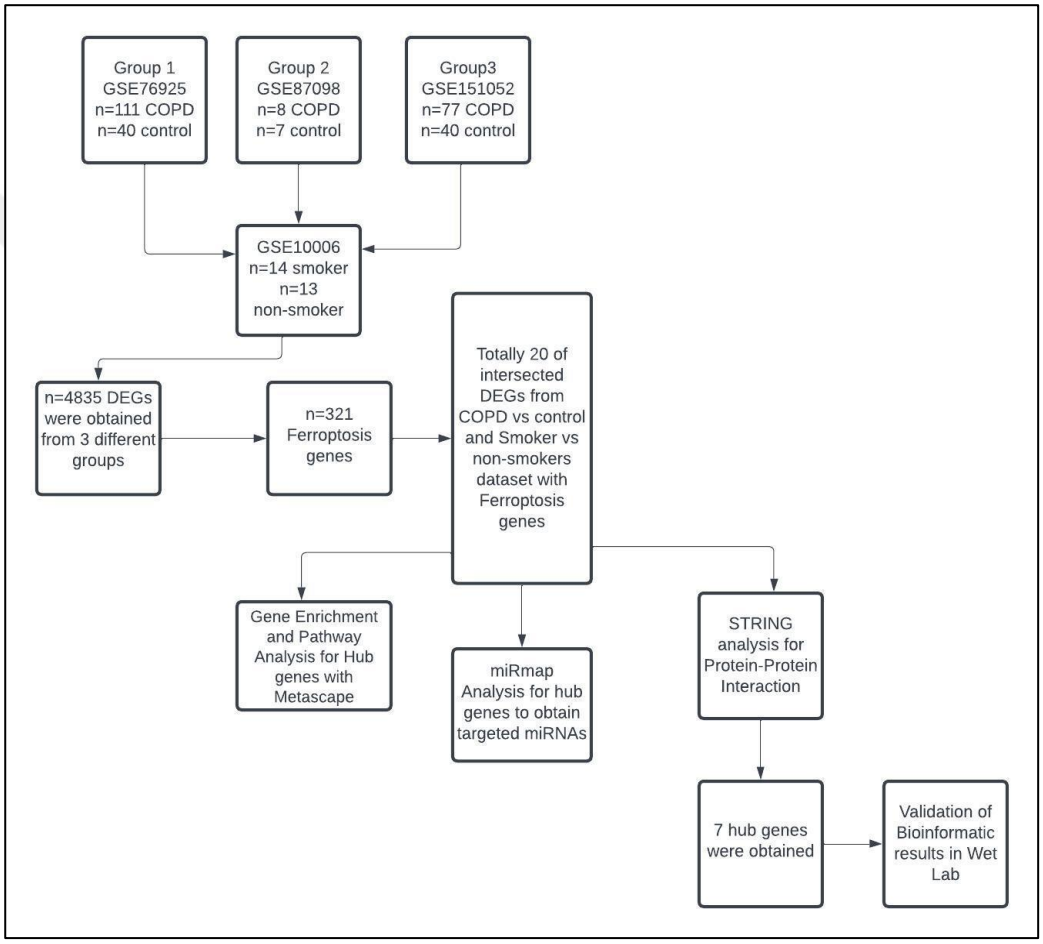

Figure 3.13: The flowchart of the study

Chapter 4:
DISCUSSION

In the current study, ferroptosis-related genes involved in the pathogenesis of COPD associated with cigarette smoke exposure were identified using an integrative bioinformatics approach. The identified genes were examined for their response to cigarette smoke exposure in both BEAS-2B cells, and primary HAEC by QRT-PCR. Bioinformatic analyses revealed that the expression of seven genes was significantly altered in individuals with cigarette smoke-related COPD and that these ferroptosis genes interacted at a high level. These genes were MDM2, EGFR, TP63, SRC, GDF15, BRD4, and CD44.

Following bioinformatic analysis, validation was performed using the QRT-PCR to understand the response of these genes to cigarette smoke. Fresh CSE at various concentrations (2.5%, 5%, and 7.5%) was prepared in SF medium using previously optimized methodologies and applied to the cells for 24 hours (Aoshiba et al. 2001; Sarı et al. 2020). In our exposure studies, CSE did not alter the expression of these genes in BEAS-2B cells. However, HAEC cells showed a significant response to CSE. In our study, none of the CSE doses altered MDM2 mRNA expression compared to the control, while the mRNA expression of EGFR, BRD4, SRC, GDF15, and CD44 was significantly reduced by CSE. This reduction was significant across all CSE doses and followed a similar trend. TP63 gene expression was not affected by 2.5% CSE, but 5% and 7.5% CSE levels significantly reduced its expression compared to the control.

The decrease in the expression levels of these genes suggests that CSE may downregulate their expression through different gene regulatory pathways. Functional pathway analysis of these seven hub genes revealed enrichment in pathways associated with the transcriptional regulation of the TP53 gene and the positive regulation of fatty acid and sulfur components involved in ferroptosis. On the other hand, based on the miRNA-gene interaction analysis of these seven genes, we found that hsa-mir-21-5p, hsa-mir-34a-3p, hsa-mir-155-5p, hsa-mir-203a-3p, and hsa-mir-218-5p were associated with these genes and could be responsible for their downregulation at the transcriptional level.

The MDM2 gene, one of the seven hub genes, is a proto-oncogene and encodes a nuclear-localized E3 ubiquitin ligase. This ligase functions as a negative regulator of the tumor suppressor gene P53 and is, in turn, regulated by the P53 gene (Bond et al., 2005). At the cellular level, the P53 gene is strongly associated with cell death pathways, playing a critical role in tumor suppression. A previous study showed that, p53 plays a crucial role in mediating ferroptosis by weakening its target SLC7A11 (Jiang et al., 2015). One of the most important upstream regulators of ferroptosis is SLC7A11, a cystine/glutamate antiporter, that plays a critical role in cystine uptake to propel GSH synthesis and relieve oxidative stress (Fu et al.,2024). Research indicates that SLC7A11 knockdown indirectly reduces GPX4 function by lowering intracellular cystine levels and decreasing GSH production. This ultimately results in fatal lipid peroxidation that triggers ferroptosis (Maschalidi et al.,2022). Mizuno, et al., demonstrated that p53 and MDM2 gene polymorphisms are associated with apoptotic signaling and smoking-related emphysematous lung changes in smokers (Mizuno et al., 2017). Additionally, MDM2 regulates the ferroptosis process by regulating ACSL4 ubiquitination (Ji et al., 2024). ACSL4 is a critical determinant of ferroptosis, executing ferroptosis by catalyzing lipid biosynthesis (Mou et al., 2019; Jiang et.al., 2021).

Cigarette smoke exposure induces oxidative stress at the cellular level, leading to the activation of NF-κB, which in turn triggers an increase in inflammation (Shen et al., 2009). Pro-inflammatory cytokines such as IL-1B, IL-6, IL-8, and TNF-α are regulated by NF-κB, and they also regulate NF-κB production in a feedback loop (Shen et al., 2009). NF-κB has been shown to play a role not only in the pathogenesis of COPD associated with cigarette smoke exposure but also in inflammation-induced carcinogenesis (Gu et al. 2018). Given that cigarette smoke is a known carcinogen, NF-κB may represent a linked pathway in the overlap between COPD and lung cancer. Studies have demonstrated that NF-κB promotes tumor survival and suppresses tumor apoptosis. Furthermore, NF-κB activation has been shown to lead to a reduction in P53 protein levels by promoting the polyubiquitination and degradation of P53 through the MDM2 E3 ligase, an inhibitor of P53 (Tergaonkar et al., 2002; Kashatus et al., 2006). Interestingly in our research, MDM2 was found to be upregulated via bioinformatic analysis, which was performed in GEO datasets. However, MDM2 was non-significant at the transcriptome level in both BEAS -2B cell line and HAEC primary cells incubated with CSE. This situation suggests that some genes identified from a pool of patient-derived samples may not exhibit the

expected changes in cell lines, as seen in the case of MDM2. This discrepancy could also be attributed to underlying factors such as the bioinformatic approach used or the influence of genotypic variations. Differences in genetic background between patient samples and cell lines might impact gene expression responses, potentially leading to inconsistent results across experimental models.

In a preprint study by Shi et al. (2024), five different COPD peripheral blood samples and five different COPD lung tissue samples were analyzed using the GEO microarray dataset. Using the limma R package with cut-off values of log2 FC > 0.995 and $P < 0.05$, the analysis identified that 24 ferroptosis-related genes showed significant changes in COPD patients. Among these genes, MDM2, which also emerged in our analysis, was highlighted as a potential biomarker for COPD. Another gene they identified was CDKN1A, also known as P21. Although CDKN1A did not emerge in our analysis, it is a gene linked to P53 and involved in mitosis and senescence, and its expression was reported to be elevated in COPD patients. Additionally, the study suggested that MDM2 could be a target of CDKN1A, and both genes were positively correlated, with their expression levels correlating positively with neutrophil count in COPD patients (Shi et al. 2024 preprint). However, there is very little data on the role of MDM2 in epithelial cells in relation to COPD and cigarette smoke response, which is an important gap addressed by our study.

In another study, it was found that MDM2 expression in smokers was associated with P53 codon 72 and MDM2 SNP 309 genotypes. MDM2 expression was higher in individuals with the GG genotype of MDM2 SNP 309 compared to those with GT and TT genotypes, with the lowest MDM2 expression seen in the TT genotype. Conversely, P53 protein levels were lowest in the GG genotype and increased progressively in the TT phenotype. The study also found that P53 protein levels were higher in moderate to severe COPD compared to mild COPD, with the highest P53 levels observed in individuals with GT and TT genotypes of MDM2 SNP 309 (Mizuno et al., 2017). Given the variability of these genotypes between individuals, it is likely that their response to cigarette smoke will also vary. Thus, the lack of MDM2 response observed in the BEAS-2B and HAEC cell lines, which are derived from a single individual, may reflect biological non-responsiveness of this gene rather than a generalizable finding.

The EGFR signaling pathway plays a pivotal role in lung development, homeostasis, and repair, making it a potential therapeutic target for chronic lung diseases such as pulmonary fibrosis, COPD, and lung cancer (Vallath et al., 2014). In particular, abnormal activation of the epidermal growth factor receptor (ERBB) family is stimulated when the lung epithelium is exposed to oxidative stress from cigarette smoke (CS) (Roskoski, 2019). Cigarette smoke exposure activates EGFR signaling, which in turn triggers phosphorylation via the ERK1/2 and MEK1/2 pathways. Additionally, CS can cause ERK1/2 phosphorylation and activation through oxidative stress, independent of EGFR signaling, and EGFR/ERK1/2-mediated wound repair is inhibited by CS-induced oxidative stress (Amatngalim et al., 2016). Studies have shown that even brief exposure to CS, for 6 or 24 hours, induces damage and affects the wound repair response through modulation of EGFR signaling, highlighting its sensitivity. Furthermore, in these studies, CS exposure led to the proliferation of p63+ basal cells at the edges of wound sites, and it was found that CS disrupts the proliferation and migration of basal cells (Amatngalim et al., 2016). Another study on the role of EGFR in COPD suggested that EGFR could play a key role in the airway changes seen in patients with COPD and chronic mucus hypersecretion (Howell, 2007).

As bronchial epithelial cells were activated by CS, EGFR stimulated the release of pro-inflammatory cytokines such as IL-8 and increased the gene expression of mucin MUC5AC. In the same study, treatment with doxycycline was shown to inhibit the release of EGFR ligands in response to CS, thereby reducing IL-8 release and MUC5AC gene expression (Howell, 2007). Additionally, CSE was found to enhance EGFR signaling via oxidative stress, leading to features associated with COPD, such as basal cell hyperplasia and goblet cell hyperplasia in the airway epithelium (Gindele, 2021).

Moreover, CS has been shown to contribute to epithelial barrier dysfunction in COPD through an EGFR-dependent mechanism. Specifically, CS can disrupt intercellular junctions by affecting proteins such as zonula occludens (ZO)1 and occludin (OCLN) through EGFR (HER1) and HER2-dependent extracellular signal-regulated kinases (Erk), leading to increased IL-6 release and subsequent epithelial barrier dysfunction (Mishra et al., 2016; Heijink et al., 2012). In our study, the observed reduction in EGFR gene expression levels in HAEC cells by 24-hour CSE exposure compared may be explained by the continuation of the oxidative stress response and the induction of ferroptosis. However, our study's limitation is the lack of direct evidence

showing the induction of ferroptosis, which would be valuable to confirm this mechanism. On the other hand, the reduction in EGFR expression observed in our study may be linked to the upregulation of miRNAs found to be associated with EGFR downregulation, specifically hsa-mir-21-5p, hsa-mir-335-5p, hsa-mir-218-5p, hsa-mir-16-5p, and hsa-mir-128-3p. The activation and increased levels of these miRNAs could contribute to the observed decrease in EGFR gene expression in airway epithelial cells following CSE exposure. Investigating the expression levels of these miRNAs would help elucidate the underlying mechanisms responsible for the reduction in EGFR during cigarette smoke exposure in airway epithelial cells.

BRD4 is a crucial epigenetic factor that regulates cancer cell proliferation, apoptosis, and various forms of programmed cell death, with varying biological outcomes (Hu, Jinfeng et al.,2022). Brd4 may have a direct role in ferroptosis by controlling the metabolism of polyunsaturated fatty acids (PUFAs), iron, and glutathione. It inhibits the autophagic degradation of ferritin and transcriptionally promotes the production of GAP4, SLC7A11, and SLC3A2, hence suppressing ferroptosis (Hu et al., 2022). Iron metabolism is crucial for ferroptosis, with iron chelators suppressing ROS accumulation and excess iron causing it (Chen et al., 2020; Dixon et al.2012; Li et al., 2017). The import, export, storage, utilization, and turnover of iron affect cell sensitivity. Ferroptosis can be induced under JQ1 treatment and Brd4 knockdown in cancer cell lines and mouse tumor xenografts. (Sui et al.,2019). Additionally, aberrant lipid metabolism, particularly polyunsaturated fatty acids (PUFAs), is associated with ferroptosis. Enzymes involved in the biosynthesis or remodeling of PUFAs can trigger or block ferroptosis. (Sui et al., 2019).

In our study, BRD4 gene did not show a significant change in BEAS 2B cells under cigarette exposure; however, in primary cells, the gene expression was downregulated by CSE. The downregulation of this gene's expression suggests that it may positively affect the ferroptosis mechanism. BRD4 may have also increased the sensitivity of cells to ferroptosis by possibly inhibiting GPX4 activity (Zhu et al., 2024). Despite evidence that BRD4 expression is increased in COPD patients (Tang et al., 2019), our study found that short-term CSE exposure led to a reduction in BRD4 mRNA levels. This decrease in BRD4 expression may be attributed to the post-transcriptional regulation by miRNAs such as hsa-mir-26b-5p and hsa-mir-204-5p. Previous studies have demonstrated the role

of another miRNAs in regulating BRD4. For instance, Tang et al. (2019) reported that BRD4 was upregulated in the lungs of COPD patients, and this increase was negatively correlated with mir-29b and IL-8. Moreover, mir-29b was found to be reduced in both the plasma and lungs of COPD patients. In vitro experiments from the same study showed that mir-29b targeted BRD4 in human bronchial epithelial cells exposed to CSE, regulating IL-8 expression. Another study found that in human lung microvascular endothelial cells exposed to CSE, mir-218-5p directly targeted BRD4, which was mediated by one of the long-noncoding genes, MIR155HG being upregulated by CSE. Functional studies revealed that this lncRNA contributed to the pathogenesis of smoking-related COPD through the mir-128-5p/BRD4 axis, regulating apoptosis and inflammatory processes (Song et al., 2020). Additionally, a separate study showed that in smoking-related COPD, BRD4 and a circular RNA, CircANKRD11, were increased in the lung tissues of both smoking and non-smoking COPD patients, while mir-145-5p was decreased. Similar results were observed in human lung microvascular endothelial cells exposed to CSE. The study demonstrated that BRD4 was targeted by mir-145-5p, contributing to the regulation of BRD4 expression in COPD (Wang et al., 2021). Several additional studies have explored the regulation of BRD4 in COPD. Notably, these studies identified that BRD4 was regulated by the miRNA circ-OSBPL2/mir-193a-5p axis, contributing to smoking-related COPD (Zheng et al., 2021). Therefore, our results also support that BRD4 is a negative regulator of ferroptosis, and it could be regulated by miRNAs.

SRC proto-oncogene, a non-receptor tyrosine kinase (SRC), is a protein that acts as a non-receptor tyrosine kinase and has been associated with pathways that regulate cell growth, division, migration, and survival (Roskoski, 2015). In a study related to liver fibrosis, it was observed that inhibiting SRC activation led to a significant increase in ferroptosis in both hepatic stellate cells (HSCs) and fibrotic liver tissues. This finding suggests a potential link between SRC and ferroptosis (Cheng et al., 2023). However, there is currently a notable gap in research directly exploring the relationship between SRC and ferroptosis in CS-related COPD. In vivo studies conducted in mouse lungs have shown that CS exposure increases c-Src phosphorylation, leading to the upregulation of this transcription factor. Moreover, prolonged CS exposure further enhances this activity. Silencing c-Src in human small airway epithelial cells was found to suppress CS-induced MAPK activation, which led to decreased levels of pro-inflammatory mediators such as

IL-1B, IL-6, and MMP-9. Additionally, the study identified that the interaction between c-Src and EGFR was a key determinant of MAPK activation, emphasizing the role of c-Src in regulating EGFR signaling in response to CS exposure (Geraghty et al., 2014). This interaction could explain why both SRC and EGFR expression levels decreased in our study following CSE exposure. The coordinated downregulation of these two factors suggests that c-Src may have a significant impact on EGFR signaling during CSE exposure, and this relationship could be a critical factor in the cellular response to CS, particularly in processes related to inflammation and tissue remodelling.

The growth/differentiation factor 15 (GDF15) gene, also known as macrophage inhibitory cytokine 1, encodes a secreted ligand of the TGF-beta (transforming growth factor-beta) superfamily of proteins. Under normal circumstances, GDF15 mRNA is minimally expressed in other organs and is most prevalent in the liver, placenta, and prostate. Under pathologic conditions, however, GDF15 expression is markedly elevated in numerous tissues or cell types (e.g. acute injury and inflammation). Elevated GDF15 could control apoptosis, inflammation, and cell division in a number of illnesses, such as viral infections, liver damage, cancer, cardiovascular disorders, and thalassemia (Wu et al., 2012). There are very few studies on GDF15 expression and function in the lung. Rats' bronchial epithelial cells express GDF15 mRNA, as shown in in situ hybridization (Böttner et al., 1999). According to a recent study, vascular endothelial cells in the lungs of patients with pulmonary arterial hypertension have much higher amounts of GDF15 protein than human normal bronchial and alveolar epithelial cells (Nickel et al., 2011). In a study, it has been showed that GDF15 knockdown promotes erastin-induced ferroptosis in a gastric cancer cell line by attenuating the expression of SLC7A11 and the function of system X_c^- (Chen et al., 2020). In COPD smoker patients, the expression of GDF15 has been observed to be higher compared to non-smokers, particularly in ciliated cells. In air-liquid interface (ALI) experiments, GDF15 was found to be responsible for the increased expression of MUC5AC in airway cells stimulated by CSE through PIK3 activation. This suggests that the differentiation status of the cells used *in vitro* could influence the response to CSE exposure. A recent study reported that GDF15 levels are generally low in normal human bronchial and alveolar epithelial cells but elevated in endothelial cells from lungs with pulmonary arterial hypertension and in well-differentiated, ciliated bronchial epithelial cells (Wu et al., 2012). This increase was particularly pronounced

following CSE exposure. In our study, the observed decrease in GDF15 expression after CSE exposure might be due to the use of submerged culture for HAEC cells, which do not differentiate as ALI cultures or in vivo conditions of the human airways. However, submerged cultures are commonly used in toxicological studies to assess the effects of toxic materials like CSE.

The protein that TP63 encodes is frequently employed as an immunohistochemical marker of squamous cell carcinoma, a malignancy that is closely linked to tobacco use (Khayyata et al., 2009; Zhang et al., 2009). TP63 is one of the transcription factors that transactivates TP53 target genes. Therefore, a change in TP63 expression would result in a change in the proliferation of the cells (Yang et al., 1998). GPX2, which encodes a glutathione peroxidase, is up regulated by p63 but not p53. P63 is also one of the basal cell markers in the airway epithelium, along with cytokeratin 5 and 14. It plays a critical role in the renewal and maintenance of the basal cell population, which is essential for airway epithelial homeostasis and repair processes. (Rock et al., 2009). CCS exposure increases the levels of p63 in basal cells, which highly express CK5, CK14, and p63, as well as EGFR levels in intermediate cells that also express basal cell markers, such as SCGB1A1 and CYP2F1 (Zuo et al., 2020). In a study, which chronic CSE exposure was performed, it was reported that the mRNA levels of basal cell markers CK5, CK14, and p63 did not change in primary bronchial epithelial cells cultured using the ALI method (Schamberger et al., 2015). More recently, we found a decrease in expression of CK5, CK14, and p63 in bronchial epithelial explants and cells cultured from these explants from both COPD and non-COPD smoker patients, indicating a reduction in basal cell numbers (Bostancieri et al., 2023). Based on the results of these studies, the reduction in p63 levels in COPD, a disease associated with aging, may be linked to cellular senescence. Considering the relationship between cigarette smoking and cellular senescence, smoking-induced cellular aging may contribute to biological aging, and all these processes could potentially be connected to ferroptosis. In our CSE exposure experiment, the reduction in TP63 levels could also be related to the increase in ferroptosis and cellular senescence, which might be associated with the decline in basal cell numbers. Since this was not one of the primary objectives of our study, further research is needed to investigate the changes in cellular senescence and basal cell populations.

CD44 is one of the efferocytosis receptors that is present at low levels on the surface of lung macrophages (Hodge et al., 2007). CD44 plays a role in the removal of hyaluronan, lipid metabolism, surfactant processing, and efferocytosis, all of which contribute to the regulation of inflammation. CD44 was found to be decreased in alveolar macrophages (AM) from smokers compared to non-smokers (Hodge et al., 2007; Pans et al., 2005). Efferocytosis is a highly regulated process involving the interaction of ligands, such as phosphatidylserine and calreticulin, present on apoptotic cells, with cell surface receptors on clearance cells, including macrophages, fibroblasts, epithelial, and endothelial cells. These receptors include the phosphatidylserine receptor, CD14, CD31, CD44, αvβ3/5 integrins, and surfactant proteins A and D, all of which facilitate the recognition and removal of apoptotic cells (Vandivier et al., 2006). AMs identify apoptotic cells through cell surface receptors, including CD44 (a hyaluronan receptor), which is expressed at lower levels in smokers. CD44 plays a crucial role in clearing apoptotic neutrophils and releasing anti-inflammatory and pro-repair mediators, such as TGF-β. Cigarette smoke (CS) has been shown to impair efferocytosis in AMs by altering the interaction between AMs and cigarette smoke-modified extracellular matrix (ECM) proteins, as well as disrupting surfactant processing (Teder et al., 2002; Kirkham et al., 2004).

It has been shown that smoking leads to a decrease in CD44 levels in alveolar macrophages. This reduction has also been found to impair the target recognition and phagocytic ability of alveolar macrophages in COPD (Hodge et al., 2007). A recent study in Cd44−/− mice demonstrated that deficiency of CD44 on alveolar macrophages disrupted surfactant lipid homeostasis (Hristova et al., 2022; Dong et al., 2020) suggested that CD44 deficiency leads to abnormal lipid accumulation and oxidation, exacerbated by oxidized lipid-induced lung inflammation. In a study conducted on airway epithelial cells, it was shown that the activation of the EGFR and CD44 interaction could lead to the upregulation of mucin (Casalino-Matsuda et al., 2006). In our study, the decrease in CD44 expression after CSE exposure suggests that cells may become less recognizable by macrophages, leading to an exacerbation of airway epithelial damage. This could potentially trigger a molecular change that promotes ferroptosis.

The present study has several limitations. Firstly, because few studies on the role of ferroptosis in COPD have been performed, and only the FerDb database currently provides information on ferroptosis-related genes, more related genes remain to be

discovered. Secondly, further experimental evidence is needed to validate the ferroptosis regulatory function of these genes in COPD. Thirdly, the experimental study should be repeated using ALI cultures, airway epithelial organoids, or primary airway epithelial cells directly obtained from patients, which could better reflect the well-differentiated state of airway epithelial cells. It is also necessary to check which cell type's specific expression is observed by examining these genes in the single-cell data set. The cells can be marked with Bodipy, a lipid peroxidation marker, and the results obtained by flow cytometry can be examined for correlation with other parameters. Erastin and RSL3, the ferroptosis driver and suppressor, exposure experiments are important. When ferroptosis is stimulated or inhibited, more clear information can be obtained about the functions of these genes and the changes in these genes. Western blotting methods must be performed for 2 genes (EGFR and SRC) which are demonstrated to be downregulated in qPCR and bioinformatic results. In this way, the transcriptome data would be confirmed at the protein level, and the role of ferroptosis in the pathogenesis of smoking-induced COPD could be explained in more detail. The release of pro-inflammatory cytokines, such as IL-1B, IL-6, IL-8, GM-CSF, and TNF-a levels could be analysed in the supernatant from cell cultures treated with CSE by ELISA.

In conclusion, we have revealed the relationship between ferroptosis and six hub genes except MDM2 in the pathogenesis of CSE-induced COPD, by bioinformatics analysis, which was validated by qPCR and our findings suggest this, as a potential therapeutic target for future studies.

BIBLIOGRAPHY

Adeloye, D., Chua, S., Lee, C., Basquill, C., Papana, A., Theodoratou, E., Nair, H., Gasevic, D., Sridhar, D., Campbell, H., Chan, K. Y., Sheikh, A., Rudan, I., & Global Health Epidemiology Reference Group (GHERG) (2015). Global and regional estimates of COPD prevalence: Systematic review and meta-analysis. *Journal of global health*, *5*(2), 020415.

Adeloye, D., Song, P., Zhu, Y., Campbell, H., Sheikh, A., Rudan, I., & NIHR RESPIRE Global Respiratory Health Unit (2022). Global, regional, and national prevalence of, and risk factors for, chronic obstructive pulmonary disease (COPD) in 2019: a systematic review and modelling analysis. *The Lancet. Respiratory medicine*, *10*(5), 447–458.

Aghapour, M., Raee, P., Moghaddam, S. J., Hiemstra, P. S., & Heijink, I. H. (2018). Airway Epithelial Barrier Dysfunction in Chronic Obstructive Pulmonary Disease: Role of Cigarette Smoke Exposure. *American journal of respiratory cell and molecular biology*, *58*(2), 157–169.

Agusti, A., Böhm, M., Celli, B., Criner, G. J., Garcia-Alvarez, A., Martinez, F., ... & Vogelmeier, C. F. (2024). GOLD COPD DOCUMENT 2023: a brief update for practicing cardiologists. *Clinical Research in Cardiology*, *113*(2), 195-204.

Agustí, A., & Hogg, J. C. (2019). Update on the Pathogenesis of Chronic Obstructive Pulmonary Disease. *The New England journal of medicine*, *381*(13), 1248–1256.

Amatngalim, G. D., Broekman, W., Daniel, N. M., van der Vlugt, L. E., van Schadewijk, A., Taube, C., & Hiemstra, P. S. (2016). Cigarette Smoke Modulates Repair and Innate Immunity following Injury to Airway Epithelial Cells. *PloS one*, *11*(11), e0166255.

Antunes, M. A., Lopes-Pacheco, M., & Rocco, P. R. M. (2021). Oxidative Stress-Derived Mitochondrial Dysfunction in Chronic Obstructive Pulmonary Disease: A Concise Review. *Oxidative medicine and cellular longevity*, *2021*, 6644002.

Aoshiba, K., Tamaoki, J., & Nagai, A. (2001). Acute cigarette smoke exposure induces apoptosis of alveolar macrophages. *American Journal of Physiology-Lung Cellular and Molecular Physiology*, *281*(6), L1392-L1401.

Bao, H., Zhou, Q., Li, Q., Niu, M., Chen, S., Yang, P., Liu, Z., & Xia, L. (2020). Differentially expressed circular RNAs in a murine asthma model. *Molecular medicine reports*, *22*(6), 5412–5422.

Barnes P. J. (2015). Therapeutic approaches to asthma-chronic obstructive pulmonary disease overlap syndromes. *The Journal of allergy and clinical immunology*, *136*(3), 531–545.

Barnes P. J. (2016). Inflammatory mechanisms in patients with chronic obstructive pulmonary disease. *The Journal of allergy and clinical immunology*, *138*(1), 16–27.

Barnes P. J. (2020). COPD 2020: new directions needed. *American journal of physiology. Lung cellular and molecular physiology*, *319*(5), L884–L886.

Barnes, P. J., & Celli, B. R. (2009). Systemic manifestations and comorbidities of COPD. *The European respiratory journal*, *33*(5), 1165–1185.

Barrett, T., Wilhite, S. E., Ledoux, P., Evangelista, C., Kim, I. F., Tomashevsky, M., Marshall, K. A., Phillippy, K. H., Sherman, P. M., Holko, M., Yefanov, A., Lee, H., Zhang, N., Robertson, C. L., Serova, N., Davis, S., & Soboleva, A. (2013). NCBI GEO: archive for functional genomics data sets--update. *Nucleic acids research*, *41*(Database issue), D991–D995.

Bartos, A., & Sikora, J. (2023). Bioinorganic Modulators of Ferroptosis: A Review of Recent Findings. *International journal of molecular sciences*, *24*(4), 3634.

Beeh, K. M., Beier, J., Kornmann, O., Mander, A., & Buhl, R. (2003). Long-term repeatability of induced sputum cells and inflammatory markers in stable, moderately severe COPD. *Chest*, *123*(3), 778–783.

Benam, K. H., Novak, R., Nawroth, J., Hirano-Kobayashi, M., Ferrante, T. C., Choe, Y., Prantil-Baun, R., Weaver, J. C., Bahinski, A., Parker, K. K., & Ingber, D. E. (2016). Matched-Comparative Modeling of Normal and Diseased Human Airway Responses Using a Microengineered Breathing Lung Chip. *Cell systems*, *3*(5), 456–466.e4.

Bond, G. L., Hu, W., & Levine, A. J. (2005). MDM2 is a central node in the p53 pathway: 12 years and counting. *Current cancer drug targets*, *5*(1), 3-8.

Boschetto, P., Quintavalle, S., Zeni, E., Leprotti, S., Potena, A., Ballerin, L., Papi, A., Palladini, G., Luisetti, M., Annovazzi, L., Iadarola, P., De Rosa, E., Fabbri, L. M., & Mapp, C. E. (2006). Association between markers of emphysema and more severe chronic obstructive pulmonary disease. *Thorax*, *61*(12), 1037–1042.

Bostancieri, N., Bakir, K., Kul, S., Eralp, A., Kayalar, O., Konyalilar, N., Rajabi, H., Yuncu, M., Yildirim, A.Ö. and Bayram, H., 2023. The effect of multiple outgrowths from bronchial tissue explants on progenitor/stem cell number in primary bronchial epithelial cell cultures from smokers and patients with COPD. *Frontiers in Medicine*, *10*, p.1118715.

Böttner, M., Laaff, M., Schechinger, B., Rappold, G., Unsicker, K., & Suter-Crazzolara, C. (1999). Characterization of the rat, mouse, and human genes of growth/differentiation factor-15/macrophage inhibiting cytokine-1 (GDF-15/MIC-1). *Gene*, *237*(1), 105-111.

Brehm, J. M., Hagiwara, K., Tesfaigzi, Y., Bruse, S., Mariani, T. J., Bhattacharya, S., Boutaoui, N., Ziniti, J. P., Soto-Quiros, M. E., Avila, L., Cho, M. H., Himes, B., Litonjua, A. A., Jacobson, F., Bakke, P., Gulsvik, A., Anderson, W. H., Lomas, D. A., Forno, E., Datta, S., … Celedón, J. C. (2011). Identification of FGF7 as a novel susceptibility locus for chronic obstructive pulmonary disease. *Thorax*, *66*(12), 1085–1090.

Brightling, C., & Greening, N. (2019). Airway inflammation in COPD: progress to precision medicine. *The European respiratory journal*, *54*(2), 1900651.

Carolan, B. J., Harvey, B. G., De, B. P., Vanni, H., & Crystal, R. G. (2008). Decreased expression of intelectin 1 in the human airway epithelium of smokers compared to nonsmokers. *The Journal of Immunology*, *181*(8), 5760-5767.

Chen, L., Qiao, L., Bian, Y., & Sun, X. (2020). GDF15 knockdown promotes erastin-induced ferroptosis by decreasing SLC7A11 expression. *Biochemical and biophysical research communications*, *526*(2), 293-299.

Chen, H., & Boutros, P. C. (2011). VennDiagram: a package for the generation of highly-customizable Venn and Euler diagrams in R. *BMC bioinformatics*, *12*, 35.

Chen, J., Deng, X., Xie, H., Wang, C., Huang, J., & Lian, N. (2024). Circular RNA_0025843 Alleviated Cigarette Smoke Extract Induced Bronchoalveolar Epithelial Cells Ferroptosis. *International journal of chronic obstructive pulmonary disease*, *19*, 363–374.

Chen, X., Yu, C., Kang, R., & Tang, D. (2020). Iron Metabolism in Ferroptosis. *Frontiers in cell and developmental biology*, *8*, 590226.

Cheng, Z., Zhang, X., Chen, P., Wang, H., Wang, K., & Shen, Y. (2023). Sarcoma protein kinase inhibition alleviates liver fibrosis by promoting hepatic stellate cells ferroptosis. *Open Life Sciences*, *18*(1), 20220781.

Cho, M.H., Castaldi, P.J., Wan, E.S., Siedlinski, M., Hersh, C.P., Demeo, D.L., Himes, B.E., Sylvia, J.S., Klanderman, B.J., Ziniti, J.P. and Lange, C., 2012. A genome-wide association study of COPD identifies a susceptibility locus on chromosome 19q13. *Human molecular genetics*, *21*(4), pp.947-957.

Chung K. F. (2001). Cytokines in chronic obstructive pulmonary disease. *The European respiratory journal. Supplement*, *34*, 50s–59s.

Chung, K. F., & Adcock, I. M. (2008). Multifaceted mechanisms in COPD: inflammation, immunity, and tissue repair and destruction. *European Respiratory Journal*, *31*(6), 1334-1356.

Conrad, M., & da Silva, M. C. (2020). Ferroptosis: Physiological and pathophysiological aspects. In *Oxidative stress* (pp. 149-166). Academic Press.

Demedts, I. K., Demoor, T., Bracke, K. R., Joos, G. F., & Brusselle, G. G. (2006). Role of apoptosis in the pathogenesis of COPD and pulmonary emphysema. *Respiratory research*, *7*(1), 53.

D'Herde, K., & Krysko, D. V. (2017). Ferroptosis: Oxidized PEs trigger death. *Nature chemical biology*, *13*(1), 4–5.

Díaz-Peña, R., Boekstegers, F., Silva, R. S., Jaime, S., Hosgood Iii, H. D., Miravitlles, M., Agustí, À., Lorenzo Bermejo, J., & Olloquequi, J. (2020). Amerindian Ancestry Influences Genetic Susceptibility to Chronic Obstructive Pulmonary Disease. *Journal of personalized medicine*, *10*(3), 93.

Dixon, S. J., Lemberg, K. M., Lamprecht, M. R., Skouta, R., Zaitsev, E. M., Gleason, C. E., Patel, D. N., Bauer, A. J., Cantley, A. M., Yang, W. S., Morrison, B., 3rd, & Stockwell, B. R. (2012). Ferroptosis: an iron-dependent form of nonapoptotic cell death. *Cell*, *149*(5), 1060–1072.

Dixon, S. J., Patel, D. N., Welsch, M., Skouta, R., Lee, E. D., Hayano, M., Thomas, A. G., Gleason, C. E., Tatonetti, N. P., Slusher, B. S., & Stockwell, B. R. (2014). Pharmacological inhibition of cystine-glutamate exchange induces endoplasmic reticulum stress and ferroptosis. *eLife*, *3*, e02523.

Dixon, S. J., Winter, G. E., Musavi, L. S., Lee, E. D., Snijder, B., Rebsamen, M., Superti-Furga, G., & Stockwell, B. R. (2015). Human Haploid Cell Genetics Reveals

Roles for Lipid Metabolism Genes in Nonapoptotic Cell Death. *ACS chemical biology*, *10*(7), 1604–1609.

Dong, Y., Arif, A.A., Guo, J., Ha, Z., Lee-Sayer, S.S., Poon, G.F., Dosanjh, M., Roskelley, C.D., Huan, T. and Johnson, P., 2020. CD44 loss disrupts lung lipid surfactant homeostasis and exacerbates oxidized lipid-induced lung inflammation. *Frontiers in immunology*, *11*, p.29.

Dos Santos, A. F., Fazeli, G., da Silva, T. N. X., & Angeli, J. P. F. (2023). Ferroptosis: mechanisms and implications for cancer development and therapy response. *Trends in cell biology*, *33*(12), 1062-1076.

Dowdle, W.E., Nyfeler, B., Nagel, J., Elling, R.A., Liu, S., Triantafellow, E., Menon, S., Wang, Z., Honda, A., Pardee, G. and Cantwell, J., 2014. Selective VPS34 inhibitor blocks autophagy and uncovers a role for NCOA4 in ferritin degradation and iron homeostasis in vivo. *Nature cell biology*, *16*(11), pp.1069-1079.

Feng, Y., Li, M., Yangzhong, X., Zhang, X., Zu, A., Hou, Y., Li, L., &; Sun, S. (2022). Pyroptosis in inflammation-related respiratory disease. *Journal of physiology and biochemistry*, *78(4)*, 721–737.

Ferrarotti, I., Thun, G. A., Zorzetto, M., Ottaviani, S., Imboden, M., Schindler, C., von Eckardstein, A., Rohrer, L., Rochat, T., Russi, E. W., Probst-Hensch, N. M., & Luisetti, M. (2012). Serum levels and genotype distribution of α1-antitrypsin in the general population. *Thorax*, 67(8), 669–674.

Fu, R., You, Y., Wang, Y., Wang, J., Lu, Y., Gao, R., Pang, M., Yang, P., & Wang, H. (2024). Sanggenol L induces ferroptosis in non-small cell lung cancer cells via regulating the miR-26a-1-3p/MDM2/p53 signaling pathway. *Biochemical pharmacology*, *226*, 116345.

Gadgil, A., & Duncan, S. R. (2008). Role of T-lymphocytes and pro-inflammatory mediators in the pathogenesis of chronic obstructive pulmonary disease. *International journal of chronic obstructive pulmonary disease*, *3*(4), 531–541.

Geraghty, P., Hardigan, A. and Foronjy, R.F., 2014. Cigarette smoke activates the proto-oncogene c-src to promote airway inflammation and lung tissue destruction. *American journal of respiratory cell and molecular biology*, *50*(3), pp.559-570.

Gharib, S. A., Manicone, A. M., & Parks, W. C. (2018). Matrix metalloproteinases in emphysema. *Matrix biology : journal of the International Society for Matrix Biology*, *73*, 34–51.

Ghio, A. J., Hilborn, E. D., Stonehuerner, J. G., Dailey, L. A., Carter, J. D., Richards, J. H., Crissman, K. M., Foronjy, R. F., Uyeminami, D. L., & Pinkerton, K. E. (2008). Particulate matter in cigarette smoke alters iron homeostasis to produce a biological effect. *American journal of respiratory and critical care medicine*, *178*(11), 1130–1138.

Gindele, J.A., 2021. *Characterization of the molecular mechanisms underlying the pathophysiological differentiation of small airway epithelial cells in Chronic Obstructive Pulmonary Disease (COPD)* (Doctoral dissertation, Universität Ulm).

Goldklang, M., & Stockley, R. (2016). Pathophysiology of emphysema and implications. *Chronic obstructive pulmonary diseases*, *3*(1), 454.

Gryzik, M., Asperti, M., Denardo, A., Arosio, P., & Poli, M. (2021). NCOA4-mediated ferritinophagy promotes ferroptosis induced by erastin, but not by RSL3 in HeLa cells. *Biochimica et biophysica acta. Molecular cell research*, *1868*(2), 118913.

Gu, L., Wang, Z., Zuo, J., Li, H., & Zha, L. (2018). Prognostic significance of NF-κB expression in non-small cell lung cancer: A meta-analysis. *PloS one*, *13*(5), e0198223.

Gu, Zuguang et alComplex heatmaps reveal patterns and correlations in multidimensional genomic data. *Bioinformatics (Oxford, England)*, *32*(18), 2847–2849.

Guo, P., Li, R., Piao, T. H., Wang, C. L., Wu, X. L., & Cai, H. Y. (2022). Pathological mechanism and targeted drugs of COPD. *International journal of chronic obstructive pulmonary disease*, 1565-1575.

Guo, Y., Gong, Y., Pan, C., Qian, Y., Shi, G., Cheng, Q., Li, Q., Ren, L., Weng, Q., Chen, Y., Cheng, T., Fan, L., Jiang, Z., & Wan, H. (2012). Association of genetic polymorphisms with chronic obstructive pulmonary disease in the Chinese Han population: a case-control study. *BMC medical genomics*, *5*, 64.

Günes Günsel, G., Conlon, T. M., Jeridi, A., Kim, R., Ertüz, Z., Lang, N. J., ... & Yildirim, A. Ö. (2022). The arginine methyltransferase PRMT7 promotes extravasation of monocytes resulting in tissue injury in COPD. *Nature communications*, *13*(1), 1303.

Hancock, D. B., Eijgelsheim, M., Wilk, J. B., Gharib, S. A., Loehr, L. R., Marciante, K. D., ... & London, S. J. (2010). Meta-analyses of genome-wide association studies identify multiple loci associated with pulmonary function. *Nature genetics*, *42(1)*, 45-52.

Hao, W., Li, M., Zhang, C., Zhang, Y., & Xue, Y. (2019). High Serum Fractalkine/CX3CL1 in Patients with Chronic Obstructive Pulmonary Disease: Relationship with Emphysema Severity and Frequent Exacerbation. *Lung*, *197*(1), 29–35.

Halpin, D. M., Criner, G. J., Papi, A., Singh, D., Anzueto, A., Martinez, F. J., ... & Vogelmeier, C. F. (2021). Global initiative for the diagnosis, management, and prevention of chronic obstructive lung disease. The 2020 GOLD science committee report on COVID-19 and chronic obstructive pulmonary disease. *American journal of respiratory and critical care medicine*, *203*(1), 24-36.

Hardin, M., Cho, M., McDonald, M. L., Beaty, T., Ramsdell, J., Bhatt, S., van Beek, E. J., Make, B. J., Crapo, J. D., Silverman, E. K., & Hersh, C. P. (2014). The clinical and genetic features of COPD-asthma overlap syndrome. *The European respiratory journal*, 44(2), 341–350.

Hata, H., Yoshimoto, T., Hayashi, N., Hada, T., & Nakanishi, K. (2004). IL-18 together with anti-CD3 antibody induces human Th1 cells to produce Th1-and Th2-cytokines and IL-8. *International immunology*, *16(12)*, 1733-1739.

Heijink, I. H., Brandenburg, S. M., Postma, D. S., & van Oosterhout, A. J. (2012). Cigarette smoke impairs airway epithelial barrier function and cell-cell contact recovery. *The European respiratory journal*, *39*(2), 419–428.

Hikichi, M., Mizumura, K., Maruoka, S., & Gon, Y. (2019). Pathogenesis of chronic obstructive pulmonary disease (COPD) induced by cigarette smoke. *Journal of thoracic disease*, *11*(Suppl 17), S2129–S2140.

Hobbs, B. D., Morrow, J. D., Wang, X. W., Liu, Y. Y., DeMeo, D. L., Hersh, C. P., ... & Cho, M. H. (2023). Identifying chronic obstructive pulmonary disease from integrative omics and clustering in lung tissue. BMC Pulmonary Medicine, 23(1), 115.

Hodge S, Hodge G, Ahern J. Smoking alters alveolar macrophage recognition and phagocytic ability: implications in chronic obstructive pulmonary disease. American journal of respiratory cell and molecular biology 2007; 37:748–55.

Hogg, J. C., Paré, P. D., & Hackett, T. L. (2017). The Contribution of Small Airway Obstruction to the Pathogenesis of Chronic Obstructive Pulmonary Disease. *Physiological reviews*, *97*(2), 529–552.

Hou, W., Hu, S., Li, C., Ma, H., Wang, Q., Meng, G., Guo, T., & Zhang, J. (2019). Cigarette Smoke Induced Lung Barrier Dysfunction, EMT, and Tissue Remodeling: A

Possible Link between COPD and Lung Cancer. *BioMed research international*, *2019*, 2025636.

Howell, T. (2007). *The role of the epidermal growth factor receptor and its ligands in the regulation of the bronchial epithelial phenotype in smoking related lung disease* (Doctoral dissertation, University of Southampton).

Hristova, V. A., Watson, A., Chaerkady, R., Glover, M. S., Ackland, J., Angerman, B., Belfield, G., Belvisi, M. G., Burke, H., Cellura, D., Clark, H. W., Etal, D., Freeman, A., Heinson, A. I., Hess, S., Hühn, M., Hall, E., Mackay, A., Madsen, J., McCrae, C., … MICA II Study group (2022). Multiomics links global surfactant dysregulation with airflow obstruction and emphysema in COPD. *ERJ open research*, *9*(3), 00378-2022.

Hu, J., Pan, D., Li, G., Chen, K., & Hu, X. (2022). Regulation of programmed cell death by Brd4. *Cell death & disease*, *13*(12), 1059.

Imai, H., Matsuoka, M., Kumagai, T., Sakamoto, T., & Koumura, T. (2017). Lipid Peroxidation-Dependent Cell Death Regulated by GPx4 and Ferroptosis. *Current topics in microbiology and immunology*, *403*, 143–170.

Jeridi, A., Kapellos, T. S., & Yildirim, A. Ö. (2023). Fumarate hydratase: a new checkpoint of metabolic regulation in inflammatory macrophages. *Signal transduction and targeted therapy*, *8*(1), 332.

Ji, Q., Zhang, L., & Ye, H. (2024). Melatonin improves stroke through MDM2-mediated ubiquitination of ACSL4. *Aging (Albany NY)*, *16*(2), 1925.

Jiang, L., Kon, N., Li, T., Wang, S. J., Su, T., Hibshoosh, H., Baer, R., & Gu, W. (2015). Ferroptosis as a p53-mediated activity during tumour suppression. *Nature*, *520*(7545), 57–62.

Jiang, X., Stockwell, B. R., & Conrad, M. (2021). Ferroptosis: mechanisms, biology and role in disease. *Nature reviews. Molecular cell biology*, *22*(4), 266–282.

Kanehisa, M., & Goto, S. (2000). KEGG: kyoto encyclopedia of genes and genomes. *Nucleic acids research*, *28*(1), 27–30.

Kanehisa, M., Furumichi, M., Sato, Y., Ishiguro-Watanabe, M., & Tanabe, M. (2021). KEGG: integrating viruses and cellular organisms. *Nucleic acids research*, *49*(D1), D545–D551.

Kanehisa, M., Furumichi, M., Sato, Y., Kawashima, M., & Ishiguro-Watanabe, M. (2023). KEGG for taxonomy-based analysis of pathways and genomes. *Nucleic acids research*, *51*(D1), D587–D592.

Kashatus D, Cogswell P, Baldwin AS. Expression of the Bcl-3 proto-oncogene suppresses p53 activation. Genes Dev. 2006;20(2):225–35.

Kaur, M., Chandel, J., Malik, J., & Naura, A. S. (2022). Particulate matter in COPD pathogenesis: an overview. *Inflammation Research*, *71*(7), 797-815.

Kayalar, Ö., Rajabi, H., Konyalilar, N., Mortazavi, D., Aksoy, G. T., Wang, J., & Bayram, H. (2024). Impact of particulate air pollution on airway injury and epithelial plasticity; underlying mechanisms. *Frontiers in immunology*, *15*, 1324552.

Keatings, V. M., Collins, P. D., Scott, D. M., & Barnes, P. J. (1996). Differences in interleukin-8 and tumor necrosis factor-alpha in induced sputum from patients with chronic obstructive pulmonary disease or asthma. *American journal of respiratory and critical care medicine*, *153*(2), 530–534.

Khawas, S., & Sharma, N. (2024). Cell death crosstalk in respiratory diseases: unveiling the relationship between pyroptosis and ferroptosis in asthma and COPD. *Molecular and Cellular Biochemistry*, *1-22*.

Khayyata, S., Yun, S., Pasha, T., Jian, B., McGrath, C., Yu, G., Gupta, P., & Baloch, Z. (2009). Value of P63 and CK5/6 in distinguishing squamous cell carcinoma from adenocarcinoma in lung fine-needle aspiration specimens. *Diagnostic cytopathology*, *37*(3), 178–183.

Kirkham, P. A., Spooner, G., Rahman, I., & Rossi, A. G. (2004). Macrophage phagocytosis of apoptotic neutrophils is compromised by matrix proteins modified by cigarette smoke and lipid peroxidation products. *Biochemical and biophysical research communications*, *318*(1), 32–37.

Kong, X., Cho, M. H., Anderson, W., Coxson, H. O., Muller, N., Washko, G., Hoffman, E. A., Bakke, P., Gulsvik, A., Lomas, D. A., Silverman, E. K., Pillai, S. G., & ECLIPSE Study NETT Investigators (2011). Genome-wide association study identifies BICD1 as a susceptibility gene for emphysema. *American journal of respiratory and critical care medicine*, *183*(1), 43–49.

Kwon, O. S., Kwon, E. J., Kong, H. J., Choi, J. Y., Kim, Y. J., Lee, E. W., Kim, W., Lee, H., & Cha, H. J. (2020). Systematic identification of a nuclear receptor-enriched predictive signature for erastin-induced ferroptosis. *Redox biology*, *37*, 101719.

Levra, S., Rosani, U., Gnemmi, I., Brun, P., Leonardi, A., Carriero, V., ... & Di Stefano, A. (2023). Impaired autophagy in the lower airways and lung parenchyma in stable COPD. *ERJ Open Research*, 9(6).

Li, H., Ma, Y., Li, T., Zeng, Z., Luo, L., Liu, X., Li, Y., & Chen, Y. (2024). CAPN5 attenuates cigarette smoke extract-induced apoptosis and inflammation in BEAS-2B cells. *Tobacco induced diseases*, *22*, 10.18332/tid/186183.

Li, J., Cao, F., Yin, H. L., Huang, Z. J., Lin, Z. T., Mao, N., Sun, B., & Wang, G. (2020). Ferroptosis: past, present and future. *Cell death & disease*, *11*(2), 88.

Li, Q., Han, X., Lan, X., Gao, Y., Wan, J., Durham, F., Cheng, T., Yang, J., Wang, Z., Jiang, C., Ying, M., Koehler, R. C., Stockwell, B. R., & Wang, J. (2017). Inhibition of neuronal ferroptosis protects hemorrhagic brain. *JCI insight*, *2*(7), e90777.

Li, X., Zhao, F., Wang, A., Cheng, P., & Chen, H. (2021). Role and mechanisms of autophagy in lung metabolism and repair. *Cellular and Molecular Life Sciences*, *78*, 5051-5068.

Li, Y., Yang, Y., Guo, T., Weng, C., Yang, Y., Wang, Z., Zhang, L., & Li, W. (2023). Heme oxygenase-1 determines the cell fate of ferroptotic death of alveolar macrophages in COPD. *Frontiers in immunology*, *14*, 1162087.

Liang, X., Qin, Y., Wu, D., Wang, Q., & Wu, H. (2024). Pyroptosis: a double-edged sword in lung cancer and other respiratory diseases. *Cell communication and signaling: CCS*, *22(1)*, 40.

Liu, M., Kong, X.Y., Yao, Y., Wang, X.A., Yang, W., Wu, H., Li, S., Ding, J.W. and Yang, J., 2022. The critical role and molecular mechanisms of ferroptosis in antioxidant systems: a narrative review. *Annals of translational medicine*, *10*(6).

Liao, C.M., Wulfmeyer, V.C., Chen, R., Erlangga, Z., Sinning, J., von Mässenhausen, A., Sörensen-Zender, I., Beer, K., von Vietinghoff, S., Haller, H. and Linkermann, A., 2022. Induction of ferroptosis selectively eliminates senescent tubular cells. *American Journal of Transplantation*, *22*(9), pp.2158-2168.

Liu, M., Kong, X. Y., Yao, Y., Wang, X. A., Yang, W., Wu, H., ... & Yang, J. (2022). The critical role and molecular mechanisms of ferroptosis in antioxidant systems: a narrative review. *Annals of translational medicine*, *10*(6).Liu, X., Huang, X., & Xu, F. (2023). The influence of pyroptosis-related genes on the development of chronic obstructive pulmonary disease. *BMC pulmonary medicine*, *23(1)*, 167.

Liu, X., Ma, Y., Luo, L., Zong, D., Li, H., Zeng, Z., Cui, Y., Meng, W., & Chen, Y. (2022). Dihydroquercetin suppresses cigarette smoke induced ferroptosis in the pathogenesis of chronic obstructive pulmonary disease by activating Nrf2-mediated

pathway. *Phytomedicine: international journal of phytotherapy and phytopharmacology*, *96*, 153894.

Livak, K. J., & Schmittgen, T. D. (2001). Analysis of relative gene expression data using real-time quantitative PCR and the 2(-Delta Delta C(T)) Method. *Methods (San Diego, Calif.)*, *25*(4), 402–408.

Love, M. I., Huber, W., & Anders, S. (2014). Moderated estimation of fold change and dispersion for RNA-seq data with DESeq2. *Genome biology*, *15*(12), 550.

Lv, X., Li, K., & Hu, Z. (2020). Chronic Obstructive Pulmonary Disease and Autophagy. *Advances in experimental medicine and biology*, *1207*, 559–567.

Manisalidis, I., Stavropoulou, E., Stavropoulos, A., & Bezirtzoglou, E. (2020). Environmental and Health Impacts of Air Pollution: A Review. *Frontiers in public health*, *8*, 14.

Mannino, D. M., Watt, G., Hole, D., Gillis, C., Hart, C., McConnachie, A., ... & Vestbo, J. (2006). The natural history of chronic obstructive pulmonary disease. *European Respiratory Journal*, *27*(3), 627-643.

Maschalidi, S., Mehrotra, P., Keçeli, B.N., De Cleene, H.K., Lecomte, K., Van der Cruyssen, R., Janssen, P., Pinney, J., van Loo, G., Elewaut, D. and Massie, A., 2022. Targeting SLC7A11 improves efferocytosis by dendritic cells and wound healing in diabetes. *Nature*, *606*(7915), pp.776-784.

Meng, D., Zhu, C., Jia, R., Li, Z., Wang, W., & Song, S. (2023). The molecular mechanism of ferroptosis and its role in COPD. *Frontiers in Medicine*, *9*, 1052540.

Mercer, B. A., & D'Armiento, J. M. (2006). Emerging role of MAP kinase pathways as therapeutic targets in COPD. *International journal of chronic obstructive pulmonary disease*, *1*(2), 137–150.

Miller, M. R., Hankinson, J., Brusasco, V., Burgos, F., Casaburi, R., Coates, A., Crapo, R., Enright, P., van der Grinten, C. P., Gustafsson, P., Jensen, R., Johnson, D. C., MacIntyre, N., McKay, R., Navajas, D., Pedersen, O. F., Pellegrino, R., Viegi, G., Wanger, J., & ATS/ERS Task Force (2005). Standardisation of spirometry. *The European respiratory journal*, *26*(2), 319–338.

Mishra, R., Foster, D., Vasu, V.T., Thaikoottathil, J.V., Kosmider, B., Chu, H.W., Bowler, R.P. and Finigan, J.H., 2016. Cigarette smoke induces human epidermal receptor 2–dependent changes in epithelial permeability. *American journal of respiratory cell and molecular biology*, *54*(6), pp.853-864.

Mizumura, K., & Gon, Y. (2021). Iron-Regulated Reactive Oxygen Species Production and Programmed Cell Death in Chronic Obstructive Pulmonary Disease. *Antioxidants (Basel, Switzerland)*, *10*(10), 1569.

Mizuno, S., Ishizaki, T., Kadowaki, M., Akai, M., Shiozaki, K., Iguchi, M., Oikawa, T., Nakagawa, K., Osanai, K., Toga, H. and Gomez-Arroyo, J., 2017. p53 signaling pathway polymorphisms associated with emphysematous changes in patients with COPD. *Chest*, *152*(1), pp.58-69.

Moerke, C., Theilig, F., Kunzendorf, U., & Krautwald, S. (2019). ACSL4 as the first reliable biomarker of ferroptosis under pathophysiological conditions. *Ferroptosis in health and disease*, 111-123.Tang, H. M., & Tang, H. L. (2019). Cell recovery by reversal of ferroptosis. *Biology open*, *8*(6), bio043182.

Morrow, J.D., Zhou, X., Lao, T., Jiang, Z., DeMeo, D.L., Cho, M.H., Qiu, W., Cloonan, S., Pinto-Plata, V., Celli, B. and Marchetti, N., 2017. Functional interactors of three genome-wide association study genes are differentially expressed in severe chronic obstructive pulmonary disease lung tissue. *Scientific reports*, *7*(1), p.44232.

Mou, Y., Wang, J., Wu, J., He, D., Zhang, C., Duan, C., & Li, B. (2019). Ferroptosis, a new form of cell death: opportunities and challenges in cancer. *Journal of hematology & oncology*, *12*, 1-16.

Nickel, N., Jonigk, D., Kempf, T., Bockmeyer, C.L., Maegel, L., Rische, J., Laenger, F., Lehmann, U., Sauer, C., Greer, M. and Welte, T., 2011. GDF-15 is abundantly expressed in plexiform lesions in patients with pulmonary arterial hypertension and affects proliferation and apoptosis of pulmonary endothelial cells. *Respiratory research*, *12*, pp.1-11.

Park, E. J., Park, Y. J., Lee, S. J., Lee, K., & Yoon, C. (2019). Whole cigarette smoke condensates induce ferroptosis in human bronchial epithelial cells. *Toxicology Letters*, *303*, 55-66.

Parris, B. A., O'Farrell, H. E., Fong, K. M., & Yang, I. A. (2019). Chronic obstructive pulmonary disease (COPD) and lung cancer: common pathways for pathogenesis. *Journal of thoracic disease*, *11*(Suppl 17), S2155–S2172.

Pathak, R. K., Singh, D. B., & Singh, R. (2022). Introduction to basics of bioinformatics. In *Bioinformatics* (pp. 1-15). Academic Press.

Pierrou, S., Broberg, P., O'Donnell, R. A., Pawłowski, K., Virtala, R., Lindqvist, E., ... & Djukanovic, R. (2007). Expression of genes involved in oxidative stress responses

in airway epithelial cells of smokers with chronic obstructive pulmonary disease. *American journal of respiratory and critical care medicine*, *175*(6), 577-586.

Pillai, S. G., Ge, D., Zhu, G., Kong, X., Shianna, K. V., Need, A. C., Feng, S., Hersh, C. P., Bakke, P., Gulsvik, A., Ruppert, A., Lødrup Carlsen, K. C., Roses, A., Anderson, W., Rennard, S. I., Lomas, D. A., Silverman, E. K., Goldstein, D. B., & ICGN Investigators (2009). A genome-wide association study in chronic obstructive pulmonary disease (COPD): identification of two major susceptibility loci. *PLoS genetics*, *5*(3), e1000421.

Rahman I. (2005). Oxidative stress in pathogenesis of chronic obstructive pulmonary disease: cellular and molecular mechanisms. *Cell biochemistry and biophysics*, *43*(1), 167–188.

Rajabi, H., Mortazavi, D., Konyalilar, N., Aksoy, G.T., Erkan, S., Korkunc, S.K., Kayalar, O., Bayram, H. and Rahbarghazi, R., 2022. Forthcoming complications in recovered COVID-19 patients with COPD and asthma; possible therapeutic opportunities. *Cell Communication and Signaling*, *20*(1), p.173.

Reddel, R. R., Ke, Y., Gerwin, B. I., McMenamin, M. G., Lechner, J. F., Su, R. T., Brash, D. E., Park, J. B., Rhim, J. S., & Harris, C. C. (1988). Transformation of human bronchial epithelial cells by infection with SV40 or adenovirus-12 SV40 hybrid virus, or transfection via strontium phosphate coprecipitation with a plasmid containing SV40 early region genes. *Cancer research*, *48*(7), 1904–1909.

Rock JR, Onaitis MW, Rawlins EL, Lu Y, Clark CP, Xue Y, Randell SH, Hogan B L. Basal cells as stem cells of the mouse trachea and human airway epithelium. Proc Natl Acad Sci USA 2009; 106:12771–12775.

Roskoski R., Jr (2019). Small molecule inhibitors targeting the EGFR/ErbB family of protein-tyrosine kinases in human cancers. *Pharmacological research*, *139*, 395–411.

Roskoski R., Jr (2015). Src protein-tyrosine kinase structure, mechanism, and small molecule inhibitors. *Pharmacological research*, *94*, 9–25.

Saferali, A., Yun, J. H., Parker, M. M., Sakornsakolpat, P., Chase, R. P., Lamb, A., Hobbs, B. D., Boezen, M. H., Dai, X., de Jong, K., Beaty, T. H., Wei, W., Zhou, X., Silverman, E. K., Cho, M. H., Castaldi, P. J., Hersh, C. P., COPDGene Investigators, & International COPD Genetics Consortium Investigators (2019). Analysis of genetically driven alternative splicing identifies FBXO38 as a novel COPD susceptibility gene. *PLoS genetics*, *15*(7), e1008229.

Sari, E., Oztay, F., & Tasci, A. E. (2020). Vitamin D modulates E-cadherin turnover by regulating TGF-β and Wnt signalings during EMT-mediated myofibroblast differentiation in A459 cells. *The Journal of Steroid Biochemistry and Molecular Biology*, *202*, 105723.

Sato, K., Inoue, S., Igarashi, A., Tokairin, Y., Yamauchi, K., Kimura, T., Nishiwaki, M., Nemoto, T., Nakano, H., Sato, M., Machida, H., Yang, S., Minegishi, Y., Furuyama, K., Watanabe, M., & Shibata, Y. (2020). Effect of Iron Deficiency on a Murine Model of Smoke-induced Emphysema. *American journal of respiratory cell and molecular biology*, *62*(5), 588–597.

Sayers, E. W., Beck, J., Bolton, E. E., Bourexis, D., Brister, J. R., Canese, K., Comeau, D. C., Funk, K., Kim, S., Klimke, W., Marchler-Bauer, A., Landrum, M., Lathrop, S., Lu, Z., Madden, T. L., O'Leary, N., Phan, L., Rangwala, S. H., Schneider, V. A., Skripchenko, Y., … Sherry, S. T. (2021). Database resources of the National Center for Biotechnology Information. *Nucleic acids research*, *49*(D1), D10–D17.

Scanlon, P. D., Connett, J. E., Waller, L. A., Altose, M. D., Bailey, W. C., Buist, A. S., Tashkin, D. P., & Lung Health Study Research Group (2000). Smoking cessation and lung function in mild-to-moderate chronic obstructive pulmonary disease. The Lung Health Study. *American journal of respiratory and critical care medicine*, *161*(2 Pt 1), 381–390.

Schamberger, A.C., Staab-Weijnitz, C. A., Mise-Racek, N., & Eickelberg, O. (2015). Cigarette smoke alters primary human bronchial epithelial cell differentiation at the air-liquid interface. *Scientific reports*, *5*(1), 8163.

Shannon, P., Markiel, A., Ozier, O., Baliga, N. S., Wang, J. T., Ramage, D., Amin, N., Schwikowski, B., & Ideker, T. (2003). Cytoscape: a software environment for integrated models of biomolecular interaction networks. *Genome research*, *13*(11), 2498–2504.

Shaykhiev, R., & Crystal, R. G. (2014). Early events in the pathogenesis of chronic obstructive pulmonary disease. Smoking-induced reprogramming of airway epithelial basal progenitor cells. *Annals of the American Thoracic Society*, *11 Suppl 5*(Suppl 5), S252–S258.

Shen, H. M., & Tergaonkar, V. (2009). NFκB signaling in carcinogenesis and as a potential molecular target for cancer therapy. *Apoptosis*, *14*, 348-363.

Shen, S. Q., Chang, H., Wang, Z. X., Chen, H. Y., Chen, L. F., Gao, F., & Yan, X. W. (2018). The Acute Effects of Cigarette Smoking on the Functional State of High Density Lipoprotein. *The American journal of the medical sciences*, *356*(4), 374–381.

Shi, R., Wang, L., Du, X., Bai, C., Wang, F., Wang, C., ... & Yang, W. (2024). Ferroptosis-related genes MDM2 and CDKN1A as reliable biomarkers for COPD.

Siedlinski, M., Postma, D. S., van Diemen, C. C., Blokstra, A., Smit, H. A., & Boezen, H. M. (2008). Lung function loss, smoking, vitamin C intake, and polymorphisms of the glutamate-cysteine ligase genes. *American journal of respiratory and critical care medicine*, *178*(1), 13-19.

Simpson, J. L., McDonald, V. M., Baines, K. J., Oreo, K. M., Wang, F., Hansbro, P. M., & Gibson, P. G. (2013). Influence of age, past smoking, and disease severity on TLR2, neutrophilic inflammation, and MMP-9 levels in COPD. *Mediators of inflammation*, *2013*, 462934.

Song, J., Wang, Q., & Zong, L. (2020). LncRNA MIR155HG contributes to smoke-related chronic obstructive pulmonary disease by targeting miR-128-5p/BRD4 axis. *Bioscience Reports*, *40*(3), BSR20192567.

Song, Q., Chen, P., & Liu, X. M. (2021). The role of cigarette smoke-induced pulmonary vascular endothelial cell apoptosis in COPD. *Respiratory research*, *22(1)*, 39.

Soriano, J. B., Kendrick, P. J., Paulson, K. R., Gupta, V., Abrams, E. M., Adedoyin, R. A., ... & Moradi, M. (2020). Prevalence and attributable health burden of chronic respiratory diseases, 1990–2017: a systematic analysis for the Global Burden of Disease Study 2017. *The Lancet Respiratory Medicine*, *8*(6), 585-596.

Stockley R. A. (1999). Neutrophils and protease/antiprotease imbalance. *American journal of respiratory and critical care medicine*, *160*(5 Pt 2), S49–S52.

Stoyanovsky, D. A., Tyurina, Y. Y., Shrivastava, I., Bahar, I., Tyurin, V. A., Protchenko, O., ... & Kagan, V. E. (2019). Iron catalysis of lipid peroxidation in ferroptosis: Regulated enzymatic or random free radical reaction?. *Free Radical Biology and Medicine*, *133*, 153-161.

Subramanian, I., Verma, S., Kumar, S., Jere, A., & Anamika, K. (2020). Multi-omics data integration, interpretation, and its application. *Bioinformatics and biology insights*, *14*, 1177932219899051.

Subramanian, A., Tamayo, P., Mootha, V. K., Mukherjee, S., Ebert, B. L., Gillette, M. A., ... & Mesirov, J. P. (2005). Gene set enrichment analysis: a knowledge-based

approach for interpreting genome-wide expression profiles. *Proceedings of the National Academy of Sciences*, *102*(43), 15545-15550.

Sui, S., Zhang, J., Xu, S., Wang, Q., Wang, P., & Pang, D. (2019). Ferritinophagy is required for the induction of ferroptosis by the bromodomain protein BRD4 inhibitor (+)-JQ1 in cancer cells. *Cell death & disease*, *10*(5), 331.

Sun, Y., Chen, P., Zhai, B., Zhang, M., Xiang, Y., Fang, J., Xu, S., Gao, Y., Chen, X., Sui, X. and Li, G., 2020. The emerging role of ferroptosis in inflammation. *Biomedicine & Pharmacotherapy*, *127*, p.110108.

Szklarczyk, D., Gable, A. L., Nastou, K. C., Lyon, D., Kirsch, R., Pyysalo, S., Doncheva, N. T., Legeay, M., Fang, T., Bork, P., Jensen, L. J., & von Mering, C. (2021). The STRING database in 2021: customizable protein-protein networks, and functional characterization of user-uploaded gene/measurement sets. *Nucleic acids research*, *49*(D1), D605–D612.

Szklarczyk, D., Kirsch, R., Koutrouli, M., Nastou, K., Mehryary, F., Hachilif, R., Gable, A. L., Fang, T., Doncheva, N. T., Pyysalo, S., Bork, P., Jensen, L. J., & von Mering, C. (2023). The STRING database in 2023: protein-protein association networks and functional enrichment analyses for any sequenced genome of interest. *Nucleic acids research*, *51*(D1), D638–D646.

Tang, K., Zhao, J., Xie, J., & Wang, J. (2019). Decreased miR-29b expression is associated with airway inflammation in chronic obstructive pulmonary disease. *American Journal of Physiology-Lung Cellular and Molecular Physiology*, *316*(4), L621-L629.

Tang, D., Chen, X., Kang, R., & Kroemer, G. (2021). Ferroptosis: molecular mechanisms and health implications. *Cell research*, *31*(2), 107–125.

Teder, P., Vandivier, R. W., Jiang, D., Liang, J., Cohn, L., Puré, E., Henson, P. M., & Noble, P. W. (2002). Resolution of lung inflammation by CD44. *Science (New York, N.Y.)*, *296*(5565), 155–158.

Tergaonkar, V., Pando, M., Vafa, O., Wahl, G., & Verma, I. (2002). p53 stabilization is decreased upon NFkappaB activation: a role for NFkappaB in acquisition of resistance to chemotherapy. *Cancer cell*, *1*(5), 493–503.

Trapnell, C., Roberts, A., Goff, L., Pertea, G., Kim, D., Kelley, D. R., Pimentel, H., Salzberg, S. L., Rinn, J. L., & Pachter, L. (2012). Differential gene and transcript expression analysis of RNA-seq experiments with TopHat and Cufflinks. *Nature protocols*, *7*(3), 562–578.

US Department of Health and Human Services, May 2024, Secondhand Cigarette Smoke is Harmful and Deadly, https://www.health.ny.gov/prevention/tobacco_control/

Vallath, S., Hynds, R. E., Succony, L., Janes, S. M., & Giangreco, A. (2014). Targeting EGFR signalling in chronic lung disease: therapeutic challenges and opportunities. *European Respiratory Journal*, *44*(2), 513-522.

Van Buren, E., Radicioni, G., Lester, S., O'Neal, W.K., Dang, H., Kasela, S., Garudadri, S., Curtis, J.L., Han, M.K., Krishnan, J.A. and Wan, E.S., 2023. Genetic regulators of sputum mucin concentration and their associations with COPD phenotypes. *PLoS genetics*, *19*(6), p.e1010445.

van der Does, A. M., Mahbub, R. M., Ninaber, D. K., Rathnayake, S. N. H., Timens, W., van den Berge, M., Aliee, H., Theis, F. J., Nawijn, M. C., Hiemstra, P. S., & Faiz, A. (2022). Early transcriptional responses of bronchial epithelial cells to whole cigarette smoke mirror those of in-vivo exposed human bronchial mucosa. *Respiratory research*, *23*(1), 227.

Vandivier, R. W., Henson, P. M., & Douglas, I. S. (2006). Burying the dead: the impact of failed apoptotic cell removal (efferocytosis) on chronic inflammatory lung disease. *Chest*, *129*(6), 1673-1682.

Vejnar, C. E., & Zdobnov, E. M. (2012). MiRmap: comprehensive prediction of microRNA target repression strength. *Nucleic acids research*, *40*(22), 11673–11683.

Veljkovic, E., Jiricny, J., Menigatti, M., Rehrauer, H., & Han, W. (2011). Chronic exposure to cigarette smoke condensate in vitro induces epithelial to mesenchymal transition-like changes in human bronchial epithelial cells, BEAS-2B. *Toxicology in vitro : an international journal published in association with BIBRA*, *25*(2), 446–453.

Vlahos, R., & Bozinovski, S. (2014). Role of alveolar macrophages in chronic obstructive pulmonary disease. *Frontiers in immunology*, *5*, 435.

Wang, B., Yang, J., Xiao, J., Liang, B., Zhou, H. X., Su, Z., ... & Feng, Y. (2014). Association of XRCC5 polymorphisms with COPD and COPD-related phenotypes in the Han Chinese population: a case-control cohort study. *Genet Mol Res*, *13*(3), 7070-7078.

Wang, Z., Zuo, Y., & Gao, Z. (2021). CircANKRD11 knockdown protects HPMECs from cigarette smoke extract-induced injury by regulating miR-145-5p/BRD4 axis. *International journal of chronic obstructive pulmonary disease*, 887-899.

Wang, B., Liang, B., Yang, J., Xiao, J., Ma, C., Xu, S., Lei, J., Xu, X., Liao, Z., Liu, H., Ou, X., & Feng, Y. (2013). Association of FAM13A polymorphisms with COPD and

COPD-related phenotypes in Han Chinese. *Clinical biochemistry*, *46*(16-17), 1683–1688.

Wang, B., Wang, Y., Zhang, J., Hu, C., Jiang, J., Li, Y., & Peng, Z. (2023). ROS-induced lipid peroxidation modulates cell death outcome: mechanisms behind apoptosis, autophagy, and ferroptosis. *Archives of toxicology*, *97*(6), 1439-1451.

Wang, B., Zhou, H., Yang, J., Xiao, J., Liang, B., Li, D., Zhou, H., Zeng, Q., Fang, C., Rao, Z., Yu, H., Ou, X., & Feng, Y. (2013). Association of HHIP polymorphisms with COPD and COPD-related phenotypes in a Chinese Han population. *Gene*, *531*(1), 101–105.

Wang, Y., & Tang, M. (2019). PM2. 5 induces ferroptosis in human endothelial cells through iron overload and redox imbalance. *Environmental pollution*, *254*, 112937.

Wang, Z., Gerstein, M., & Snyder, M. (2009). RNA-Seq: a revolutionary tool for transcriptomics. *Nature reviews. Genetics*, *10*(1), 57–63.

Wohnhaas, C. T., Gindele, J. A., Kiechle, T., Shen, Y., Leparc, G. G., Stierstorfer, B., Stahl, H., Gantner, F., Viollet, C., Schymeinsky, J., & Baum, P. (2021). Cigarette Smoke Specifically Affects Small Airway Epithelial Cell Populations and Triggers the Expansion of Inflammatory and Squamous Differentiation Associated Basal Cells. *International journal of molecular sciences*, *22*(14), 7646.

World Health Organization (2020, September 22). Retrieved from: https://www.who.int/news-room/fact-sheets/detail/chronic-obstructive-pulmonary-disease-(copd)

Wu, Q., Jiang, D., & Chu, H. W. (2012). Cigarette smoke induces growth differentiation factor 15 production in human lung epithelial cells: implication in mucin over-expression. *Innate immunity*, *18*(4), 617-626.

Wu, L., Xian, X., Tan, Z., Dong, F., Xu, G., Zhang, M., & Zhang, F. (2023). The role of iron metabolism, lipid metabolism, and redox homeostasis in Alzheimer's disease: from the perspective of ferroptosis. *Molecular Neurobiology*, *60*(5), 2832-2850.

Xu, F., Vasilescu, D. M., Kinose, D., Tanabe, N., Ng, K. W., Coxson, H. O., Cooper, J. D., Hackett, T. L., Verleden, S. E., Vanaudenaerde, B. M., Stevenson, C. S., Lenburg, M. E., Spira, A., Tan, W. C., Sin, D. D., Ng, R. T., & Hogg, J. C. (2022). The molecular and cellular mechanisms associated with the destruction of terminal bronchioles in COPD. *The European respiratory journal*, *59*(5), 2101411.

Yamamoto, C., Yoneda, T., Yoshikawa, M., Fu, A., Tokuyama, T., Tsukaguchi, K., & Narita, N. (1997). Airway inflammation in COPD assessed by sputum levels of interleukin-8. *Chest*, *112*(2), 505–510.

Yang, A., Kaghad, M., Wang, Y., Gillett, E., Fleming, M. D., Dötsch, V., ... & McKeon, F. (1998). p63, a p53 homolog at 3q27–29, encodes multiple products with transactivating, death-inducing, and dominant-negative activities. *Molecular cell*, *2*(3), 305-316.

Yang, D., Xu, D., Wang, T., Yuan, Z., Liu, L., Shen, Y., & Wen, F. (2021). Mitoquinone ameliorates cigarette smoke-induced airway inflammation and mucus hypersecretion in mice. *International immunopharmacology*, *90*, 107149.

Yang, W. S., & Stockwell, B. R. (2016). Ferroptosis: Death by Lipid Peroxidation. *Trends in cell biology*, *26*(3), 165–176.

Yang, W. S., Kim, K. J., Gaschler, M. M., Patel, M., Shchepinov, M. S., & Stockwell, B. R. (2016). Peroxidation of polyunsaturated fatty acids by lipoxygenases drives ferroptosis. *Proceedings of the National Academy of Sciences of the United States of America*, *113*(34), E4966–E4975.

Yoon, H. K., Hu, H. J., Rhee, C. K., Shin, S. H., Oh, Y. M., Lee, S. D., Jung, S. H., Yim, S. H., Kim, T. M., Korean Obstructive Lung Disease (KOLD) Study Group, & Chung, Y. J. (2014). Polymorphisms in PDE4D are associated with a risk of COPD in non-emphysematous Koreans. *COPD*, *11*(6), 652–658.

Yoshida, M., Minagawa, S., Araya, J., Sakamoto, T., Hara, H., Tsubouchi, K., Hosaka, Y., Ichikawa, A., Saito, N., Kadota, T. and Sato, N., 2019. Involvement of cigarette smoke-induced epithelial cell ferroptosis in COPD pathogenesis. *Nature Communications*, *10*(1), p.3145.

Yu, G., Wang, L. G., Han, Y., & He, Q. Y. (2012). clusterProfiler: an R package for comparing biological themes among gene clusters. *Omics: a journal of integrative biology*, *16*(5), 284-287.

Yu, S., Jia, J., Zheng, J., Zhou, Y., Jia, D., & Wang, J. (2021). Recent Progress of Ferroptosis in Lung Diseases. *Frontiers in cell and developmental biology*, *9*, 789517.

Zhang, P., Han, Y., Huang, L., Li, Q., & Ma, D. (2009). *Zhongguo fei ai za zhi = Chinese journal of lung cancer*, *12*(9), 995–999.

Zhang, Y., Zhang, J., & Fu, Z. (2022). Role of autophagy in lung diseases and ageing. *European respiratory review : an official journal of the European Respiratory Society, 31(166)*,220134.

Zheng, T., Zhu, Z., Wang, Z., Homer, R. J., Ma, B., Riese, R. J., Jr, Chapman, H. A., Jr, Shapiro, S. D., & Elias, J. A. (2000). Inducible targeting of IL-13 to the adult lung causes matrix metalloproteinase- and cathepsin-dependent emphysema. *The Journal of clinical investigation*, *106*(9), 1081–1093.

Zhou, N., & Bao, J. (2020). FerrDb: a manually curated resource for regulators and markers of ferroptosis and ferroptosis-disease associations. *Database*, *2020*, baaa021.

Zhou, X., Baron, R.M., Hardin, M., Cho, M.H., Zielinski, J., Hawrylkiewicz, I., Sliwinski, P., Hersh, C.P., Mancini, J.D., Lu, K. and Thibault, D., 2012. Identification of a chronic obstructive pulmonary disease genetic determinant that regulates HHIP. *Human molecular genetics*, *21*(6), pp.1325-1335.

Zhou, Y., Zhou, B., Pache, L., Chang, M., Khodabakhshi, A.H., Tanaseichuk, O., Benner, C. and Chanda, S.K., 2019. Metascape provides a biologist-oriented resource for the analysis of systems-level datasets. *Nature communications*, *10*(1), p.1523.

Zhu, X., Fu, Z., Dutchak, K., Arabzadeh, A., Milette, S., Steinberger, J., Morin, G., Monast, A., Pilon, V., Kong, T. and Adams, B.N., 2024. Cotargeting CDK4/6 and BRD4 Promotes Senescence and Ferroptosis Sensitivity in Cancer. *Cancer Research*, *84*(8), pp.1333-1351.

Zuo, W.L., Rostami, M.R., Shenoy, S.A., LeBlanc, M.G., Salit, J., Strulovici-Barel, Y., O'Beirne, S.L., Kaner, R.J., Leopold, P.L., Mezey, J.G. and Schymeinsky, J., 2020. Cell-specific expression of lung disease risk-related genes in the human small airway epithelium. *Respiratory research*, *21*, pp.1-11.